

Electronic Thesis and Dissertation Repository

8-21-2017 12:00 AM

Bacterial Cellulose Nanocrystals: Production and Application

Isabela Reiniati, *The University of Western Ontario*

Supervisor: Dr. Andrew N. Hrymak, *The University of Western Ontario*

Co-Supervisor: Dr. Argyrios Margaritis, *The University of Western Ontario*

A thesis submitted in partial fulfillment of the requirements for the Doctor of Philosophy degree
in Chemical and Biochemical Engineering

© Isabela Reiniati 2017

Follow this and additional works at: <https://ir.lib.uwo.ca/etd>

 Part of the [Biochemical and Biomolecular Engineering Commons](#)

Recommended Citation

Reiniati, Isabela, "Bacterial Cellulose Nanocrystals: Production and Application" (2017). *Electronic Thesis and Dissertation Repository*. 4826.

<https://ir.lib.uwo.ca/etd/4826>

This Dissertation/Thesis is brought to you for free and open access by Scholarship@Western. It has been accepted for inclusion in Electronic Thesis and Dissertation Repository by an authorized administrator of Scholarship@Western. For more information, please contact wlsadmin@uwo.ca.

Abstract

The aims of this study were to investigate the effect of culture conditions on the production of bacterial cellulose (BC) by *Komagataeibacter xylinus* (*K. xylinus*), to assess the feasibility of tailoring the surface properties of bacterial cellulose nanocrystals (BCNs) through the culture conditions, and to use the BCNs in an aqueous system for drug adsorption application. BC fibers production improved with increased agitation rates in a stirred tank bioreactor resulting in yields of 0.54 and 1.13 g of BC per litre at agitation rates of 500 rpm and 700 rpm, respectively. Separation and purification of bacterial cellulose were achieved in a one-step process, while also preserving the crystalline cellulose structure. Stirred-tank bioreactors represent a promising avenue for scale up to achieve high yields of bacterial cellulose.

A shake flask study was conducted to investigate the yield of BCNs in relation to the BC fibers production. Rotational speed significantly affected the production of BC fibers and yield of BCNs. It was observed that the highest BC production also generated the maximum total mass of BCNs per volume of the culture medium. The optimal medium that achieved the highest amount of BCNs contained 25 g of fructose l⁻¹ and 35 g of CSS l⁻¹ at a pH of 4.5, when cultivated in a rotary shaker incubator at 250 rpm.

BCNs obtained from sulfuric acid hydrolysis were used as an adsorbent for ionizable antibiotic tetracycline hydrochloride (TCH) from concentrated aqueous suspension. After 6 hours of adsorption, both pH and rotational speed did not significantly affect the adsorption capacity of antibiotic tetracycline hydrochloride (TCH) on BCNs, reaching a maximum loading of 54.5 mg of TCH per gram of BCNs at 25°C and pH 3.

Modification of BC fibers production parameters increased the yield of BCNs and affected the BCNs size distribution. The adsorption kinetics of TCH on BCNs followed pseudo-second order kinetic model with a better fit on the higher BCNs dosage. In addition, this study demonstrates that bacterial-derived cellulose nanocrystals are an effective adsorbent for tetracycline hydrochloride drug delivery excipient in an aqueous system.

Keywords

Bacterial cellulose fiber, bacterial cellulose nanocrystal, *Komagataeibacter xylinus*, bioreactor, adsorption, tetracycline hydrochloride.

Co-Authorship Statement

In the development of this work, four papers were written and co-authored. The extent of the collaboration of the co-authors is stated below.

Chapter 2: Recent developments in the production and applications of bacterial cellulose fibers and nanocrystals.

Isabela Reiniati, Andrew N. Hrymak, and Argyrios Margaritis

A version of this chapter has been published in *Critical Reviews in Biotechnology*, 37, 4, 510-524, 2017. (<http://dx.doi.org/10.1080/07388551.2016.1189871>).

Isabela Reiniati: technical and theoretical advisor, literature review, writing, and corrections of several drafts and final paper.

Dr. Andrew N. Hrymak: paper review and corrections.

Dr. Argyrios Margaritis: supervision, paper review, and corrections.

Chapter 4: Kinetics of Cell Growth and Crystalline Nanocellulose Production by *Komagataeibacter xylinus*.

Isabela Reiniati, Andrew N. Hrymak, and Argyrios Margaritis

A version of this chapter has been accepted and published online in *Biochemical Engineering Journal*, In Press, 22 July 2017 (<https://doi.org/10.1016/j.bej.2017.07.007>).

Isabela Reiniati: experimental design, laboratory work, data analysis, paper writing, and corrections of several drafts and final paper.

Dr. Andrew N. Hrymak: paper review and corrections.

Dr. Argyrios Margaritis: supervision, critical data interpretation, and corrections.

Chapter 5: Bacterial cellulose nanocrystals by *Komagataeibacter xylinus*: yield and adsorption capacity.

Isabela Reiniati, Andrew N. Hrymak, and Argyrios Margaritis

This paper is ready for submission to a journal.

Isabela Reiniati: experimental design, laboratory work, data analysis, paper writing, and corrections of several drafts and final paper.

Dr. Andrew N. Hrymak: experimental design, technical advisor, paper review and corrections.

Dr. Argyrios Margaritis: paper review and corrections.

Chapter 6: Adsorption of model drug tetracycline hydrochloride on bacterial cellulose nanocrystals

Isabela Reiniati, Andrew N. Hrymak, and Argyrios Margaritis

This paper is ready for submission to a journal.

Isabela Reiniati: experimental design, laboratory work, data analysis, paper writing, and corrections of several drafts and final paper.

Dr. Andrew N. Hrymak: supervision, paper review and corrections.

Dr. Argyrios Margaritis: paper review and corrections.

Acknowledgments

I would like to express my sincere gratitude to my thesis co-supervisors, Dr. Argyrios Margaritis and Dr. Andrew N. Hrymak, for the opportunity to be part of their research group, for their guidance, continuous support, and funding throughout my PhD. I thank them for the numerous discussion and encouragement when I encountered difficulties in my research.

I would like to thank my current and past lab mates/colleagues: Dr. Shahram Amirnia, Cody Bulmer, Koosha Azhie, Thirumalai Nambi Thiruvengadathan, and Timothy McDougald for their help, company, and encouragements during this research work. Especially to Reyna Gomez-Flores, thank you for being an extraordinary lab mate, fermentation guru, and a dear friend since the start of our graduate studies. To Elizabeth K. Tomaszewski, thank you for many coffee chats, noon masses we attended in Brescia, and for critically correcting my English. Thank you for your friendship and being my moral compass. I am indebted to my friends and colleagues for providing a stimulating environment and safe space to grow, specially Dr. Yira Aponte, Dr. Angel Lanza, Vanessa Rodgher, Maritza Gomez-Flores, Dr. Ana Maria-Aguirre, and Dr. Gabriela Navarro. I would also like to thank Dr. Kalin Penev for his positive outlook and motivation. Thank you all for the good times, friendships, and all the invaluable things I have learned from all of you.

I thank Dr. Emily Cranston of McMaster University for her insights on cellulose nanocrystals production technique. I am very thankful to Dr. Hugo de Lasa for his encouragement and wisdom. I thank Pastor Solano-Flores for his help in XRD techniques, Ying Zhang for assistance in FTIR, Souheil Afara and Brian Dennis, for their willingness to help and being the most hands-on helpers. Thank you for your technical assistance and cheerful moments. I would also like to thank all current and former CBE department staff who helped me during my PhD: Joseph Cole Handsaeme, Ashley Jokhu, Kara Malott, Sarah Williams, Myriam Delgado, Katherine Manweiler, Paul Sheller, and Stephen Mallinson. A special thank you to Florencia de Lasa and Dr. Rika Anderson for their assistance in the editing of this thesis.

I am grateful to for an amazing family here in London: my mother-in-law, Win Nio Lie, who supported me with her delicious home cook meals, my sister-in-law, Lian Hoa Lie, with her cheerfulness, Shirleen Iskandar with her wonderful dishes when I still lived in the basement,

and little Matthew Soenjaya with his adorable smiles and cuteness. To Dr. Yohannes Soenjaya, Calvin Soenjaya, Desi, Muriel Silva, Edgar Pena, Olivia Siswanto, and Theo Surjo, thank you for your moral support and friendships. I cherished our gatherings and enjoyed your company.

My greatest gratitude is to my mom, Betisari Latidjan, and my dad, Didik Waluyo, for encouraging me in all of my pursuits, inspiring me to be a better person, and loving me unconditionally. To my brothers, Benedictus Ariestika and Dionisius Rianto, for being my strength and greatest life supporters. To Odelia, Keira, Kelzie, Friska, and Abelle for cheering me and loving my brothers and parents. It does not matter where we are, distance has only brought us closer to each other.

This work could never have done without the unfailing support of my lovely husband, Riki Lie, who was always there for me, cheering me up when things get tough, and helping me to stand on my feet when I felt weak. There are no words to fully describe his support, understanding and care.

Finally, to the Heavenly Father, I praise you and thank you for your blessings and all that you are.

With God all things are possible

~Matthew 19:26

Table of Contents

Abstract.....	i
Co-Authorship Statement.....	iii
Acknowledgments.....	v
Table of Contents.....	vii
List of Tables.....	xiii
List of Figures.....	xv
List of Appendices.....	xx
Nomenclature.....	xxi
Abbreviation.....	xxiv
Chapter 1.....	1
1 Introduction.....	1
1.1 Research Objectives and Contributions.....	1
1.1.1 Main Objective.....	1
1.1.2 Specific Objectives.....	2
1.2 Thesis Organization.....	3
1.3 Research Contribution.....	4
Chapter 2.....	6
2 Literature Review: Recent developments in the production and applications of bacterial cellulose fibers and nanocrystals.....	6
2.1 Abstract.....	6
2.2 Introduction.....	6
2.3 Bacterial cellulose biosynthesis.....	14
2.4 Effects of culture media composition on BC production.....	17

2.5	Effects of culture media composition and BC production conditions on BC physical properties.....	20
2.6	Effects of bioprocess parameters on BC production.....	21
2.7	Separation and purification of BC from broth	23
2.8	Production of cellulose nanocrystals (CNs).....	23
2.8.1	Acid hydrolysis	25
2.8.2	Oxidation.....	28
2.8.3	Enzymatic hydrolysis.....	29
2.8.4	Ionic Liquids	30
2.9	Challenges.....	31
2.10	Conclusions.....	32
2.11	References.....	33
Chapter 3.....		45
3	Batch Growth of <i>Komagataeibacter xylinus</i> and Measurement of Bacterial Cellulose Crystallinity.....	45
3.1	Abstract.....	45
3.2	Introduction.....	45
3.3	Materials and methods	48
3.3.1	Microorganism and culture media	48
3.3.2	Preparation of stock culture	48
3.3.3	Production of cellulose in shake flasks.....	49
3.3.4	Measurement of bacterial cellulose and cell dry weight.....	49
3.3.5	Measurement of sugar concentration	50
3.3.6	Scanning electron microscope (SEM) of bacterial cellulose fibers	50
3.3.7	Attenuated Total Reflectance Fourier-Transform Infrared Spectroscopy (ATR-FTIR) of bacterial cellulose fibers	51
3.3.8	X-ray Diffraction (XRD) of bacterial cellulose fibers.....	51

3.3.9	Data analysis	52
3.4	Results and Discussion	52
3.4.1	Bacterial cellulose morphology	52
3.4.2	Effect of production conditions and cultivation time on bacterial cellulose fibers production	55
3.4.3	Evaluation of changes in bacterial cellulose crystallinity measured with XRD and ATR-FTIR	60
3.5	Conclusions.....	68
3.6	Reference	69
Chapter 4	75
4	Kinetics of Cell Growth and Crystalline Nanocellulose Production by <i>Komagataeibacter xylinus</i>	75
4.1	Abstract.....	75
4.2	Introduction.....	75
4.3	Materials and experimental methods	78
4.3.1	Microorganism.....	78
4.3.2	Culture media.....	78
4.3.3	Inoculum and culture conditions.....	79
4.3.4	Operational conditions	80
4.3.5	Measurement of bacterial cellulose and cell dry weight.....	82
4.3.6	Measurement of sugar concentration	82
4.3.7	Separation and purification of bacterial cellulose fibers.....	82
4.3.8	Protein quantification.....	83
4.3.9	Scanning electron microscope (SEM)	83
4.3.10	Fourier-Transform Infrared Spectroscopy (FTIR).....	83
4.3.11	X-ray Diffraction (XRD)	84
4.3.12	Cell growth kinetics	84

4.3.13	Measurement of oxygen uptake rate (OUR).....	85
4.4	Results and Discussion	87
4.4.1	Bacterial cellulose formation	87
4.4.2	Bacterial cellulose production in a stirred-tank bioreactor.....	88
4.4.3	Separation and purification of bacterial cellulose fibers.....	95
4.4.4	Cellulose crystallinity	97
4.5	Conclusion	102
4.6	References.....	103
Chapter 5	108
5	Bacterial cellulose nanocrystals by <i>Komagataeibacter xylinus</i> : yield and drug adsorption capacity.....	108
5.1	Abstract.....	108
5.2	Introduction.....	108
5.3	Materials and methods	110
5.3.1	Microorganism and culture media	110
5.3.2	Shake flask experiment for one-factor-at-a-time optimization approach.....	111
5.3.3	Experimental design.....	111
5.3.4	Analytical methods	112
5.3.5	Bacterial cellulose nanocrystals (BCNs) preparation	113
5.3.6	Adsorption of tetracycline hydrochloride (TCH)	114
5.3.7	Zeta potential measurements.....	115
5.3.8	Data analysis	115
5.4	Results and Discussion	115
5.4.1	Effect of culture conditions on BC production using one-factor-at-a-time approach.....	115
5.4.2	Screening of factors using fractional factorial design.....	118
5.4.3	Adsorption study.....	121

5.5 Conclusion	123
5.6 Reference	124
Chapter 6.....	127
6 Adsorption of model drug tetracycline hydrochloride on bacterial cellulose nanocrystals	127
6.1 Abstract.....	127
6.2 Introduction.....	127
6.3 Materials and experimental methods	129
6.3.1 Bacterial cellulose (BC) production.....	129
6.3.2 Preparation of bacterial cellulose nanocrystals (BCNs)	129
6.3.3 Scanning electron microscope (SEM)	130
6.3.4 Transmission electron microscope (TEM).....	130
6.3.5 X-ray diffraction (XRD)	130
6.3.6 Zeta potential measurements.....	131
6.3.7 Effect of pH on TCH adsorption.....	131
6.3.8 Adsorption kinetics of TCH on BCNs	132
6.3.9 Drug release kinetics.....	132
6.4 Results and Discussion	132
6.4.1 TCH morphology and BCNs crystallinity	132
6.4.2 Size distribution of BCNs	134
6.4.3 Effect of solution pH.....	135
6.4.4 Effect of BCNs dosage on TCH adsorption kinetics	138
6.4.5 Drug release kinetics.....	142
6.5 Conclusion	143
6.6 Reference	144
Chapter 7.....	146

7	Conclusions and Recommendations	146
7.1	Conclusions.....	146
7.2	Recommendations.....	148
	Appendices.....	150
	Appendix A: Pictures of bacterial cellulose and bacterial cellulose nanocrystals	150
	Appendix B: Characterization of bacterial cellulose nanocrystals via sulfuric acid hydrolysis	153
	Appendix B1: Bacterial cellulose nanocrystals (BCNs) production.....	153
	Appendix B2: Size distribution of bacterial cellulose nanocrystals (BCNs) and Avicel cellulose nanocrystals (Avi-CNs) obtained at different acid hydrolysis times.	156
	Appendix C: Calibration curves for TCH in 10 mM PBS at pH 7 and in deionized water at pH 3 to 7.....	158
	Curriculum Vitae	160

List of Tables

Table 2.1 Comparison criteria for plant-derived cellulose and bacterial cellulose fiber	9
Table 2.2 Different applications of bacterial cellulose (BC) using different processing methods	10
Table 2.3 Bacterial cellulose production under different culture conditions.....	19
Table 2.4 Physical characteristics of cellulose nanocrystal (CNs) from different sources.....	24
Table 2.5. Summary of acid hydrolysis conditions for the production of cellulose nanocrystals	27
Table 3.1 Bacterial cellulose (BC) production by <i>K. xylinus</i> grown in a fructose-CSS solution medium in shake flasks with fructose and CSS concentration of 25 g/l and 35 g/l, respectively. Values represent average \pm standard deviations from triplicate experiments (n=3).....	55
Table 3.2 Summary of cellulose crystallinity indices of bacterial cellulose produced by <i>K. xylinus</i> in shake flasks at 30°C for 5 days. Legend: A (250 rpm, without baffles), B (250 rpm, with baffles), C (150 rpm, without baffles), and D (150 rpm, with baffles). Avicel is presented for comparison.	67
Table 4.1. Process parameters for bacterial cellulose production, substrate consumption, and cell growth of <i>K. xylinus</i> in fructose-corn steep solid solution medium in a 3-L stirred-tank bioreactor at 30°C for 72 h. The values reported were obtained from duplicate runs and expressed as mean \pm standard deviation.	92
Table 4.2. Crystallinity indices of bacterial cellulose fibers produced in a 3-L bioreactor agitated at 700 rpm for 72 h, measured using XRD and ATR-FTIR.....	99
Table 5.1 Factors assigned at different levels for one-factor-at-a-time optimization method.	111
Table 5.2 Factors and their levels in fractional factorial design for bacterial cellulose (BC) production in a rotary shaker incubator.	112

Table 5.3 Fractional factorial design of experiments to study the effects of the culture process parameters on bacterial cellulose (BC) production and bacterial cellulose nanocrystals (BCNs) yield.....	112
Table 5.4 Adsorption capacity of TCH onto BCNs and zeta potentials of BCNs and TCH mixture after 2 and 6 hours of adsorption in deionized water at pH 3 at ambient temperature of 25°C. The mean values are average of triplicates and are presented with standard error. ...	122
Table 6.1 Zeta potentials of bacterial cellulose nanocrystals (BCNs) in deionized water (H ₂ O) at 25°C and different pH. Zeta potential values are expressed as an average of three measurements.....	136
Table 6.2. Kinetic parameters of TCH adsorption on BCNs in deionized water at 25°C. ...	142

List of Figures

Figure 1.1 Research framework.....	4
Figure 2.1 Schematic process flow diagram of bacterial cellulose (BC) and bacterial cellulose nanocrystals (BCNs) production.....	14
Figure 2.2 A schematic showing the major metabolic pathways of <i>A. xylinum</i> and the assembly of cellulose molecules into nanofibrils. Obtained from Lee et al. (Lee et al., 2014) with permission. Copyright, 2014, Wiley – VCH Verlag GmbH & Co. KGaA, Weinheim.....	15
Figure 3.1 Schematic of shake flasks (a) without and (b and c) with baffles for bacterial cellulose production.....	49
Figure 3.2 Images of <i>K. xylinus</i> , bacterial culture, and bacterial cellulose in shake flasks. ..	53
Figure 3.3 SEM images of bacterial cellulose produced by <i>K. xylinus</i> grown for 5 days in a fructose-CSS medium at 250 rpm: (a) and (b) showing bacterial cellulose being produced from the bacterial cells, (c) and (d) showing pure bacterial cellulose after being treated with 0.1 N NaOH. Scale bar for (a) and (c) is 10 μm while for (b) and (d) it is 5 μm . ..	54
Figure 3.4 Bacterial cellulose production by <i>K. xylinus</i> in fructose-CSS medium incubated in an orbital shaker set at 30°C and with a rotational speed of 250 rpm in shake flasks (A) without baffles and (B) with baffles. Legend: ■: bacterial cellulose concentration, ●: cell concentration, ▲: fructose concentration, ◆: pH.	58
Figure 3.5 Bacterial cellulose production by <i>K. xylinus</i> in fructose-CSS medium incubated in an orbital shaker set at 30°C and with a rotational speed of 150 rpm in shake flasks (C) without baffles and (D) with baffles. Legend: ■: bacterial cellulose concentration, ●: cell concentration, ▲: fructose concentration, ◆: pH.	59
Figure 3.6 X-ray diffractogram of bacterial cellulose fibers produced by <i>K. xylinus</i> in shake flask culture using two different rotational speeds: A (250 rpm, without baffles), B (250 rpm, with baffles), C (150 rpm, with baffles), and D (150 rpm, without baffles) at different cultivation days (as labelled on the graphs).....	61

Figure 3.7 X-ray diffractogram of bacterial cellulose fibers produced by <i>K. xylinus</i> after 5 days of cultivation in an orbital shaker set at 30°C in shake flasks: A (250 rpm, without baffles), B (250 rpm, with baffles), C (150 rpm, without baffles), and D (150 rpm, with baffles). Avicel is presented for comparison.....	62
Figure 3.8 XRD crystallinity indices of bacterial cellulose fibers produced in shake flasks filled with fru-CSS medium, incubated from 1 to 10 days inside a 30°C orbital shaker set at 250 rpm (A: without baffles, B: with baffles), and at 150 rpm (C: without baffles, D: with baffles) as determined using (a) the peak area fitting method and (b) the peak intensity method.	63
Figure 3.9 ATR-FTIR spectra of bacterial cellulose fibers produced by <i>K. xylinus</i> after 5 days of cultivation in an orbital shaker set at 30°C in shake flasks: A (250 rpm, without baffles), B (250 rpm, with baffles), C (150 rpm, without baffles), and D (150 rpm, with baffles). Avicel is presented for comparison.....	65
Figure 3.10 IR Cellulose crystallinity indices (a) $Cr_1 = A_{1428}/A_{897}$ and (b) $Cr_2 = A_{1372}/A_{2898}$ of bacterial cellulose fibers produced by <i>K. xylinus</i> in an orbital shaker set at 30°C in shake flasks: A (250 rpm, without baffles), B (250 rpm, with baffles), C (150 rpm, without baffles), and D (150 rpm, with baffles). Avicel is presented for comparison.	68
Figure 4.1. Schematic diagram of bacterial cellulose production.....	80
Figure 4.2. Schematic diagram of (A) a 3-L bioreactor used in batch fermentation for bacterial cellulose production (not to scale): 1) air supply, 2) flow meter, 3) air filter, 4) compressed nitrogen gas, 5) inoculum bottle, 6) peristaltic pump for inoculum feeding, 7) sampling tube, 8) syringe, 9) level probe, 10) temperature electrode, 11) pH electrode, 12) DO probe, 13) head plate, 14) strap heater, 15) air sparger, 16) Rushton turbine impeller, 17) baffles, 18) agitation motor, 19) gas outlet, 20) control panel. Legends for diagram (B): diameter of bioreactor, $D=12.5$ cm, height of liquid media, $H=17.5$ cm, baffle ($F/D=0.08$), 6-bladed Rushton-type turbine impellers ($d/D=0.44$), $H/D=1.4$, $h_1/H=0.35$, $h_2/H=0.39$, $h_3/H=0.26$	81
Figure 4.3. Results obtained during dynamic gassing-out for k_{La} and OUR determination during cultivation of <i>K. xylinus</i>	86

Figure 4.4. SEM images of *K. xylinus* and bacterial cellulose fibers produced in a 3-L stirred-tank bioreactor agitated at 700 rpm collected at different times: (A) 7 h, (B) 17 h, (C) 30 h, and (D) 72 h. Scale bar for (A) and (D) is 2 μm while for (B) and (C) is 1 μm 88

Figure 4.5 Growth kinetics of *K. xylinus* and bacterial cellulose production in a 3-L stirred-tank bioreactor with dual Rushton turbines set at agitation rates of 500 rpm (A and B), air supplied at 1 vvm, initial pH fructose-corn steep solid solution medium of 4.5 and kept at a constant temperature of 30°C. Legends: cellulose concentration (■), cell concentration (●), fructose concentration (▲), dissolved oxygen (DO) saturation (◆), and pH (▼). The values reported were obtained from duplicate runs and expressed as mean \pm standard deviation. ... 90

Figure 4.6 Growth kinetics of *K. xylinus* and bacterial cellulose production in a 3-L stirred-tank bioreactor with dual Rushton turbines set at agitation rates 700 rpm (A and B), air supplied at 1 vvm, initial pH fructose-corn steep solid solution medium of 4.5 and kept at a constant temperature of 30°C. Legends: cellulose concentration (■), cell concentration (●), fructose concentration (▲), dissolved oxygen (DO) saturation (◆), and pH (▼). The values reported were obtained from duplicate runs and expressed as mean \pm standard deviation. 91

Figure 4.7. Experimental data for oxygen uptake rate (OUR), specific oxygen uptake rate (q_{O_2}), and bacterial cellulose concentration (C_x) in a bioreactor agitated at (A) 500 rpm and (B) 700 rpm. Legends: OUR (○), q_{O_2} (▲), and C_x (■)..... 94

Figure 4.8. (A) Absorbance reading at 600 nm and (B) protein concentration profile of supernatant samples from each washing cycle. The mean is average of triplicates. 95

Figure 4.9. SEM images of bacterial cellulose fibers produced by *K. xylinus* in a 3-L stirred-tank bioreactor at 700 rpm after being treated with 0.1 N NaOH solution at 90°C for (A) 30 min and (B) 1 h in a small batch (25 ml sample size). Scale bar is 200 nm. 96

Figure 4.10. SEM images of bacterial cellulose fibers from 500 ml broth culture after purification treatment with 0.1 M NaOH solution at 90°C: (A) bacterial cellulose fibers, *K. xylinus* cell, and cell debris after 1 h treatment, (B) pure bacterial cellulose fibers after 2 h treatment. Scale bar is 1 μm 97

Figure 4.11. X-ray diffractogram of pure bacterial cellulose fibers produced in a 3-L stirred-tank bioreactor agitated at 700 rpm for 72 h.....	98
Figure 4.12. ATR-FTIR spectra of pure bacterial cellulose fibers produced by <i>K. xylinus</i> for 72 h at 30°C in a 3-L stirred-tank bioreactor agitated at 700 rpm: (A) full spectrum; (B) absorption bands at 750 and 710 cm ⁻¹ correspond to cellulose I _α and I _β , respectively.	100
Figure 5.1. Schematic diagram of a) bacterial cellulose (BC) fibers production and b) bacterial cellulose nanocrystals production.	114
Figure 5.2. Effect of fructose concentration, CSS concentration, pH medium, and shaker speed on bacterial cellulose (BC) production, cell production, BC yield, and pH of broth (numerical values are presented at the bottom graph). Results are the mean of three replicates ± standard error.	117
Figure 5.3 (A) Bacterial cellulose (BC) produced by <i>Komagataeibacter xylinus</i> in baffled shake flasks kept in an orbital incubator shaker at 30°C at 250 rpm and 150 rpm. (B) Bacterial cellulose nanocrystals (BCNs) yield was calculated by dividing a final freeze-dried weight of BCNs (g) after acid hydrolysis by an initial freeze-dried weight of BC fibers (g). The run numbers refer to experimental conditions described in Table 5.3. Legend: ■: BC production, ●: cell production, ▲: BCNs yield. Results show the data spread of three replicates.	120
Figure 5.4. BCNs dispersion in deionized water.	122
Figure 6.1 Scanning electron micrograph of tetracycline hydrochloride (TCH) powder as received.	133
Figure 6.2. a) X-ray diffraction pattern on freeze-dried bacterial cellulose nanocrystals (BCNs). Prominent peaks at 2 θ (°) of 14.6, 16.8, and 22.7 indicated cellulose I. b) Scanning electron micrograph of BCNs in deionized distilled water.....	133
Figure 6.3 The length distribution of BCNs (a) obtained from TEM images and morphology of BCNs (b).....	135
Figure 6.4. Molecular structure and functional groups of tetracycline hydrochloride (adapted from (Ali, 1984)).	137

Figure 6.5. Effect of initial pH on biosorption of TCH to BCNs in deionized water (initial TCH concentration: 100 µg/ml; volume: 10 ml; BCNs: 10 mg; temperature: 25°C; agitation rate: 150 rpm; incubation time: 2 h).....	138
Figure 6.6. Adsorption kinetics of TCH to BCNs in water (initial pH: 3; TCH concentration: 1000 µg/ml; volume: 2 ml; BCNs: 1 and 2 mg; temperature: 25°C).....	139
Figure 6.7. Linear regression adsorption kinetics of TCH of 0.5 mg BCNs/ml solution (a & b) and 1 mg BCNs/ml solution (c & d) following pseudo-first-order model and pseudo-second-order model.	141
Figure 6.8. The release kinetics of tetracycline hydrochloride (TCH) from bacterial cellulose nanocrystals (BCNs) in 10 mM phosphate buffered saline at 37°C (initial TCH concentration: 1000 µg/ml; volume: 2 ml; BCNs: 2 mg; temperature: 37°C)	143

List of Appendices

Appendix A: Pictures of bacterial cellulose and bacterial cellulose nanocrystals.....	150
Appendix B: Characterization of bacterial cellulose nanocrystals via sulfuric acid hydrolysis	153
Appendix C: Calibration curves for TCH in 10 mM PBS at pH 7 and in deionized water at pH 3 to 7	158

Nomenclature

μ	Specific growth rate of the microorganisms, /h
μ_{\max}	Maximum specific growth rate, /h
B	The width of baffle, cm
$C^*_{O_2}$	Equilibrium dissolved oxygen concentration, mg/L
C_0	Drug concentrations in the aqueous phase before adsorption (C_0 , mg/L)
C_e	Drug concentrations in the aqueous phase after adsorption (C_e , mg/L)
C_{\max}	Maximum cell concentration, g/L
C_{O_2}	Instantaneous dissolved oxygen concentration given by the probe, mg/L
Cr	Cellulose crystallinity index
Cr_1	Cellulose crystallinity index determined using ratios of the ATR-FTIR absorption intensity at wavenumber 1428 and 897 cm^{-1}
Cr_2	Cellulose crystallinity index determined using ratios of the absorption intensity at wavenumber 1372 and 2898 cm^{-1}
Cr_A	Crystallinity index determined by the peak area method obtained using XRD
C_X	Cell concentration, mg/L

d	Diameter of the 6-bladed Rushton turbine impeller, cm
D	Inner diameter of the 3L bioreactor, cm
dC_{O_2}/dt	Accumulation oxygen rate in the liquid phase, mg/L-h
fru	Fructose
h	Height, cm
H ₂ SO ₄	Sulfuric acid
k_{La}	Volumetric mass transfer coefficient, /h
K_s	Monod saturation constant, g/L
m	Mass of bacterial cellulose nanocrystals (g)
NaOH	Sodium hydroxide
q_e	Amount of drug adsorbed at equilibrium (mg/g)
q_{O_2}	Specific uptake rate of oxygen, L/mg-h
Q_P	Bacterial cellulose production rate, g/L-h
Q_S	Fructose consumption rate, g/L-h
q_t	Amount of drug adsorbed at different time (mg/g)
r	The width of impeller's blade

V	Volume of drug solution (L)
$Y_{P/S}$	Bacterial cellulose production based on the substrate consumed, g dry weight/ g substrate
$Y_{P/X}$	Bacterial cellulose production based on the cell concentration, g dry weight/ g dry weight
$Y_{X/S}$	Cell concentration based on the substrate consumed, g dry weight/ g dry weight

Abbreviation

ATR	Attenuated Total Reflectance
BC	Bacterial cellulose
BCN	Bacterial cellulose nanocrystals
CMC	Carboxymethyl cellulose
CN	Cellulose nanocrystals
CSS	Corn steep solid
DNS	Dinitrosalicylic acid
DO	Dissolved oxygen
FTIR	Fourier-transform Infrared
IL	Ionic liquid
MCC	Microcrystalline cellulose
MFC	Microfibrillated cellulose
OTR	Oxygen transfer rate
OUR	Oxygen uptake rate
PBS	Phosphate buffered saline

SEM	Scanning Electron Microscopy
TCH	Tetracycline hydrochloride
TEM	Transmission Electron Microscopy
XRD	X-ray Diffraction

Chapter 1

1 Introduction

Cellulose nanocrystals are attractive nanomaterials that are biodegradable, non-toxic, favor surface functionalization, and have a multitude of applications. The main sources of cellulose nanocrystals are wood and plants. Alternate sources include algae, tunicate, and bacteria. Production of cellulose from bacteria offers advantages, such as, the ability to control the production rate for extraction of high purity cellulose, and to control the properties (size, shape, and crystallinity) of bacterial cellulose (BC) fibers. Despite the advantages, the implementation of bacterial cellulose nanocrystals (BCNs) as novel materials in an industrial scale is challenging. Several issues related to the BC production process need to be addressed, such as, increasing productivity, producing BC with high cellulose crystallinity, increasing the yield of BCNs, and ability to control desirable BCNs properties.

Different strategies are proposed to increase the yield of BCNs. Increasing the BC fiber production by varying production conditions, such as sugar and nitrogen content, initial pH of liquid medium, and different agitation rates. Producing BC fibers with high cellulose crystallinity may potentially result in higher BCNs yield. Different acid hydrolysis conditions can affect the yield and size of the nanocrystals. Even though there are advantages in using bacteria to produce cellulose fiber and nanocrystals, only a few reports are available on the effect of culture conditions on BCNs yield and surface properties, making this area of high interest for research. With an increasing demand in the use of non-toxic nanocarriers for drugs, an adsorption study of model drug antibiotic tetracycline hydrochloride on BCNs was investigated.

1.1 Research Objectives and Contributions

1.1.1 Main Objective

The main objective of this research was to investigate the feasibility of tailoring the BCNs surface properties by varying the BC fiber culture conditions.

1.1.2 Specific Objectives

The general objective of this research was to develop a method for using cellulose nanocrystals produced by bacteria in selected industrial applications such as pharmaceutical application.

Objective 1: To produce and characterize bacterial cellulose fibers by *Komagataeibacter xylinus* (*Gluconacetobacter xylinus*) under different growing conditions.

- a). Investigate the effect of fructose concentration, corn steep solid concentration, pH medium, and rotational speed on the yield of bacterial cellulose (BC) fiber.
- b). Assess the effect of cultivation time on BC fiber production and degree of crystallinity.

Objective 2: To evaluate the impact of agitation speeds on the production of BC fiber in a 3L stirred tank bioreactor.

- a). Separation and purification of BC fiber from broth.
- b). Kinetics of growth of *Komagataeibacter xylinus* and BC fiber production.
- c). Investigation of in-situ oxygen uptake rate and oxygen transfer rate.

Objective 3: To characterize the bacterial cellulose nanocrystals (BCNs) prepared via acid hydrolysis.

- a). Investigate the effect of acid loading ratio and hydrolysis time on the yield and the size distributions of BCNs.
- b). Assess the effect of different BC fiber production method on the cellulose crystallinity and the size distribution of the BCNs.

Objective 4: To evaluate the adsorption of tetracycline hydrochloride (TCH) on BCNs in an aqueous system.

- a). Identify parameters which contribute to increase drug adsorption, pH and BCNs loading.
- b). Study the effect of pH on the adsorption of TCH onto BCNs.
- c). Study the adsorption kinetics of TCH on BCNs.

Objective 5: To investigate the impact of cultivation parameters on the BCNs production.

- a). Screen parameters affecting the production of BC fiber and BCNs yield.
- b). Measure cellulose crystallinity.

1.2 Thesis Organization

The thesis was divided into seven chapters and conforms to the “integrated” format as outlined by the Thesis Regulation Guide by the School of Graduate and Postdoctoral Studies (SGPS) of the University of Western Ontario. The chapters are organized as shown in Figure 1.1.

Chapter 1 introduces the research, its objectives, and thesis structure, Chapter 2 covers the literature review and gives the general background on production of bacterial cellulose fibers, bacterial cellulose nanocrystals characterizations, and applications. Chapter 3 deals with the batch growth of *Komagataeibacter xylinus* and cellulose crystallinity measurement. Chapter 4 presents the kinetics of growth of *Komagataeibacter xylinus* and bacterial cellulose production in a 3L bioreactor. This chapter also covers the oxygen uptake rate and oxygen transfer rate measured in-situ. Chapter 5 describes the detailed investigation of bacterial cellulose production at different cultivation conditions, the corresponding yield of bacterial cellulose nanocrystals (BCNs), and the surface characteristics of BCNs. Chapter 6 shows the use of BCNs for binding of antibiotic tetracycline hydrochloride (TCH). Chapter 7 summarizes the conclusions of the study and provides recommendations for future work. Appendix A describes the preparation method and the size distribution of bacterial cellulose nanocrystals.

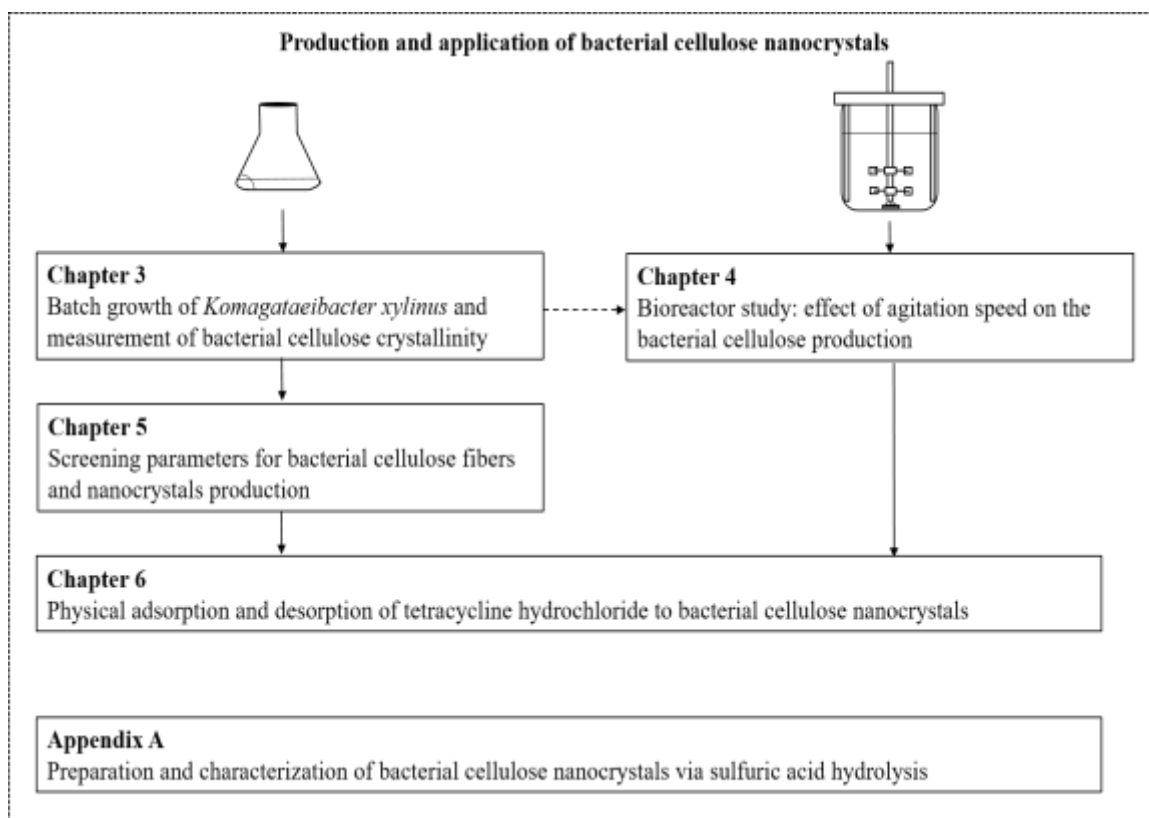


Figure 1.1 Research framework.

1.3 Research Contribution

Bacterial cellulose (BC) is highly crystalline and is free of lignin and hemicellulose. The unique properties along with the ease of modifying in-situ properties attract the wide interest of academic and industrial research communities. Determination of microbial kinetics is crucial for scale up studies of BC production in bioreactors. Dissolved oxygen and substrate availability play major role in the growth of bacterial cells, however, their measurement in-situ is difficult. Characterization of bacterial cellulose nanocrystals obtained via acid hydrolysis is essential to determine the potential applications. The main contributions of this research are:

- Determine the microbial kinetics growth of *Komagataeibacter xylinus* on fructose medium in a 3L stirred-tank bioreactor.
- Measurement of *in situ* oxygen uptake rate by *Komagataeibacter xylinus*.

- Investigate the relationship of BC production parameters on BCNs yield and surface properties.
- Size distribution of BCNs obtained via acid hydrolysis.
- The use of BCNs for the adsorption of TCH.

Chapter 2

2 Literature Review: Recent developments in the production and applications of bacterial cellulose fibers and nanocrystals

Information presented in this chapter has been slightly modified to fulfill formatting requirements. This chapter is based on the paper “Recent developments in the production and applications of bacterial cellulose fibers and nanocrystals”, published in *Critical Reviews in Biotechnology*, 2017, 37, 4, 510-524. (<http://dx.doi.org/10.1080/07388551.2016.1189871>).

2.1 Abstract

Cellulosic nanomaterials provide a novel and sustainable platform for the production of high performance materials enabled by nanotechnology. Bacterial cellulose (BC) is a highly crystalline material and contains pure cellulose without lignin and hemicellulose. BC offers an opportunity to provide control of the products’ properties in-situ, via specific BC production methods and culture conditions. The BC potential in advanced material applications are hindered by limited knowledge of optimal BC production conditions, efficient process scale-up, separation methods, and purification methods. There is a growing body of work on the production of bacterial cellulose nanocrystals (BCNs) from BC fibers; however, there is limited information on the effect of BC fibers’ characteristics on the production of nanocrystals. This review describes developments in BC and BCNs production methods and factors affecting their yield and physical characteristics.

2.2 Introduction

The current widespread interest in nanotechnology and nanomaterials promoted the growth of research in the cellulosic nanomaterials. As particle sizes decreases toward atomic scale, the properties of the materials are altered or enhanced, exhibiting new capabilities or

improvement for novel value-added materials. Bacterial cellulose (BC) has been gaining interest as it produces three-dimensional nanoporous fibers network with fibers diameter of approximately 30-50 nm (Tokoh et al., 1998), much thinner than plant cellulose. BC features a high purity without the presence of hemicellulose and lignin and its simple production and purification process make BC attractive. BC features a high crystallinity (up to 90%), a high degree of polymerization (up to 8000), biocompatibility, high surface area, superior mechanical properties (Young's modulus about 15-35 GPa and tensile strength of 200-300 MPa), and high-water content (Klemm et al., 2005, Klemm et al., 2006). The degree of crystallinity describes the relative amount of crystalline regions in the cellulose biopolymer and help to quantify changes in cellulose structure resulting from chemical, physicochemical, and biological treatments. The β -1,4-D-glucan chains in cellulose associate strongly via hydrogen bonding and are responsible for high degree of crystallinity and good mechanical stability of cellulose (Klemm et al., 2011, Son et al., 2003).

Bacterial cellulose (BC) is synthesized in highly crystalline form by many bacteria such as *Gluconacetobacter* (formerly *Acetobacter*), *Agrobacterium*, *Rhizobium*, and *Sarcina* with *Gluconacetobacter xylinus* being the most widely studied producer of extra-cellular pure cellulose (Ross et al., 1991). Table 2.1 shows the comparison criteria between plant-derived cellulose and BC fibers, which emphasizes the simplicity and advantageous method of producing cellulose using bacteria. Furthermore, depending on the cultivation methods, different shape of BC can be produced such as: membrane, pellets, or thin fibrous materials. BC properties can be easily modified after the bioprocess, for example by coating with polymers or chemicals (Lee et al., 2011, Oshima et al., 2011). These post-modification methods are similar to modification procedures employed for plant derived cellulose. However, the capability for in-situ properties modification of BC during bioprocess offers a great advantage over its counterpart. For example, BC can be molded in-situ during cultivation period allowing the formation of tubular shaped BC that can be used as a digestive tract and vascular grafts (Czaja et al., 2006, Bodin et al., 2007). Moreover, the morphology of BC can be controlled by changing the type of bacterial strains, addition of nutrients to medium, different methods and growing conditions, and post-processing drying methods (Gatenholm and Klemm, 2010). In addition, inclusion of

water soluble polymers in the liquid medium (e.g. carboxymethyl cellulose, sodium alginate, and agar alters the crystallinity, porosity and mechanical properties (Bae et al., 2004, Cheng et al., 2009, Zhou et al., 2007). Addition of particles, hydrophilic, or hydrophobic molecules to the fermentation medium alters the BC morphology by interfering with the cellulose crystallization and polymerization processes. The effect of different additives varied considerably, and in some cases the additives are not incorporated in BC while others lead to morphological change in the BC nanocomposites (Haigler et al., 1982).

Several reviews detail the history of cellulosic nanomaterials, their preparation methods, characterization, and applications (Habibi et al., 2010, Klemm et al., 2011, Klemm et al., 2006, Moon et al., 2011, Peng et al., 2011, Gatenholm and Klemm, 2010). Both plant and bacteria are versatile raw material that can exist in many morphological forms leading to different physicochemical properties. Cellulose microfibrils (CMF) achieved using mechanical treatment have different properties than cellulose nanocrystals (CN) obtained from acid hydrolysis, including specific physicochemical properties, high specific strength, and surface properties. Cellulose nanowhiskers (CNW) and nanocrystalline cellulose (NCC) are terms that are sometimes used interchangeably with CNs. With many capabilities and potentials, this BC fibers and nanocrystals are currently under intensive investigation for a broad range of applications. Several review papers describe BC's versatility for manufacturing strong and biorenewable nanocomposites (Blaker et al., 2011), as well as rapidly growing biocompatible materials for biomedical applications (Petersen and Gatenholm, 2011, Klemm et al., 2005, Klemm et al., 2006, Klemm et al., 2001, Czaja et al., 2006) and drug delivery system (Abeer et al., 2014). Furthermore, previous publications present comprehensive BC applications and patents on MFC, CNs, and BC (Lin et al., 2013, Charreau et al., 2013). Table 2.2 summarizes the BC applications, processing and highlights elucidating the different morphology of BC creates platforms for other applications.

Table 2.1 Comparison criteria for plant-derived cellulose and bacterial cellulose fiber

Criteria	Plant-derived cellulose	Bacteria-derived cellulose
Production time	Years, depending on tree species	Days, depending on bacterial species and growth rate
Growth conditions	Soil type, nutrients, climate conditions, and susceptible to insect pest infestation	Sugars used from agricultural and food processing wastes, controlled bioreactor conditions: pH, temperature, mixing, aeration, and nutrients
Composition	Mainly wood components: cellulose, lignin, hemicellulose	Pure cellulose produced after bacterial cells removal, no lignin or other components present
Energy requirement	Harvesting and transportation of logs, high temperature wood chipping, pulp processing, including lignin removal	Sterilization of nutrients and BC production equipment, including bioreactor used to produce pure cellulose
Processing steps	Multiple steps, involving different mechanical, physical, chemical, and size reduction processes	Main bioprocess steps involving sugars utilization bacterial cells, separation of fibers, and cells removal
Environmental impact	Pulp and paper mills still have serious problems regarding environmental impacts in solid waste, air and water pollution	Bioprocesses involve bacterial culture performed at mild temperatures and pressures with low level of solid, liquid, and air pollution
Process commercialization	Commercial process is established	Produced industrially and sold as food product called nata de coco. Several scale-up facilities produce BC membranes for biomedical devices/wound healing. More improved process is needed to facilitate high yield BC production in shorter time.

Table 2.2 Different applications of bacterial cellulose (BC) using different processing methods

Applications	BC processing	Highlight	References
<i>BC without chemical modification</i>			
Acoustic diaphragms	BC sheets are pressed between two steel plates	BC sheets with Young's Modulus reaching 30 GPa	(Nishi et al., 1990)
Artificial skin and blood vessels	Tubular shape of BC is cultivated in situ to mimic blood vessel shape	High mechanical strength in wet state, low roughness of the inner surface, high water retention	(Klemm et al., 2001)
Dietary food, thickening agent	Grown statically and in a bioreactor	High water retention, high thermal stability, able to prevent flow after melting	(Nakagaito et al., 2005, Okiyama et al., 1992, Okiyama et al., 1993)
Vascular graft	BC is grown at different oxygen concentrations on the top of silicon tubes and the BC tubes are composed of layers	Young's modulus (5MPa) is unaffected by the oxygen ratio Can produce branched tubes with unlimited length and inner diameters	(Bodin et al., 2007)
Support for cell immobilization	Yeast producing wine is immobilized using BC	BC-immobilized yeast has an increased metabolic activities and improved flavor by reducing volatile acid production	(Nguyen et al., 2009)
Barrier membrane for bone tissue regeneration	BC membrane is grown in static culture Cells are seeded on a BC and collagen membrane surfaces	Compared to collagen membrane, BC membrane has lower cell proliferation on the surface, shows significantly higher tensile strain, tensile stress, and Young's modulus	(Lee et al., 2015)
Cardiovascular tissues	BC suspensions are added with different concentrations of polyvinyl alcohol (PVA)	Similar mechanical properties with porcine aorta and aortic heart valves	(Millon and Wan, 2006)
Emulsions stabilizer	Varying concentrations of BC nanofibers are added to oil-in-water emulsions	Compared to HPMC and CMC emulsions, BC emulsions show largest droplet size and the highest stability in responds to changes in pH, temperature or ionic strength	(Paximada et al., 2016)
Drug delivery system	BC membrane is bounded with a model drug, serum albumin	Freeze dried BC shows lower uptake capacity than the wet native BC The biological activity and integrity of the proteins are maintained during loading and release processes	(Müller et al., 2013)
<i>BC with chemical modification</i>			
Scaffold for tissue engineering	BC sheets are phosphorylated and sulfated	High compressive modulus Supported proliferation of chondrocytes	(Svensson et al., 2005)
Protein adsorbent	BC membranes with different degrees of phosphorylation (Oshima et al., 2011) and carboxymethylation (Lin et al., 2015)	Adsorption quantity of proteins and zeta potentials increased with the increase of degree of substitution Phosphorylated bacterial cellulose has larger specific surface area and higher adsorption capacity of proteins than phosphorylated plant cellulose	(Lin et al., 2015, Oshima et al., 2011)
Reinforced composites (for	BC sheets are immersed in poly(L-lactic acid) (PLLA) dissolved in chloroform	Transparent films have two fold of tensile strength of pure PLLA and	(Kim et al., 2009)

display device and food packaging)		increased nanocomposites crystallinity	
Nanocomposite for biomedical application	BC sheets are soaked with chitosan dissolved in acetic acid solution	BC-chitosan composite shows an increased thermal stability, decreased the degree of crystallinity, and better cells adhesion better than pristine BC	(Kim et al., 2010)
Ion-conducting membrane for uses in batteries	BC is immersed in triethanolamine (TEA) aqueous solution	TEA is incorporated into bulk and BC surface facilitating aggregation of BC fibril High water retention and enhanced conductivity	(Salvi et al., 2014)
Antimicrobial packaging films, drug delivery	BC membranes are immersed in antibacterial molecules named nisin	Nisin is absorbed but does not physically bind to the BC membrane and nisin is released in a timely manner Nisin-containing BC films effectively inhibit growth of <i>Listeria monocytogenes</i>	(Nguyen et al., 2008)
<i>Impregnation</i>			
Optically transparent composite	BC sheets are impregnated with thermosetting resins such as epoxy and acrylic	BC shows a highly transparent membrane with a low thermal expansion, and an increased Young's Modulus by 5 times compared to engineered plastics	(Yano et al., 2005)
Antimicrobial films	BC membranes grown in different carbon sources are impregnated with silver nitrate (AgNO ₃) solution	Sucrose-derived BC membranes show smaller porosity and lower crystallinity compared to glucose and maltose-derived membrane	(Yang et al., 2012)
Nanocomposite membranes	BC nanofibers are incorporated with hydroxyapatite in a wet state	Does not cause inflammatory effect in soft tissue unlike plant derived cellulose Accelerates bone regeneration	(Saska et al., 2011)
<i>In-situ modification</i>			
Nanocomposite	BC is grown in medium added with different concentrations of polyethylene oxide (PEO)	Fine dispersed BC/PEO composites with lower crystallinity and melting point Thermal and mechanical properties depend on the composition and morphology	(Brown and Laborie, 2007)
Nanocomposite	Different concentrations of carboxymethyl cellulose (CMC) are added into the medium	CMC-altered BC shows a slightly reduced crystal size and degree of crystallinity The CMC addition increases thermal stability but decreases mechanical strength significantly	(Cheng et al., 2009)
Tablet excipient	In-situ fermentation of BC together with hydroxypropyl methylcellulose (HPMC)	Addition of HPMC decreases the degree of crystallinity, improves rehydration and small molecules absorption of the membranes	(Huang et al., 2011)
Nanocomposite for biomedical field and food packaging	Variable amount of hydrophobic polycaprolactone (PCL) powder is added to the BC culture medium	PCL is fully incorporated into the BC network and does not change the BC morphology Nanocomposite shows improved mechanical properties and thermal stability compared to pristine PCL	(Figueiredo et al., 2015)

Nanocomposite	HPMC and insoluble bioplastic poly-3-hydroxybutyrate (PHB) are added to the growth media	PHB is incorporated into the BC fibrils Semicrystalline PHB interferes with BC crystallization, thus, decreases the crystallinity of BC BC-PHB films have better mechanical properties than neat PHB	(Ruka et al., 2013)
<hr/>			
Bacterial cellulose nanocrystals			
Emulsions stabilizer	BC is hydrolyzed with hydrochloric acid (HCl) and sonicated Suspensions examined have various concentrations of bacterial cellulose nanocrystals (BCNs)	BCNs stabilize irreversibly an oil-in-water Pickering emulsions Results in monodispersed and deformable oil-in-water droplets around 4 μm in diameter	(Kalashnikova et al., 2011)
Edible and biodegradable food packaging	Wet BC is hydrolyzed with HCl and boiled for 4 hours Different concentrations of BCNs are added to gelatin solutions	Addition of BCNs to gelatin matrix reduces the moisture sorption and water vapor permeability, as well as increases the degradation temperature	(George and Siddaramaiah, 2012)
Nanocomposite	BC is hydrolyzed with sulfuric acid at different length of hydrolysis times	Produces rod shape cellulose I nanocrystals allomorph with aspect ratio ranging from 20 to 50 Longer hydrolysis times result in remarkable decrease of thermal stability and increase in crystallinity index	(Martínez-Sanz et al., 2011)

The physical properties of nanocrystals such as crystallite sizes, size distribution, and surface characteristics depend on the cellulose source and reaction conditions. Studies on the impact of production conditions on bacterial-synthesized nanocrystals or bacterial cellulose nanocrystals (BCNs) properties and its behaviors in different systems (e.g. nanocomposite, suspension and emulsion) supplement the use of BCNs for specific applications. Surface characteristics and behavior in suspension play a key role in many applications such as in the controlled release of drugs and proteins (Akhlaghi et al., 2013, Jackson et al., 2011, Wang and Roman, 2011, Akhlaghi et al., 2014). Suspensions with CNs have more stable viscosity profiles that are less susceptible to variations in temperature, pH, or ionic strength, compared to that of other water-soluble hydrocolloids used for viscosity enhancers owing to the fact that cellulose is insoluble in water (Mihrianyan et al., 2012). Furthermore, BC-emulsions show more stable emulsions against

those changes (Paximada et al., 2016). Although BCNs have many potentials for various applications, reports on processes with high BCNs yield and methods to control BCNs properties are very few. In order to push forward the feasibility of using BCNs in a large scale and exploit its potential benefits for adsorption based-drug delivery system, there must exist an economical way to produce the BC fibers while simultaneously, enhancing the understanding to control the properties of the produced BCNs.

A perusal of the research literature on BC revealed the need in several areas that require further investigation a) a new improved bacterial strain of *G. xylinus* that has high cellulose yield and rate of cell growth, b) formulation of low-cost growth media that maximizes cell growth and BC yield, c) development of novel bioreactor design that promotes on-line measurement and optimal control of pH, dissolved oxygen, and temperature to maximize BC productivity, d) development of a low-cost method for the downstream BC separation and purification, e) low-cost methods to produce BCNs with commercial interest and many potential applications.

There are ways to make BC-based applications more feasible and industrially attractive including firstly by improving BC fibers production yield and secondly by enhancing acid hydrolysis processes to control the BCNs characteristics (Figure 2.1). These two major objectives have been intensively researched, yet individually. Since cultivation methods not only affect the yield but also BC fibers morphology, they will also influence the BCNs properties. However, this area of study has not been explored in-depth previously. The ability to manipulate BCNs characteristics beginning at the bioprocessing level gives BC a clear advantage over plant-derived cellulose. This thesis chapter provides a summary of factors affecting the yield and structure of the produced BC and nanocrystals focusing on the opportunities of tailoring the BC nanocrystals structures and properties.

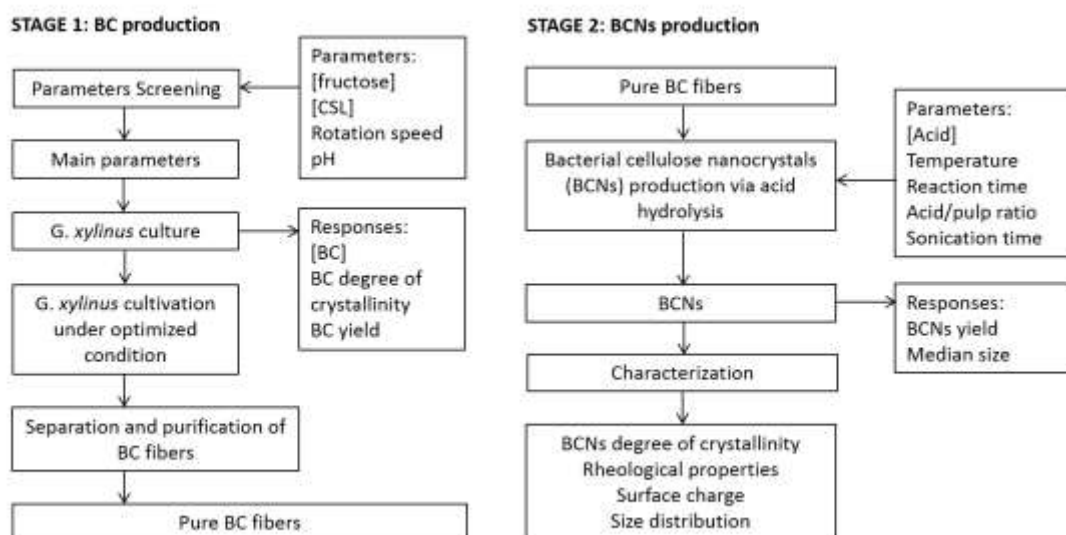


Figure 2.1 Schematic process flow diagram of bacterial cellulose (BC) and bacterial cellulose nanocrystals (BCNs) production.

2.3 Bacterial cellulose biosynthesis

BC biosynthesis, production, and applications have been reported in detail elsewhere (Chawla et al., 2009, Ross et al., 1991, Lin et al., 2013). Cellulose biosynthesis follows two steps: the first step involves the polymerization of β -1-4 glucan chains to cellulose and the second step involves cellulose chain assembly and crystallization. Figure 2.2 shows a schematic diagram of the *G. xylinus* cell and the BC biosynthesis (Lee et al., 2014). *In vivo* cellulose biosynthesis by *G. xylinus*, a rod shaped bacterium 0.5-0.7 μm in diameter and 1.2-2.2 μm in length (Rani et al., 2011), is investigated first using a dynamic process and monitored by darkfield light microscopy, which shows elongated microfibrillar ribbons attached to the bacteria cell surface (Brown et al., 1976). Cellulose microfibrils are synthesized inside the bacteria and extruded between the outer and cytoplasm membranes of the cell. These ribbons are composed of approximately 50 microfibrils in parallel with a width of 133 μm and are observed to grow only at the air-liquid interface at a rate of 2 $\mu\text{m}/\text{min}$.

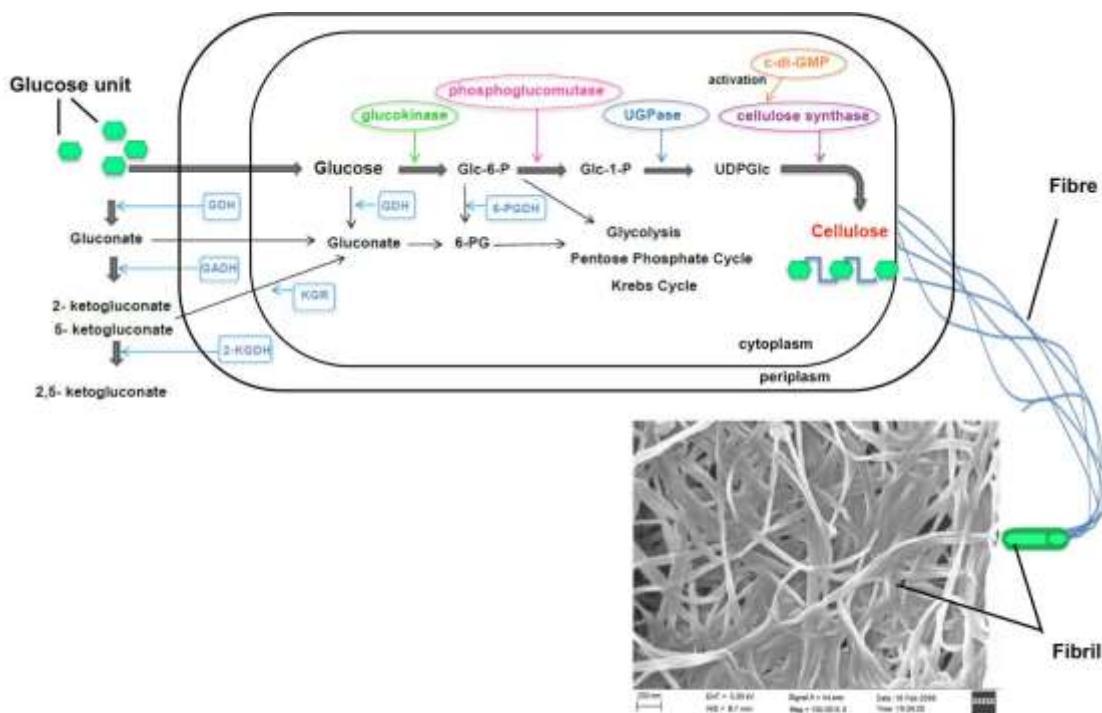


Figure 2.2 A schematic showing the major metabolic pathways of *A. xylinum* and the assembly of cellulose molecules into nanofibrils. Obtained from Lee et al. (Lee et al., 2014) with permission. Copyright, 2014, Wiley – VCH Verlag GmbH & Co. KGaA, Weinheim.

Cellulose-producing bacteria metabolize glucose via pentose-phosphate cycle or the Krebs cycle, depending on the physiological state of the cell coupled with gluconeogenesis (Ross et al., 1991). Cellulose biosynthesis is a multi-step reaction involving individual enzymes, catalytic complexes, and regulatory proteins. The four key enzymatic steps for glucose conversion to pure BC are: 1) the phosphorylation of glucose by glucokinase, 2) the isomerization of glucose-6-phosphate (Glc-6-P) to glucose-1-phosphate (Glc-1-P) by phosphoglucomutase, 3) the synthesis of uridine diphosphoglucose (UDPGlc) by UDPGlc-phyrophosphorylase(UGPase), and 4) the cellulose synthase reaction (Ross et al., 1991).

The cellulose synthesis immediate precursor is UDPGlc, which is produced in two steps from Glc-6-P. The cellulose synthase reaction is greatly enhanced by novel cyclic dinucleotide molecules cyclic diguanylic acid (c-di-GMP). In the absence of c-di-GMP, cellulose synthase stays inactive or exhibits low enzyme activity. Cellulose synthesis

occurs when glucose is polymerized into a β -1,4 glucan chain that combines with other chains to form the ribbon-like structure of cellulose, which protrudes from the cell as self-woven fibrils (Chawla et al., 2009, Tokoh et al., 1998). The aggregates of self-aligned β -1,4 glucan chains form insoluble layered sheets reinforced by dispersion forces between their stack heterocyclic rings and promote a high degree of crystallinity (Ross et al., 1991). Polymerization and crystallization are cell-directed, coupled processes, and the rate of crystallization determines the polymerization rate (Haigler et al., 1982). This coupling needs to occur for the biosynthesis of crystalline cellulose I.

The cellulose biosynthesis process is complex and not fully understood. Bacteria produce cellulose via a protein complex consisting of at least three subunits (bcsA, bcsB, bcsC) (Ross et al., 1991). The first subunit is the first gene in the operon encoded by bcsA (bacterial cellulose synthesis). The second subunit, encoded bcsB, is the c-di-GMP binding protein. Both bcsA and bcsB are often fused into single polypeptides and are essential for cellulose synthesis. bcsC is required for cellulose synthesis *in vivo* but not *in vitro*. The most recent study describes the molecular mechanism by which BC synthesis is regulated (Morgan et al., 2013). Morgan *et al.* (Morgan *et al.*, 2013) presented a crystal structure of bcsA and bcsB forming a complex with a translocating polysaccharide. This structure revealed more details on the architecture of cellulose synthase and demonstrates how a bcsA complex forms a cellulose-conducting channel to extend the cellulose chain, one glucose molecule at a time (Morgan et al., 2013).

In static culture, the cellulose pellicle forms at the air-liquid interface after two days of incubation and eventually becomes thicker over time. It is speculated that BC is formed as a self-defense mechanism to protect bacteria from the damaging effects of UV light (Williams and Cannon, 1989) or to help bacteria float at the air-liquid interface in order to secure sufficient oxygen supply (Schramm and Hestrin, 1954). Moreover, mutations of cellulose-producing bacteria have been previously reported, especially when cultivated under agitation (Valla and Kjosbakken, 1982). Schramm and Hestrin (Hestrin and Schramm, 1954) noted that *G. xylinus* wild-type (Cel⁺) mutated spontaneously to non-cellulose producing mutants (Cel⁻) when sub-cultured repeatedly. Unlike the wild type, Cel⁻ mutants lack UDPGlc-pyrophosphorylase (Ross et al., 1991) and produce water-

soluble polysaccharides identified as acetan (Chao et al., 2000). Strain selection and process optimization were investigated to improve BC production. *G. xylinus subsp. sucrofermentans* (BPR2001) (ATTC# 700178) was reported to produce a significantly higher BC yield under agitation conditions compared to other strains studied (Toyosaki et al., 1995). Since then, many studies were conducted to understand the BC production process by this strain (Bae and Shoda, 2004, Bae and Shoda, 2005a, Bae et al., 2004, Bae and Shoda, 2005b, Chao et al., 2000, Joseph et al., 2003, Kouda et al., 1997, Kouda et al., 1996).

2.4 Effects of culture media composition on BC production

Design of the culture medium is one of the key factors affecting the growth of microorganisms and BC yield. Two main media components vital for growth are the carbon and nitrogen sources. Various carbon sources including monosaccharides, oligosaccharides, organic acids, and alcohols have been proposed to increase BC production (Masaoka et al., 1993, Son et al., 2003). BC production strongly depends on the initial concentration of sugar in the medium. Bacteria grown in glucose media form the by-product gluconic acid (Bae and Shoda, 2004, Naritomi et al., 1998a, Naritomi et al., 1998b, Masaoka et al., 1993), which decreases the pH of the media and reduces BC production. The highest BC yield was obtained with glucose concentration between 1.5-2% (w/w) (Son et al., 2003). Ruka *et al.* (2012) studied the BC yield grown in different culture media and reported that the highest yield of BC was achieved using the media described by Zhou (Zhou et al., 2007) and Yamanaka (Yamanaka et al., 1989), both of which had high carbon source concentration. Media described by Son et al. (2003) was added with 2 % (v/v) of corn steep liquor (CSL) and it was found effective in BC production, despite its low carbon source concentration. CSL is a liquid by-product of corn wet milling that is rich in amino acids, minerals, and other vitamins. Various nitrogen sources were studied to assess the effects on BC production, using yeast extract concentration of 0.5% to 2%, polypeptone, CSL, and other nitrogen sources (Jung et al., 2010a). BC production was highest in the medium with yeast extract, followed by polypeptone and CSL (Son et al., 2001).

The cost of fermentation media accounts for the majority of the total process cost and several studies have been devoted to finding new low-cost production process. The ability of *Cel*⁺ to metabolize a variety of carbon and nitrogen sources (Mikkelsen et al., 2009, Moon et al., 2006, Zeng et al., 2011b), including agricultural waste (Carreira et al., 2011, Castro et al., 2011, Dahman et al., 2010, Jung et al., 2010b, Keshk et al., 2006, Moosavi-Nasab and Yousefi, 2011, Rani et al., 2011), food waste (Song et al., 2009, Moon et al., 2006), and CSL (Chao et al., 2001b, Naritomi et al., 1998a, Naritomi et al., 1998b, Toyosaki et al., 1995), provides an opportunity to lower production costs and promotes environmental sustainability.

The addition of substances to the cultivation media, such as, ethanol (Park et al., 2004, Son et al., 2001), polyacrylamide-co-acrylic acid (Joseph et al., 2003), carboxymethyl cellulose (Cheng et al., 2009), sodium alginate (Zhou et al., 2007), and agar (Bae and Shoda, 2005a) has been reported to improve the BC yield. Ethanol is utilized as an energy source for ATP generation when used as the main carbon source for BC production (Naritomi et al., 1998a). The addition of water-soluble polysaccharides increase the broth viscosity and facilitates dispersion of BC pellets, thereby increasing the amount of free cells that can accelerate the consumption of sugar and BC production (Bae and Shoda, 2005a, Ishida et al., 2003, Zhou et al., 2007).

Table 2.3 shows the BC yield, carbon sources, nitrogen sources, and production rates reported in the research literature. The conventional method of static culture is not adaptable to mass production since it requires a long cultivation time and a large facility (Czaja et al., 2006). This has led to an effort to increase BC production rate and BC production yield through medium optimization, cultivation methods variation, and additional substance for increased BC production activity (Lu et al., 2011). Genetic engineering geared towards improving bacterial strains is a promising method to enhance BC production, which has been covered in detail elsewhere.

Table 2.3 Bacterial cellulose production under different culture conditions

Strain	Bioreactor Type	Carbon and Nitrogen Source	BC Production (g/L)	BC production rate (g/L.h)	References
<i>G. xylinus</i> ATTC 53524	Static flask	Fructose*	2.81	0.03	(Mikkelsen et al., 2009)
<i>G. hansenii</i> UAC 09	Static flask	Glucose*	1.76	0.01	(Rani et al., 2011)
<i>G. xylinus</i> ATTC 700178	Shaken flask	Fructose – CSL	5.65	0.03	(Dahman et al., 2010)
<i>G. xylinus</i> ATTC 700178	Shaken flask	Agricultural wastes – CSL	5.2	0.03	(Dahman et al., 2010)
<i>A. xylinum</i> BPR2001	Shaken flask	Fructose – CSL	2.7	0.02	(Joseph et al., 2003)
<i>Acetobacter</i> sp. V6	Shaken flask	Glucose*	4.16	0.02	(Son et al., 2003)
<i>A. xylinum</i> BPR2001	1-L jar fermentor	Fructose – CSL	7.7	0.11	(Toyosaki et al., 1995)
<i>A. xylinum</i> BPR3001A	3-L jar fermentor	Fructose – CSL	8	0.22	(Naritomi et al., 1998b)
<i>A. xylinum</i> BPR2001	10-L jar fermenter	Fructose – CSL	8	0.11	(Bae et al., 2004)
<i>A. xylinum</i> BRC5	10-L jar fermenter	Glucose – CSL	15.3	0.31	(Hwang et al., 1999)
<i>A. xylinum</i> BPR2001	10-L jar fermenter	Molasses – CSL	5.3	0.07	(Bae and Shoda, 2005b)
<i>A. xylinum</i> BPR2001	50-L internal loop airlift	Fructose – CSL	6.4	0.13	(Chao et al., 2001a)
<i>G. xylinus</i> BPR2001	Modified air-lift with net plates	Glucose*	2.6	0.03	(Wu and Li, 2015)
<i>G. xylinus</i> KJ1	10-L and 50-L air lift-type bubble column	Saccharified food wastes (SFW)	5.0-5.8	0.07-0.08	(Song et al., 2009)
<i>Gluconacetobacter</i> sp. RKY5	Rotating disk bioreactor	Glucose*	5.7	0.06	(Kim et al., 2007)

*Nitrogen sources: peptone and yeast extract.

2.5 Effects of culture media composition and BC production conditions on BC physical properties

In order to make BC more competitive in the market, there is a need to improve BC production with a minimum negative impact on BC fibers' properties. The cellulose I structure has two polymorphs, a triclinic structure (I_α) and a monoclinic structure (I_β), with the I_α/I_β ratio varying depending on the source. BC is typically cellulose I with I_α as a dominant polymorph. Moon *et al.* (Moon et al., 2011) described the difference between these polymorphs and the importance of hydrogen bonding within the I_α and I_β structures with respect to cellulose properties.

The BC degree of crystallinity refers to the fraction of the ordered molecules (crystalline regions) with respect to the less ordered molecules (amorphous regions) in the polymer chain. X-ray diffraction methods (XRD) while it is a powerful analytical method for fingerprint characterization of crystalline materials and their structure determination, the results have to be analyzed cautiously since measurement and peak fitting methods will variably affect the reported degree of crystallinity (Park et al., 2010). The most commonly used method, peak height comparison, results in a higher degree of crystallinity compared to other methods.

BC produced from different carbon sources had similar molecular and microscopic properties, with all samples exhibiting similar degrees of crystallinity between 80 and 90% and having identical ratios of cellulose allomorph (I_α/I_β) as revealed by NMR spectroscopy (Mikkelsen et al., 2009). Different media resulted in BC with similar crystallite size and cellulose I_α content, ranging from 68 to 79% (Ruka et al., 2012). Jung *et al.* (Jung et al., 2010b) reported that the degree of crystallinity of BC grown in shake flasks using glucose and molasses media were 83% and 67%, respectively, showing that medium composition altered the structural arrangement at the molecular level.

Addition of sodium alginate and mannan to the growth medium interrupted hydrogen bonding and reduced the degree of crystallinity. BC grown in medium with sodium alginate showed a smaller crystallite size and a lower degree of crystallinity of 59% compared to 78% in control medium (Zhou et al., 2007). Mannan caused a reduction of cellulose I_α peak

intensity which decreased the cellulose I_{α}/I_{β} ratio (Tokoh et al., 1998). Similar phenomenon was also observed when BC was grown in agroindustrial wastes where other polysaccharides are typically present (Castro et al., 2011). This indicated that the presence of the aforementioned substances altered cellulose crystallization process and affected the aggregation of cellulose chains.

Moreover, BC culturing methods play role in affecting cellulose I_{α} peak intensity and crystallite size. Agitation interfered with microfibrils crystallization process favoring the formation of smaller crystallite sizes and lower degree of crystallinity (Czaja et al., 2004). Measured using Segal's peak intensity method (Segal et al., 1959), Moon *et al.* (Moon et al., 2006) reported that the degree of crystallinity of BC was 84.1% when grown in static culture, 86.5% in air circulated culture, and the lowest of 51.2% in shaken culture. Lower degree of crystallinity translated to a reduced BC mechanical property. BC grown in a static culture exhibited a tensile strength of 92 MPa compared to 22 MPa for BC cultivated in a rotating disk bioreactor (Krystynowicz et al., 2002). While making efforts to improve the BC yield, it is important to also consider the impact of these cultivation conditions on the physical properties of BC.

2.6 Effects of bioprocess parameters on BC production

Stirred tank bioreactors provide better control of the cultivation environment by allowing on-line measurement and control of pH, temperature, agitation, and level of dissolved oxygen (DO). Microorganisms quickly adapt to changes in these factors by altering their protein synthesis and changing their cell morphology. Optimum pH for cell growth and BC production depends on bacterial strain and is usually between 4.0 and 7.0. An initial pH of 4.0 and 5.0 resulted in high BC production rate and bacterial growth (Verschuren et al., 2000, Hwang et al., 1999). When the pH was allowed to change naturally from 4.0 to 5.0 through the consumption of gluconic acid by the cells, the BC yield was 5.89 g/L, which was 1.5 fold higher than that of the 4.1 g/L yield at constant pH 5.0.

BC cultivated in a rotating disk bioreactor without pH control produces substantially higher BC yield and cell concentration than the pH-controlled bioreactor (Kim et al., 2007). Culture broth in the rotating disk bioreactor is almost static, creating poor mixing of acid

and/or alkali used to adjust the pH and causing an inhibitory effect. While BC can be produced over a wide range of pH, the degree of crystallinity is independent of the culture medium pH (Zeng et al., 2011b).

Aeration conditions directly influence the DO, amount of oxygen dissolved in the medium, which is crucial for cell growth and BC production. High DO concentration in growth medium increases the gluconic acid concentration that reduces the BC production. However, DO limitation impedes bacterial growth and BC production. Hwang *et al.* (Hwang et al., 1999) studied the effect of DO concentration from 2 to 15% saturation in fed-batch culture and reported 10% saturation of DO generated the highest BC concentration reaching 15.3 g/L compared to 10.2 g/L with 2% DO concentration. In another study, the DO concentration in a 10-L jar fermenter was varied from 20 to 40% of saturation concentration with two turbines by an automatic change of the agitation speed (Bae and Shoda, 2005a). The optimal DO concentration for BC production was 30% and was higher than previously reported (Hwang et al., 1999), which was attributed to the presence of agar in the medium.

In addition to pH and DO, temperature control was found to be important for BC production and crystalline structure. BC production at different temperatures, ranging from 20 to 40°C for *Acetobacter sp.* A9 under shaken conditions showed 30°C as the optimum temperature (Son et al., 2001). Furthermore, Hirai *et al.* (Hirai et al., 1997) reported that *A. xylinum* (ATCC 23769) produced BC with a band shape comprising of cellulose II when cultured at 4°C, and with twisting ribbons of cellulose I when cultured at 28°C. Other studies confirmed this finding when the production temperature was between 25 and 30°C (Zeng et al., 2011a). At 4°C, cell movement was limited and extrusion of band material was in the direction perpendicular to their longitudinal axis. In contrast, at room temperature, cells moved at a steady rate of 2 µm/min and rotated around their longitudinal axis producing elongated ribbons (Brown et al., 1976). According to Hirai *et al.* (Hirai et al., 1997), bacterial cell movement determined if cellulose crystallized as cellulose I or cellulose II. The exact mechanisms and conditions regarding the formation of cellulose I and cellulose II are not well understood.

2.7 Separation and purification of BC from broth

Centrifugation and washing are two important purification steps in separation of BC from the broth containing remaining nutrients. The resulting pellets are thoroughly washed and boiled with a dilute alkali solution such as sodium hydroxide (NaOH) or potassium hydroxide (KOH) to lyse the cells. After NaOH treatment, BC pellicles are repeatedly washed with distilled water. Although alkali treatment lyses bacterial cells almost completely, a fraction of cell debris is still embedded in the BC fibers (Rani et al., 2011). Solutions to debris entrapment can include 1) applying a more stringent NaOH treatment conditions, 2) adding several distilled water wash cycles, and 3) subjecting BC to ultrasound treatment. This impurity removal by dilute NaOH solution also increases the BC mechanical properties. BC sheets treated with 2.5 wt.% NaOH solution rated twice as high on Young's modulus compared to untreated sheets (Gea et al., 2011). Dilute 0.1 N NaOH did not significantly affect tensile strain or Young's modulus of BC harvested at different cultivation periods (McKenna et al., 2009); however, a concentration of NaOH solution above 6% causes deformation and shrinkage (Nishi et al., 1990). Alkali treatment using concentrated NaOH solutions damages BC microfibrils, modifies their mechanical properties (McKenna et al., 2009), and may transform cellulose I to cellulose II in prolonged treatment periods (Shibazaki et al., 1997).

2.8 Production of cellulose nanocrystals (CNs)

CNs are generally produced by a two-step process: 1) initial hydrolysis to remove the amorphous regions of the cellulosic materials, and 2) breaking the aggregation of nanocrystals. Although acid hydrolysis is the most commonly used method to produce rod-shaped CNs, other methods demonstrate the capability to extract CNs from cellulosic materials. The cellulose source and the degree of crystallinity influence the size distribution of the liberated CNs. For example, cotton, wood, and MCC yield a narrow distribution of highly crystalline (90%) nanocrystals, while bacteria, algae, and tunicin generate nanocrystals with larger polydispersities and dimensions (Klemm et al., 2011) (Table 2.4).

Table 2.4 Physical characteristics of cellulose nanocrystal (CNs) from different sources

Sources	Length (nm)	Width (nm)	References
bacteria	100–1000	10–50	(Araki and Kuga, 2001)
	855*	17*	(Kalashnikova et al., 2011)
	30–50	6–10	(Tokoh et al., 1998)
	1450 ± 407	28 ± 9	(Martínez-Sanz et al., 2011)
	1103 ± 698	14 ± 7.4	(Sacui et al., 2014)
	290 ± 130	20 ± 5	(George and Siddaramaiah, 2012)
wood	100–150	4–5	(Beck-Candanedo et al., 2005)
	90 ± 10	8 ± 1	(Boluk et al., 2012)
	130 ± 67	5.9 ± 1.8	(Sacui et al., 2014)
	149 ± 40	9 ± 2	(Han et al., 2013)
cotton	25–320	6–70	(Elazzouzi-Hafraoui et al., 2008)
	40–300	8–44	(Ureña-Benavides et al., 2011)
tunicate	1073	28	(Elazzouzi-Hafraoui et al., 2008)
	1187 ± 1066	9.4 ± 5.0	(Sacui et al., 2014)
MCC	35–265	3–48	(Elazzouzi-Hafraoui et al., 2008)
	200–400	10	(Bondeson et al., 2006)

Nano-enabled performance and CNs applications depend on the nanocrystals' size, thus controlling the process that allows for CNs with narrow size distribution is important. All CNs production methods reduce the amorphous region, thus increasing the degree of crystallinity. The following section describes several BCNs production methods using acid hydrolysis, oxidation, enzymatic hydrolysis and ionic liquids. Some of these methods have

only been applied to CNs production, however, these methods can also be used for BCNs production.

2.8.1 Acid hydrolysis

Cellulosic nanomaterials are typically prepared by subjecting them to a strong acid under strict control of agitation, temperature, and hydrolysis time. Differing hydrolysis conditions and cellulose sources generate diverse CNs morphologies. The acid cleavage of the glycosidic bonds is attributed to differences in the kinetics of hydrolysis between amorphous and crystalline regions (Habibi et al., 2010). The hydronium ions preferentially penetrate the loosely bundled, disordered amorphous domain instead of the tightly packed crystalline region (de Souza Lima and Borsali, 2004).

Then, the resulted suspension is diluted with water to quench the hydrolysis reaction. After several washes and centrifugations, the turbid supernatant is dialyzed against distilled water to remove acids, centrifuged and sonicated. CNs neutralization involves an ion exchange process, and this is an important process as it assists in CNs dispersibility in water (Beck et al., 2012). CNs preparations commonly utilize sulfuric acid or hydrochloric acid. Hydrolysis treatment using sulfuric acid generates rod-like CNs with negative charge surface acid groups ($\text{OSO}_3^-/\text{H}^+$), while hydrochloric acid generates neutral CNs and limits their dispersion ability. These charged groups induce the electrostatic stabilization of nanocrystals in aqueous medium and promote an impeccable homogeneous dispersion. The anionic group on the surface of CNs produced by sulfuric acid is a sulfate ester, and this surface charge is sufficient to have a stable colloidal dispersion in water (Habibi et al., 2010).

Although cellulose sources significantly affect the properties of CNs, there are a few common parameters influencing the properties of CNs such as hydrolysis time, temperature, type of acid, acid concentration, and ratio of acid to substrate. Table 2.5 summarizes CNs production and properties from various acid hydrolysis treatment conditions. Acid hydrolysis induces a rapid decrease in its degree of polymerization (DP), down to the so-called level-off DP (LODP) (Habibi et al., 2010). At prolonged hydrolysis times, DP decreases much slower. The LODP value depends on cellulose origin with

typical values of 140 to 250 recorded for hydrolyzed wood pulp and cotton, and up to 10,000 for BC. The acid hydrolysis of bacterial, tunicate, *Valonia*, or cotton results in a higher polydispersity in the molecular weight, without evidence of LODP; perhaps because these cellulosic materials feature no regular amorphous region distribution. Phosphoric acid hydrolysis increases the degree of crystallinity of BCNs by 10% from 75% for the untreated to 85% for the treated one and produced BCNs with narrower size distribution and lower water retention capability (Amin et al., 2014).

While methodical study for BCNs is not readily available, CNs have been extensively studied and can help elucidate some parameters that influence the properties and yield of BCNs. Beck-Candanedo *et al.* (Beck-Candanedo et al., 2005) reported the effects of reaction time on CNs suspension properties. Prolonged hydrolysis time digested the cellulose completely and broke it down to its component sugar molecules; while a too short reaction time yielded aggregates and non-dispersible fibers with wide size distribution. Hydrolysis time of 45 min resulted in a smaller mean particle length of 120 ± 5 nm than the 141 ± 6 nm length achieved by 25 min reaction time. Longer hydrolysis time led to a narrower and smaller polydispersity in size distribution.

While high acid concentration and long hydrolysis treatment duration produce short cellulose crystals and promote uniform dispersion (Elazzouzi-Hafraoui et al., 2008), they reduce the nanocrystals yield. The CNs' yield ranged between 21% and 38% with a degree of crystallinity greater than 80% from acid hydrolyzed softwood kraft pulp (Hamad and Hu, 2010). Another method, determining the yield from the mass loss during hydrolysis, resulted in a significantly higher yield of 78% for BCNs (Winter et al., 2010). There is little information available on the effect of acid concentration and hydrolysis treatment on the yield of BCNs. Yield determination from different extraction processes needs a standardized method in order to provide a fair comparison.

Table 2.5. Summary of acid hydrolysis conditions for the production of cellulose nanocrystals

Source	Temperature (°C)	Reaction time	Acid, w/w %	Acid/pulp (ml/g)	Yield (%)	Degree of crystallinity	References
BC	70	30 min	65 % H ₂ SO ₄	-	-	-	(Araki and Kuga, 2001)
BC	70	2 h	2.5 M HCl	-	78	-	(Winter et al., 2010)
BC	50	2 h	55.4% H ₂ SO ₄	80 - 100	-	79.1 ± .4	(Martínez-Sanz et al., 2011)
	50	48 h	55.4% H ₂ SO ₄	80 -100	-	90.3 ±0.8	
MCC	45	60 min	64 % H ₂ SO ₄	8.75	43.5	-	(Dong et al., 1998)
MCC	44	130.3 min	63.5 % H ₂ SO ₄	10.2	40.35	-	(Bondeson et al., 2006)
MCC	Room temperature	24 h	Distilled water	300	-	81	(Li et al., 2012)
				300	-	73	
Softwood	65	25 min	40% H ₂ SO ₄	8.75	87.4	84	(Hamad and Hu, 2010)
	65		64		32.9	83.8	
	85		40		69.7	85.7	
	85		64		20.9	82.6	

*BC: Bacterial cellulose, MCC: microcrystalline cellulose, H₂SO₄: sulfuric acid.

Generally, sulfuric acid treatment, even at short reaction times, decreases cellulosic materials' thermal stability considerably. However, a combination of both sulfuric and hydrochloric acids during hydrolysis steps results in spherical CNs, which demonstrates better thermal stability than the rod CNs counterpart, likely due to fewer sulfate groups on its surface (Habibi et al., 2010). Storage and handling of CNs suspensions are important factors in bringing CNs applications forward. Different methods of drying (never dried,

air-drying, spray-drying, and freeze drying) have shown to affect the properties of CNs and BCNs (Amin et al., 2014, Beck et al., 2012). Dispersibility in water and low aggregation of dried CNs are desirable features. The neutralization increases CNs and BCNs dispersibility in water giving colloidal CNs suspensions having similar properties to suspensions prior to the drying step (Beck et al., 2012). Acid hydrolysis treatment provides an economical process to produce BCNs but a better understanding to control the end-product properties and enhance the process yield are still necessary.

2.8.2 Oxidation

While most research on CNs has focused on the product of sulfuric acid hydrolysis, CNs have also been prepared by oxidation with strong oxidants such as ammonium persulfate (Leung et al., 2011, Castro-Guerrero and Gray, 2014). Persulfate oxidation led to the creation of CNs by dissolving lignin, hemicellulose, and other impurities in a one-pot procedure reducing many rigorous steps in the production of CNs from biomass (Male et al., 2012). The results were CNs stabilized with surface carboxyl group instead of sulfate esters produced by sulfuric acid hydrolysis. Free radicals and hydrogen peroxide from the oxidation penetrated the amorphous regions and cleaved the β -1,4 linkage to form CNs. Leung *et al.* (Leung et al., 2011) reported that persulfate oxidation defibrillated cellulose and removed amorphous regions effectively, creating CNs with a narrow size distribution.

Another oxidative method used to prepare cellulosic nanomaterials is 2,2,6,6-tetramethylpiperidine-1-oxyl (TEMPO)-mediated oxidation, which selectively oxidizes primary alcohols. TEMPO-mediated oxidation produces carboxylated CNs that is stable and well dispersed in aqueous suspension (Qin et al., 2011). The degree of crystallinity of cellulose influences the degree of oxidation by TEMPO. Although application of TEMPO without prior acid treatment successfully defibrillates cellulose, it does not completely break down amorphous regions (Leung et al., 2011). These oxidation methods are more commonly applied to modify the surface of BC and wood fiber; however, these two methods can produce BCNs and CNs in combination with other methods.

2.8.3 Enzymatic hydrolysis

Enzymatic hydrolysis of cellulose is a multi-step heterogeneous reaction in which cellulose is broken down by a complex of enzymes: endoglucanase, cellobiohydrolase, and cellobiase that work synergistically (Satyamurthy et al., 2011). Fungi, especially *Trichoderma*, *Aspergillus*, and *Penicillium* species, produce commercial cellulases (Chen et al., 2012). The filamentous fungus *Trichoderma reesei* (*T. reesei*) is one of the most efficient producers of extracellular cellulase enzyme and is currently the cellulase of choice for CNs production (Satyamurthy et al., 2011).

The enzymatic process is affected by the surface area of the cellulose substrate, reaction temperature, concentration of the enzyme, and duration of enzyme activity (George et al., 2011). The rate of enzymatic hydrolysis is higher at higher enzyme concentrations because of the expected increase of enzyme adsorption on to the cellulose fibrils. CNs derived from enzymatic hydrolysis using cellulase produced by *T. reesei* were shorter (120 nm) compared to those hydrolyzed by sulfuric acid (287 nm) (Satyamurthy et al., 2011). Enzymatic treatment of 12 h produced BCNs 100 to 300 nm in length and 10 to 15 nm in diameter (George et al., 2011). Enzyme treated BCNs showed better thermal and mechanical properties than the sulfuric acid processed BCNs, even with addition of low concentration of BCNs (George et al., 2011). Cellulose I_α of BC is preferentially hydrolyzed by the enzymes than cellulose I_β (Kafle et al., 2015). The degree of crystallinity of cellulose had been considered as one of the factors affecting the rate of enzymatic hydrolysis, however, a recent study concluded the opposite (Kafle et al., 2015). This study reported that the degree of crystallinity, degree of polymerization, and meso-scale packing of cellulose did not correlate with the decrease in hydrolysis rate.

Although enzyme hydrolysis performed on BC fibers is able to digest cellulose and transform it to glucose, the treated BC fibers show interwoven, long and thin nanofibers instead of cellulose nanocrystals (Ioelovich, 2014). In other study, cellobiohydrolase I and II showed a synergy in promoting a processive and an endo attack, corresponding to ribbon thinning and ribbon cutting, respectively (Boisset et al., 2000). Furthermore, since enzyme hydrolysis is a complex process, a combination of enzymes can potentially increase the digestion of BC to produce shorter BCNs.

2.8.4 Ionic Liquids

Ionic liquids (ILs) are a group of salts composed of an anion and a cation, where one or both are bulky ions that exist in a liquid state and exhibit low melting temperatures (<100°C). ILs have received interest as cellulose solvents and have been studied extensively for lignocellulosic biomass biorefining, polysaccharide dissolution, and cellulosic fibers preparation (Gericke et al., 2012). While the ability of ILs to dissolve biomass has been published, there are few publications on cellulose hydrolysis using ILs. In fact, several studies have reported using ILs to produce CNs from microcrystalline cellulose (MCC), (Man et al., 2011), and this method may also be applied to BC.

Cellulose is insoluble in water and it is hypothesized that cellulose solubility is dependent on the breaking of the cellulose-cellulose hydrogen bonds. However, Lindman *et al.* (Lindman et al., 2010) reasoned that since cellulose was significantly amphiphilic, the low solubility in water could be attributed to hydrophobic interactions. A few ILs that dissolved cellulose have been described in detail elsewhere (Isik et al., 2014). Among these ILs formed by a 1-butyl-3-methylimidazolium cation with different anions such as halogenides or phosphate based anions have shown to be effective.

A one-stage hydrolysis of MCC using 1-butyl-3-methylimidazolium hydrogen sulfate (bmimHSO₄) resulted in high CNs yield (48±2%) (Mao et al., 2013). The IL treated samples retained their cellulose I structure and increased their degree of crystallinity from 77% to 91% (Man et al., 2011). Moreover, the ILs treatment removed the amorphous regions of cellulose, indicated by the increase of degree of crystallinity with both temperature and treatment time. However, the treatments did not cause dissolution of microcrystalline cellulose. The treated CNs featured a needle-like shape with dimensions of 50-300 nm in length and a diameter approximately 13-21 nm (Man et al., 2011).

Although ILs' recycling is possible, a small amount of impurities affected its physical and chemical properties, including melting point, viscosity, conductivity, polarity, and reaction rates (Gericke et al., 2012). For example, the presence of water in 1-butyl-3-methylimidazolium chloride (bmimCl) decreases the cellulose's solubility through competitive hydrogen-bonding to the cellulose microfibrils (Swatloski et al., 2002).

Gericke *et al.* (Gericke et al., 2012) reviewed the difficulties, drawbacks, and the future prospects for IL-based solvents for commercial cellulose processing. The use of IL in the cellulose dissolution process is another method to produce functionalized cellulose derivatives and CNs. However, efficient and commercially viable IL-based processes for BCNs are not yet developed.

2.9 Challenges

BC has been extensively explored as an innovative framework material for many applications. However, these efforts have been done to increase the BC production rate and the BC production yield. Several approaches to improve BC fiber production yield include genetic engineering, media optimization, varying cultivation parameters, and using different types of bioreactors. While these approaches have been successful to increase the BC yield, the applied cultivation conditions, such as different sugar, agitation rate, and bioreactor type also affected the cellulose fibrils arrangement at a molecular level. Depending on the desired applications, cellulose crystallinity may not be as crucial. For example, for the use of BC as a bioadsorbent for the adsorption of metal or drug, cellulose crystallinity is not as important as compared to BC used as a reinforcing material for nanocomposite.

Furthermore, investigations of cellulose nanocrystals synthesized by bacteria has shown a focus mostly in the characterization of BCNs and applicability of BCNs as a functional material. However, these two research topics: producing BC and characterizing BCNs were done separately, thus, missing the opportunity to explore the possibility to modify the surface properties of BCNs by altering BC cultivation conditions. Currently, there is no study relating BC cultivation conditions to the yield and surface characteristics of BCNs after acid hydrolysis treatment.

Polymers have been widely used in the pharmaceutical industry and recently, natural polymers, such as cellulose and chitosan have been explored for design and development of novel pharmaceutical carriers. These natural polymers offer advantages such as low cost, biocompatibility, biodegradability, non-toxicity, and surface functionalities making them excellent candidates for drug carriers. Surface properties are important in the adsorption

mechanism by electrostatic force. Few adsorption studies have been performed using plant derived CNs and currently, there is no available drug adsorption study done using BCNs. Tetracycline hydrochloride (TCH) is a common antibiotic to treat ulcers and periodontal infection. TCH is a water soluble drug and is pH dependent due to possible protonation and deprotonation action in its functional groups. These attributes make TCH a candidate for model drug adsorption study on BCNs.

Another significant parameter that influences the application of BCNs is the size of nanocrystals. Size of nanocrystals varies due to different cellulose sources, processing methods, and acid hydrolysis conditions. Presently, the ability to consistently producing homogeneous BCNs size is a challenge. Innovation to improve BCNs process and to control BCNs properties is required to offer a robust and functional framework to appeal the interest of industries.

In the literature, there is no study on the impact of BC crystallinity on the yield of BCNs. CNs obtained from wood pulp have a controlled nanocrystal size and properties specification compared to BCNs obtained from BC. However, BCNs offer some flexibility to generate nanocrystals with longer length or different property specification.

A comprehensive study starting from the beginning of the BC synthesis to the application of BCNs is necessary to elaborate on the process resulting in high BCN yield and the potential of modifying surface properties of BCNs.

2.10 Conclusions

Although BC offers a broad spectrum of applications for many industries, BC's inefficient production technology currently limits its economic feasibility. Conservation of BC's most advantageous properties, such as its high degree of crystallinity and yield, necessitates careful production and purification conditions. BC modification can be executed in-situ by bioreactor selection, agitation vigor, and addition of soluble polymers. Low BC yield caused by mutations that transform cell producing cellulose to non-producing cellulose sometimes overrides efforts to shorten BC production times. Moreover, it is possible to tailor BC properties by selection of BC production methods and implementation of BCNs

production methods to achieve desired properties. More information about the effect of different BC fibers characteristics on the produced BCNs is required in order to have a better understanding on how to control the BCNs properties. Furthermore, meeting the growing demand of BC and BCNs as well as increasing its economic feasibility requires further development of robust industrial production, standardization for characterization methods, and manufacturing infrastructure that would allow for greater control on the properties.

2.11 References

- Abeer, M. M., Mohd Amin, M. C. I. & Martin, C. 2014. A review of bacterial cellulose-based drug delivery systems: their biochemistry, current approaches and future prospects. *Journal of Pharmacy and Pharmacology*, 66, 1047-1061.
- Akhlaghi, S., Berry, R. & Tam, K. 2013. Surface modification of cellulose nanocrystal with chitosan oligosaccharide for drug delivery applications. *Cellulose*, 20, 1747-1764.
- Akhlaghi, S. P., Tiong, D., Berry, R. M. & Tam, K. C. 2014. Comparative release studies of two cationic model drugs from different cellulose nanocrystal derivatives. *European Journal of Pharmaceutics and Biopharmaceutics*, 88, 207-215.
- Amin, M. C. I. M., Abadi, A. G. & Katas, H. 2014. Purification, characterization and comparative studies of spray-dried bacterial cellulose microparticles. *Carbohydrate Polymers*, 99, 180-189.
- Araki, J. & Kuga, S. 2001. Effect of Trace Electrolyte on Liquid Crystal Type of Cellulose Microcrystals. *Langmuir : the ACS journal of surfaces and colloids*, 17, 4493-4496.
- Bae, S. & Shoda, M. 2004. Bacterial cellulose production by fed-batch fermentation in molasses medium. *Biotechnology progress*, 20, 1366-71.
- Bae, S. & Shoda, M. 2005a. Statistical optimization of culture conditions for bacterial cellulose production using Box-Behnken design. *Biotechnology and bioengineering*, 90, 20-8.
- Bae, S., Sugano, Y. & Shoda, M. 2004. Improvement of bacterial cellulose production by addition of agar in a jar fermentor. *Journal of bioscience and bioengineering*, 97, 33-8.
- Bae, S. O. & Shoda, M. 2005b. Production of bacterial cellulose by *Acetobacter xylinum* BPR2001 using molasses medium in a jar fermentor. *Applied microbiology and biotechnology*, 67, 45-51.

- Beck-Candanedo, S., Roman, M. & Gray, D. G. 2005. Effect of reaction conditions on the properties and behavior of wood cellulose nanocrystal suspensions. *Biomacromolecules*, 6, 1048-1054.
- Beck, S., Bouchard, J. & Berry, R. 2012. Dispersibility in Water of Dried Nanocrystalline Cellulose. *Biomacromolecules*, 13, 1486-1494.
- Blaker, J. J., Lee, K.-Y. & Bismarck, A. 2011. Hierarchical Composites Made Entirely from Renewable Resources. *Journal of Biobased Materials and Bioenergy*, 5, 1-16.
- Bodin, A., Bäckdahl, H., Fink, H., Gustafsson, L., Risberg, B. & Gatenholm, P. 2007. Influence of cultivation conditions on mechanical and morphological properties of bacterial cellulose tubes. *Biotechnology and bioengineering*, 97, 425-434.
- Boisset, C., Fraschini, C., Schülein, M., Henrissat, B. & Chanzy, H. 2000. Imaging the Enzymatic Digestion of Bacterial Cellulose Ribbons Reveals the Endo Character of the Cellobiohydrolase Cel6A from *Humicola insolens* and Its Mode of Synergy with Cellobiohydrolase Cel7A. *Applied and Environmental Microbiology*, 66, 1444-1452.
- Boluk, Y., Zhao, L. & Incani, V. 2012. Dispersions of nanocrystalline cellulose in aqueous polymer solutions: Structure formation of colloidal rods. *Langmuir*, 28, 6114-6123.
- Bondeson, D., Mathew, A. & Oksman, K. 2006. Optimization of the isolation of nanocrystals from microcrystalline cellulose by acid hydrolysis. *Cellulose*, 13, 171-180.
- Brown, E. E. & Laborie, M.-P. G. 2007. Bioengineering bacterial cellulose/poly(ethylene oxide) nanocomposites. *Biomacromolecules*, 8, 3074-3081.
- Brown, R. M., Willison, J. H. M. & Richardson, C. L. 1976. Cellulose biosynthesis in *Acetobacter xylinum*: Visualization of the site of synthesis and direct measurement of the in vivo process*. *Cell Biology*, 73, 4565-4569.
- Carreira, P., Mendes, J. a. S., Trovatti, E., Serafim, L. S., Freire, C. S. R., Silvestre, A. J. D. & Neto, C. P. 2011. Utilization of residues from agro-forest industries in the production of high value bacterial cellulose. *Bioresource technology*, 102, 7354-7360.
- Castro-Guerrero, C. & Gray, D. 2014. Chiral nematic phase formation by aqueous suspensions of cellulose nanocrystals prepared by oxidation with ammonium persulfate. *Cellulose*, 21, 2567-2577.
- Castro, C., Zuluaga, R., Putaux, J.-L., Caro, G., Mondragon, I. & Gañán, P. 2011. Structural characterization of bacterial cellulose produced by *Gluconacetobacter swingsii* sp. from Colombian agroindustrial wastes. *Carbohydrate Polymers*, 84, 96-102.

- Chao, Y., Ishida, T., Sugano, Y. & Shoda, M. 2000. Bacterial cellulose production by *Acetobacter xylinum* in a 50-L internal-loop airlift reactor. *Biotechnology and bioengineering*, 68, 345-52.
- Chao, Y., Mitarai, M., Sugano, Y. & Shoda, M. 2001a. Effect of addition of water-soluble polysaccharides on bacterial cellulose production in a 50-L airlift reactor. *Biotechnology progress*, 17, 781-5.
- Chao, Y., Sugano, Y. & Shoda, M. 2001b. Bacterial cellulose production under oxygen-enriched air at different fructose concentrations in a 50-liter, internal-loop airlift reactor. *Applied microbiology and biotechnology*, 55, 673-9.
- Charreau, H., Foresti, M. L. & Vasquez, A. 2013. *Nanocellulose patents trends: A comprehensive review on patents on cellulose nanocrystals, microfibrillated and bacterial cellulose*, Bentham Science Publishers.
- Chawla, P. R., Bajaj, I. B., Survase, S. A. & Singhal, R. S. 2009. Microbial cellulose: Fermentative production and applications. *Food Technology and Biotechnology*, 47, 107-124.
- Chen, X., Deng, X., Shen, W. & Jiang, L. 2012. Controlled enzymolysis preparation of nanocrystalline cellulose from pretreated cotton fibers. *BioResources*, 7.
- Cheng, K.-C., Catchmark, J. M. & Demirci, A. 2009. Effect of different additives on bacterial cellulose production by *Acetobacter xylinum* and analysis of material property. *Cellulose*, 16, 1033-1045.
- Czaja, W., Romanovicz, D. & Brown, R. M. 2004. Structural investigations of microbial cellulose produced in stationary and agitated culture. *Cellulose*, 11, 403-411.
- Czaja, W. K., Young, D. J., Kawecki, M. & Brown, R. M. 2006. The future prospects of microbial cellulose in biomedical applications. *Biomacromolecules*, 8, 1-12.
- Dahman, Y., Jayasuriya, K. & Kalis, M. 2010. Potential of biocellulose nanofibers production from agricultural renewable resources: preliminary study. *Applied Biochemistry and Biotechnology*, 162, 1647-1659.
- De Souza Lima, M. M. & Borsali, R. 2004. Rodlike cellulose microcrystals: Structure, properties, and applications. *Macromolecular Rapid Communications*, 25, 771-787.
- Dong, X. M., Revol, J.-F. & Gray, D. G. 1998. Effect of microcrystallite preparation conditions on the formation of colloid crystals of cellulose. *Cellulose*, 5, 19-32.
- Elazzouzi-Hafraoui, S., Nishiyama, Y., Putaux, J.-L., Heux, L., Dubreuil, F. & Rochas, C. 2008. The shape and size distribution of crystalline nanoparticles prepared by acid hydrolysis of native cellulose. *Biomacromolecules*, 9, 57-65.

- Figueiredo, A. R. P., Silvestre, A. J. D., Neto, C. P. & Freire, C. S. R. 2015. In situ synthesis of bacterial cellulose/polycaprolactone blends for hot pressing nanocomposite films production. *Carbohydrate Polymers*, 132, 400-408.
- Gatenholm, P. & Klemm, D. 2010. Bacterial Nanocellulose as a Renewable Material for Biomedical Applications. *MRS Bulletin*, 35, 208-213.
- Gea, S., Reynolds, C. T., Roohpour, N., Wirjosentono, B., Soykeabkaew, N., Bilotti, E. & Peijs, T. 2011. Investigation into the structural, morphological, mechanical and thermal behaviour of bacterial cellulose after a two-step purification process. *Bioresource technology*, 102, 9105-9110.
- George, J., Ramana, K. V., Bawa, A. S. & Siddaramaiah 2011. Bacterial cellulose nanocrystals exhibiting high thermal stability and their polymer nanocomposites. *International Journal of Biological Macromolecules*, 48, 50-57.
- George, J. & Siddaramaiah 2012. High performance edible nanocomposite films containing bacterial cellulose nanocrystals. *Carbohydrate Polymers*, 87, 2031+.
- Gericke, M., Fardim, P. & Heinze, T. 2012. Ionic liquids — promising but challenging solvents for homogeneous derivatization of cellulose. *Molecules*, 17, 7458-7502.
- Habibi, Y., Lucia, L. A. & Rojas, O. J. 2010. Cellulose nanocrystals: chemistry, self-assembly, and applications. *Chemical Reviews*, 110, 3479-3500.
- Haigler, C. H., White, A. R., Brown, R. M. & Cooper, K. M. 1982. Alteration of in vivo cellulose ribbon assembly by carboxymethylcellulose and other cellulose derivatives. *Journal of Cell Biology*, 94, 64-69.
- Hamad, W. Y. & Hu, T. Q. 2010. Structure–process–yield interrelations in nanocrystalline cellulose extraction. *Canadian Journal of Chemical Engineering*, 88, 392-402.
- Han, J., Zhou, C., Wu, Y., Liu, F. & Wu, Q. 2013. Self-Assembling Behavior of Cellulose Nanoparticles during Freeze-Drying: Effect of Suspension Concentration, Particle Size, Crystal Structure, and Surface Charge. *Biomacromolecules*, 14, 1529-1540.
- Hestrin, S. & Schramm, M. 1954. Synthesis of cellulose by *Acetobacter xylinum*. II. Preparation of freeze-dried cells capable of polymerizing glucose to cellulose. *Biochemical Journal*, 58, 345-52.
- Hirai, A., Tsuji, M. & Horii, F. 1997. COMMUNICATION: Culture conditions producing structure entities composed of Cellulose I and II in bacterial cellulose. *Cellulose*, 4, 239-245.
- Huang, H.-C., Chen, L.-C., Lin, S.-B. & Chen, H.-H. 2011. Nano-biomaterials application: In situ modification of bacterial cellulose structure by adding HPMC during fermentation. *Carbohydrate Polymers*, 83, 979-987.

- Hwang, J. W., Yang, Y. K., Hwang, J. K., Pyun, Y. R. & Kim, Y. S. 1999. Effects of pH and dissolved oxygen on cellulose production by *Acetobacter xylinum* BRC5 in agitated culture. *Journal of Bioscience and Bioengineering*, 88, 183-188.
- Ioelovich, M. 2014. Study of enzymatic hydrolysis of bacterial nanocellulose. *American Journal of BioScience*, 2, 13-16.
- Ishida, T., Mitarai, M., Sugano, Y. & Shoda, M. 2003. Role of water-soluble polysaccharides in bacterial cellulose production. *Biotechnology and bioengineering*, 83, 474-478.
- Isik, M., Sardon, H. & Mecerreyes, D. 2014. Ionic Liquids and Cellulose: Dissolution, Chemical Modification and Preparation of New Cellulosic Materials. *International Journal of Molecular Sciences*, 15, 11922-11940.
- Jackson, J. K., Letchford, K., Wasserman, B. Z., Ye, L., Hamad, W. & Burt, H. M. 2011. The use of nanocrystalline cellulose for the binding and controlled release of drugs. *International Journal of Nanomedicine*, 6, 321-330.
- Joseph, G., Rowe, G. E., Margaritis, A. & Wan, W. 2003. Effects of polyacrylamide-co-acrylic acid on cellulose production by *Acetobacter xylinum*. *Journal of Chemical Technology and Biotechnology*, 78, 964-970.
- Jung, H.-I., Jeong, J.-H., Lee, O. M., Park, G.-T., Kim, K.-K., Park, H.-C., Lee, S.-M., Kim, Y.-G. & Son, H.-J. 2010a. Influence of glycerol on production and structural-physical properties of cellulose from *Acetobacter sp.* V6 cultured in shake flasks. *Bioresource technology*, 101, 3602-3608.
- Jung, H.-I., Lee, O. M., Jeong, J.-H., Jeon, Y.-D., Park, K.-H., Kim, H.-S., An, W.-G. & Son, H.-J. 2010b. Production and characterization of cellulose by *Acetobacter sp.* V6 using a cost-effective molasses-corn steep liquor medium. *Applied Biochemistry and Biotechnology*, 162, 486-497.
- Kafle, K., Shin, H., Lee, C. M., Park, S. & Kim, S. H. 2015. Progressive structural changes of Avicel, bleached softwood, and bacterial cellulose during enzymatic hydrolysis. *Scientific Reports*, 5, 15102.
- Kalashnikova, I., Bizot, H., Cathala, B. & Capron, I. 2011. New Pickering emulsions stabilized by bacterial cellulose nanocrystals. *Langmuir*, 27, 7471-7479.
- Keshk, S. M. a. S., Razek, T. M. A. & Sameshima, K. 2006. Bacterial cellulose production from beet molasses. *African Journal of Biotechnology*, 5, 1519-1523.
- Kim, J., Cai, Z., Lee, H. S., Choi, G. S., Lee, D. H. & Jo, C. 2010. Preparation and characterization of a Bacterial cellulose/Chitosan composite for potential biomedical application. *Journal of Polymer Research*, 18, 739-744.

- Kim, Y.-J., Kim, J.-N., Wee, Y.-J., Park, D.-H. & Ryu, H.-W. 2007. Bacterial cellulose production by *Gluconacetobacter* sp. PKY5 in a rotary biofilm contactor. *Applied Biochemistry and Biotechnology*, 137-140, 529-537.
- Kim, Y., Jung, R., Kim, H.-S. & Jin, H.-J. 2009. Transparent nanocomposites prepared by incorporating microbial nanofibrils into poly(l-lactic acid). *Current Applied Physics*, 9, S69-S71.
- Klemm, D., Heublein, B., Fink, H.-P. & Bohn, A. 2005. Cellulose: Fascinating biopolymer and sustainable raw material. *Angewandte Chemie International Edition*, 44, 3358-3393.
- Klemm, D., Kramer, F., Moritz, S., Lindström, T., Ankerfors, M., Gray, D. & Dorris, A. 2011. Nanocelluloses: A new family of nature-based materials. *Angewandte Chemie (International Edition)*, 50, 5438-5466.
- Klemm, D., Schumann, D., Kramer, F., Heßler, N., Hornung, M., Schmauder, H.-P. & Marsch, S. 2006. Nanocelluloses as innovative polymers in research and application. In: KLEMM, D. (ed.) *Polysaccharides II*. Springer Berlin Heidelberg.
- Klemm, D., Schumann, D., Udhardt, U. & Marsch, S. 2001. Bacterial synthesized cellulose — artificial blood vessels for microsurgery. *Progress in Polymer Science*, 26, 1561-1603.
- Kouda, T., Yano, H. & Yoshinaga, F. 1997. Effect of agitator configuration on bacterial cellulose productivity in aerated and agitated culture. *Journal of Fermentation and Bioengineering*, 83, 371-376.
- Kouda, T., Yano, H., Yoshinaga, F., Kaminoyama, M. & Kamiwano, M. 1996. Characterization of non-newtonian behavior during mixing of bacterial cellulose in a bioreactor. *Journal of Fermentation and Bioengineering*, 82, 382-386.
- Krystynowicz, A., Czaja, W., Wiktorowska-Jeziarska, A., Gonçalves-Miśkiewicz, M., Turkiewicz, M. & Bielecki, S. 2002. Factors affecting the yield and properties of bacterial cellulose. *Journal of Industrial Microbiology and Biotechnology*, 29, 189-195.
- Lee, K.-Y., Buldum, G., Mantalaris, A. & Bismarck, A. 2014. More than meets the eye in bacterial cellulose: Biosynthesis, bioprocessing, and applications in advanced fiber composites. *Macromolecular Bioscience*, 14, 10-32.
- Lee, K.-Y., Quero, F., Blaker, J., Hill, C. S., Eichhorn, S. & Bismarck, A. 2011. Surface only modification of bacterial cellulose nanofibres with organic acids. *Cellulose*, 18, 595-605.
- Lee, S.-H., Lim, Y.-M., Jeong, S. I., An, S.-J., Kang, S.-S., Jeong, C.-M. & Huh, J.-B. 2015. The effect of bacterial cellulose membrane compared with collagen

- membrane on guided bone regeneration. *The Journal of Advanced Prosthodontics*, 7, 484-495.
- Leung, A. C. W., Hrapovic, S., Lam, E., Liu, Y., Male, K. B., Mahmoud, K. A. & Luong, J. H. T. 2011. Characteristics and Properties of Carboxylated Cellulose Nanocrystals Prepared from a Novel One-Step Procedure. *Small*, 7, 302-305.
- Li, W., Yue, J. & Liu, S. 2012. Preparation of nanocrystalline cellulose via ultrasound and its reinforcement capability for poly(vinyl alcohol) composites. *Ultrasonics Sonochemistry*, 19, 479-485.
- Lin, Q., Zheng, Y., Wang, G. & Shi, X. 2015. Protein adsorption behaviors of carboxymethylated bacterial cellulose membranes. *International journal of biological macromolecules*, 73, 264-269.
- Lin, S.-P., Loira Calvar, I., Catchmark, J., Liu, J.-R., Demirci, A. & Cheng, K.-C. 2013. Biosynthesis, production and applications of bacterial cellulose. *Cellulose*, 20, 2191-2219.
- Lindman, B., Karlström, G. & Stigsson, L. 2010. On the mechanism of dissolution of cellulose. *Journal of Molecular Liquids*, 156, 76-81.
- Lu, Z., Zhang, Y., Chi, Y., Xu, N., Yao, W. & Sun, B. 2011. Effects of alcohols on bacterial cellulose production by *Acetobacter xylinum* 186. *World Journal of Microbiology and Biotechnology*, 27, 2281-2285.
- Male, K. B., Leung, A. C. W., Montes, J., Kamen, A. & Luong, J. H. T. 2012. Probing inhibitory effects of nanocrystalline cellulose: inhibition versus surface charge. *Nanoscale*, 4, 1373-1379.
- Man, Z., Muhammad, N., Sarwono, A., Bustam, M., Vignesh Kumar, M. & Rafiq, S. 2011. Preparation of Cellulose Nanocrystals Using an Ionic Liquid. *Journal of Polymers and the Environment*, 19, 726-731.
- Mao, J., Osorio-Madrado, A. & Laborie, M.-P. 2013. Preparation of cellulose I nanowhiskers with a mildly acidic aqueous ionic liquid: reaction efficiency and whiskers attributes. *Cellulose*, 20, 1829-1840.
- Martínez-Sanz, M., Lopez-Rubio, A. & Lagaron, J. M. 2011. Optimization of the nanofabrication by acid hydrolysis of bacterial cellulose nanowhiskers. *Carbohydrate Polymers*, 85, 228-236.
- Masaoka, S., Ohe, T. & Sakota, N. 1993. Production of cellulose from glucose by *Acetobacter xylinum*. *Journal of Fermentation and Bioengineering*, 75, 18-22.
- Mckenna, B., Mikkelsen, D., Wehr, J., Gidley, M. & Menzies, N. 2009. Mechanical and structural properties of native and alkali-treated bacterial cellulose produced by *Gluconacetobacter xylinus* strain ATCC 53524. *Cellulose*, 16, 1047-1055.

- Mihranyan, A., Ferraz, N. & Strømme, M. 2012. Current status and future prospects of nanotechnology in cosmetics. *Progress in Materials Science*, 57, 875-910.
- Mikkelsen, D., Flanagan, B. M., Dykes, G. A. & Gidley, M. J. 2009. Influence of different carbon sources on bacterial cellulose production by *Gluconacetobacter xylinus* strain ATCC 53524. *Journal of Applied Microbiology*, 107, 576-583.
- Millon, L. E. & Wan, W. K. 2006. The polyvinyl alcohol–bacterial cellulose system as a new nanocomposite for biomedical applications. *Journal of Biomedical Materials Research Part B: Applied Biomaterials*, 79B, 245-253.
- Moon, R. J., Martini, A., Nairn, J., Simonsen, J. & Youngblood, J. 2011. Cellulose nanomaterials review: structure, properties and nanocomposites. *Chemical Society Reviews*, 40, 3941-3994.
- Moon, S.-H., Park, J.-M., Chun, H.-Y. & Kim, S.-J. 2006. Comparisons of physical properties of bacterial celluloses produced in different culture conditions using saccharified food wastes. *Biotechnology and Bioprocess Engineering*, 11, 26-31.
- Moosavi-Nasab, M. & Yousefi, A. 2011. Biotechnological production of cellulose by *Gluconacetobacter xylinus* from agricultural waste. *Iran J Biotechnol*, 9, 94-101.
- Morgan, J. L. W., Strumillo, J. & Zimmer, J. 2013. Crystallographic snapshot of cellulose synthesis and membrane translocation. *Nature*, 493, 181-186.
- Müller, A., Ni, Z., Hessler, N., Wesarg, F., Müller, F. A., Kralisch, D. & Fischer, D. 2013. The biopolymer bacterial nanocellulose as drug delivery system: Investigation of drug loading and release using the model protein albumin. *Journal of Pharmaceutical Sciences*, 102, 579-592.
- Nakagaito, A. N., Iwamoto, S. & Yano, H. 2005. Bacterial cellulose: the ultimate nanoscalar cellulose morphology for the production of high-strength composites. *Applied Physics A: Materials Science & Processing*, 80, 93-97.
- Naritomi, T., Kouda, T., Yano, H. & Yoshinaga, F. 1998a. Effect of ethanol on bacterial cellulose production from fructose in continuous culture. *Journal of Fermentation and Bioengineering*, 85, 598-603.
- Naritomi, T., Kouda, T., Yano, H. & Yoshinaga, F. 1998b. Effect of lactate on bacterial cellulose production from fructose in continuous culture. *Journal of Fermentation and Bioengineering*, 85, 89-95.
- Nguyen, D. N., Ton, N. M. N. & Le, V. V. M. 2009. Optimization of *Saccharomyces cerevisiae* immobilization in bacterial cellulose by ‘adsorption- incubation’ method. *International Food Research Journal*, 16, 59-64.

- Nguyen, V. T., Gidley, M. J. & Dykes, G. A. 2008. Potential of a nisin-containing bacterial cellulose film to inhibit *Listeria monocytogenes* on processed meats. *Food Microbiology*, 25, 471-478.
- Nishi, Y., Uryu, M., Yamanaka, S., Watanabe, K., Kitamura, N., Iguchi, M. & Mitsuhashi, S. 1990. The structure and mechanical properties of sheets prepared from bacterial cellulose. *Journal of Materials Science*, 25, 2997-3001.
- Okiyama, A., Motoki, M. & Yamanaka, S. 1992. Bacterial cellulose II. Processing of the gelatinous cellulose for food materials. *Food Hydrocolloids*, 6, 479-487.
- Okiyama, A., Motoki, M. & Yamanaka, S. 1993. Bacterial cellulose IV. Application to processed foods. *Food Hydrocolloids*, 6, 503-511.
- Oshima, T., Taguchi, S., Ohe, K. & Baba, Y. 2011. Phosphorylated bacterial cellulose for adsorption of proteins. *Carbohydrate Polymers*, 83, 953-958.
- Park, J., Hyun, S. & Jung, J. 2004. Conversion of *G. hansenii* PJK into non-cellulose-producing mutants according to the culture condition. *Biotechnology and Bioprocess Engineering*, 9, 383-388.
- Park, S., Baker, J. O., Himmel, M. E., Parilla, P. A. & Johnson, D. K. 2010. Cellulose crystallinity index: measurement techniques and their impact on interpreting cellulase performance. *Biotechnology for Biofuels*, 3, 10-10.
- Paximada, P., Tsouko, E., Kopsahelis, N., Koutinas, A. A. & Mandala, I. 2016. Bacterial cellulose as stabilizer of o/w emulsions. *Food Hydrocolloids*, 53, 225-232.
- Peng, B. L., Dhar, N., Liu, H. L. & Tam, K. C. 2011. Chemistry and applications of nanocrystalline cellulose and its derivatives: A nanotechnology perspective. *The Canadian Journal of Chemical Engineering*, 89, 1191-1206.
- Petersen, N. & Gatenholm, P. 2011. Bacterial cellulose-based materials and medical devices: current state and perspectives. *Applied Microbiology and Biotechnology*, 91, 1277-1286.
- Qin, Z.-Y., Tong, G., Chin, Y. C. F. & Zhou, J.-C. 2011. *Preparation of ultrasonic-assisted high carboxylate content cellulose nanocrystals by TEMPO oxidation*, BioResources.
- Rani, M. U., Udayasankar, K. & Appaiah, K. a. A. 2011. Properties of bacterial cellulose produced in grape medium by native isolate *Gluconacetobacter sp.* *Journal of Applied Polymer Science*, 120, 2835-2841.
- Ross, P., Mayer, R. & Benziman, M. 1991. Cellulose biosynthesis and function in bacteria. *Microbiological Reviews*, 55, 35-58.

- Ruka, D. R., Simon, G. P. & Dean, K. M. 2012. Altering the growth conditions of *Gluconacetobacter xylinus* to maximize the yield of bacterial cellulose. *Carbohydrate Polymers*, 89, 613-622.
- Ruka, D. R., Simon, G. P. & Dean, K. M. 2013. In situ modifications to bacterial cellulose with the water insoluble polymer poly-3-hydroxybutyrate. *Carbohydrate Polymers*, 92, 1717-1723.
- Sacui, I. A., Nieuwendaal, R. C., Burnett, D. J., Stranick, S. J., Jorfi, M., Weder, C., Foster, E. J., Olsson, R. T. & Gilman, J. W. 2014. Comparison of the Properties of Cellulose Nanocrystals and Cellulose Nanofibrils Isolated from Bacteria, Tunicate, and Wood Processed Using Acid, Enzymatic, Mechanical, and Oxidative Methods. *ACS Applied Materials & Interfaces*, 6, 6127-6138.
- Salvi, D. T. B., Barud, H. S., Pawlicka, A., Mattos, R. I., Raphael, E., Messaddeq, Y. & Ribeiro, S. J. L. 2014. Bacterial cellulose/triethanolamine based ion-conducting membranes. *Cellulose*, 21, 1975-1985.
- Saska, S., Barud, H. S., Gaspar, A. M. M., Marchetto, R., Ribeiro, S. J. L. & Messaddeq, Y. 2011. Bacterial Cellulose-Hydroxyapatite Nanocomposites for Bone Regeneration. *International Journal of Biomaterials*, 2011.
- Satyamurthy, P., Jain, P., Balasubramanya, R. H. & Vigneshwaran, N. 2011. Preparation and characterization of cellulose nanowhiskers from cotton fibres by controlled microbial hydrolysis. *Carbohydrate Polymers*, 83, 122-129.
- Schramm, M. & Hestrin, S. 1954. Factors affecting production of cellulose at the air/liquid interface of a culture of *Acetobacter xylinum*. *Journal of General Microbiology*, 11, 123-9.
- Segal, L., Creely, J. J., Martin, A. E. & Conrad, C. M. 1959. An Empirical Method for Estimating the Degree of Crystallinity of Native Cellulose Using the X-Ray Diffractometer. *Textile Research Journal*, 29, 786-794.
- Shibazaki, H., Kuga, S. & Okano, T. 1997. Mercerization and acid hydrolysis of bacterial cellulose. *Cellulose*, 4, 75-87.
- Son, H. J., Heo, M. S., Kim, Y. G. & Lee, S. J. 2001. Optimization of fermentation conditions for the production of bacterial cellulose by a newly isolated *Acetobacter sp.* A9 in shaking cultures. *Biotechnology and applied biochemistry*, 33, 1-5.
- Son, H. J., Kim, H. G., Kim, K. K., Kim, H. S., Kim, Y. G. & Lee, S. J. 2003. Increased production of bacterial cellulose by *Acetobacter sp.* V6 in synthetic media under shaking culture conditions. *Bioresource technology*, 86, 215-9.
- Song, H.-J., Li, H., Seo, J.-H., Kim, M.-J. & Kim, S.-J. 2009. Pilot-scale production of bacterial cellulose by a spherical type bubble column bioreactor using saccharified food wastes. *Korean Journal of Chemical Engineering*, 26, 141-146.

- Svensson, A., Nicklasson, E., Harrah, T., Panilaitis, B., Kaplan, D. L., Brittberg, M. & Gatenholm, P. 2005. Bacterial cellulose as a potential scaffold for tissue engineering of cartilage. *Biomaterials*, 26, 419-431.
- Swatloski, R. P., Spear, S. K., Holbrey, J. D. & Rogers, R. D. 2002. Dissolution of cellulose with ionic liquids. *Journal of the American Chemical Society*, 124, 4974-4975.
- Tokoh, C., Takabe, K., Fujita, M. & Saiki, H. 1998. Cellulose synthesized by *Acetobacter xylinum* in the presence of acetyl glucomannan. *Cellulose*, 5, 249-261.
- Toyosaki, H., Naritomi, T., Seto, A., Matsuoka, M., Tsuchida, T. & Yoshinaga, F. 1995. Screening of bacterial cellulose-producing *Acetobacter* strains suitable for agitated culture. *Bioscience, Biotechnology, and Biochemistry*, 59, 1498-1502.
- Ureña-Benavides, E. E., Ao, G., Davis, V. A. & Kitchens, C. L. 2011. Rheology and Phase Behavior of Lyotropic Cellulose Nanocrystal Suspensions. *Macromolecules*, 44, 8990-8998.
- Valla, A. & Kjosbakken 1982. Cellulose-negative Mutants of *Acetobacter xylinum*. *Journal of General Microbiology*, 128, 1401-1408.
- Verschuren, P. G., Cardona, T. D., Nout, M. J. R., De Gooijer, K. D. & Van Den Heuvel, J. C. 2000. Location and limitation of cellulose production by *Acetobacter xylinum* established from oxygen profiles. *Journal of bioscience and bioengineering*, 89, 414-419.
- Wang, H. & Roman, M. 2011. Formation and Properties of Chitosan–Cellulose Nanocrystal Polyelectrolyte–Macroion Complexes for Drug Delivery Applications. *Biomacromolecules*, 12, 1585-1593.
- Williams, W. S. & Cannon, R. E. 1989. Alternative environmental roles for cellulose produced by *Acetobacter xylinum*. *Applied and Environmental Microbiology*, 5, 2448-2452.
- Winter, H. T., Cerclier, C., Delorme, N., Bizot, H., Quemener, B. & Cathala, B. 2010. Improved colloidal stability of bacterial cellulose nanocrystal suspensions for the elaboration of spin-coated cellulose-based model surfaces. *Biomacromolecules*, 11, 3144-3151.
- Wu, S.-C. & Li, M.-H. 2015. Production of bacterial cellulose membranes in a modified airlift bioreactor by *Gluconacetobacter xylinus*. *Journal of bioscience and bioengineering*, 120, 444-449.
- Yamanaka, S., Watanabe, K., Kitamura, N., Iguchi, M., Mitsunashi, S., Nishi, Y. & Uryu, M. 1989. The structure and mechanical properties of sheets prepared from bacterial cellulose. *Journal of Materials Science*, 24, 3141-3145.

- Yang, G., Xie, J., Hong, F., Cao, Z. & Yang, X. 2012. Antimicrobial activity of silver nanoparticle impregnated bacterial cellulose membrane: Effect of fermentation carbon sources of bacterial cellulose. *Carbohydrate Polymers*, 87, 839-845.
- Yano, H., Sugiyama, J., Nakagaito, A. N., Nogi, M., Matsuura, T., Hikita, M. & Handa, K. 2005. Optically Transparent Composites Reinforced with Networks of Bacterial Nanofibers. *Advanced Materials*, 17, 153-155.
- Zeng, X., Liu, J., Chen, J., Wang, Q., Li, Z. & Wang, H. 2011a. Screening of the common culture conditions affecting crystallinity of bacterial cellulose. *Journal of Industrial Microbiology and Biotechnology*, 38, 1993-1999.
- Zeng, X., Small, D. P. & Wan, W. 2011b. Statistical optimization of culture conditions for bacterial cellulose production by *Acetobacter xylinum* BPR 2001 from maple syrup. *Carbohydrate Polymers*, 85, 506-513.
- Zhou, L. L., Sun, D. P., Hu, L. Y., Li, Y. W. & Yang, J. Z. 2007. Effect of addition of sodium alginate on bacterial cellulose production by *Acetobacter xylinum*. *Journal of Industrial Microbiology and Biotechnology*, 34, 483-9.

Chapter 3

3 Batch Growth of *Komagataeibacter xylinus* and Measurement of Bacterial Cellulose Crystallinity

3.1 Abstract

Orbital shaker and shake flasks geometry are often used as main agitation system for aerobic cultures in shaken flasks. This study addresses the effects of mixing and cultivation time on bacterial cellulose production and cellulose crystallinity. Detailed investigations of bacterial cellulose production, cell production, and cellulose crystallinity were carried out in shake flasks with and without baffles at rotational speed of 150 rpm and 250 rpm. After 10 days of cultivation, bacterial cultures incubated in shake flasks with baffles and shaken with a rotational speed of 250 rpm produced a maximum of 2.64 ± 0.01 g/l of bacterial cellulose with a cellulose production yield of 0.25 ± 0.08 g/g of fructose consumed. In contrast with the trend for bacterial cellulose production, the bacterial cellulose crystallinity indices decreased with increasing cultivation time. Bacterial cellulose exhibited a substantial drop in cellulose crystallinity indices after 96 h of cultivation at 250 rpm, while it took more than 120 h of cultivation at 150 rpm, as assessed by X-ray diffraction (XRD) and Fourier-Transform Infrared (FTIR) using attenuated total reflectance (ATR) mode. This study demonstrated that the selection of shake flask geometry, shaker speeds, and cultivation time enhanced bacterial cellulose production and altered cellulose structure.

3.2 Introduction

In the past decade, many review papers have captured the extent of progress in the area of bacterial cellulose commercial applications with specific emphasis on biomedical, nanomedicine and nanocomposites (Reiniati et al., 2017, Lee et al., 2014, Cacicedo et al., 2016, Jorfi and Foster, 2015, Klemm et al., 2011, Charreau et al., 2013, Shah et al., 2013, Abeer et al., 2014, Gatenholm and Klemm, 2010). Bacterial cellulose has been recognized

as a versatile biomaterial. It has a high biocompatibility (Klemm et al., 2011, Saska et al., 2011) and possesses the ability to be tailored during cultivation, resulting in various nanoporous structures and cellulose crystallinities (Yang et al., 2012, Figueiredo et al., 2015, Huang et al., 2011). The high surface area and porosity of bacterial cellulose can be used to create protein and drug adsorption matrices (Müller et al., 2013, Oshima et al., 2011). This makes bacterial cellulose an ideal material for biomedical applications and controlled drug delivery. Moreover, bacterial cellulose has also been shown to enhance mechanical strength (Kim et al., 2009, Gea et al., 2010, Ruka et al., 2013) and improve the thermal stability of nanocomposites (Yano et al., 2005, Figueiredo et al., 2015).

Bacterial cellulose is an exopolysaccharide synthesized by aerobic bacteria. Many studies have focused around *Glunacetobacter xylinus* (*G. xylinus*), an efficient bacterial cellulose producer (Klemm et al., 2001). Bacterial cellulose is chemically pure as it does not contain impurities such as hemicellulose and lignin. The possibility of tailoring the properties of bacterial cellulose *in situ* during its production in liquid media makes bacterial cellulose more attractive and advantageous compared to plant-based cellulose (Reiniati et al., 2017).

Despite the remarkable properties of bacterial cellulose, its low production rate is one of the bottlenecks in leveraging the potential of bacterial cellulose for many applications. Improvements of bacterial cellulose production and yield are essential in positioning it on the front line of industrially attractive biomaterials. The conventional static culturing method for bacterial cellulose production requires a cultivation period of several weeks making it unsuitable for the commercial production of bacterial cellulose. Increased production rates can be achieved by using mixing to increase oxygen and nutrient mass transfer to the cells. The rotational shaker speed and the presence of baffles in shake flasks allow continuous mixing and enhance the bacterial cellulose production rate (Czaja et al., 2004, Son et al., 2003, Park et al., 2004). Shaking flasks, which have been utilized for the cultivation of microorganisms for many decades, offer a cost-efficient bioreactor system capable for a wide range of different tasks. More importantly, shaking bioreactors provide the first step of bioprocess development in a small-scale reactor system, such as culture conditions and effect of mixing.

Ruka et al. investigated different growth conditions that maximized the yield of bacterial cellulose and found that agitation and media composition altered cellulose crystallinity (Ruka et al., 2012). Moreover, the addition of water soluble polymers, such as carboxymethyl cellulose (Cheng et al., 2011), agar (Bae et al., 2004, Cheng et al., 2009), and sodium alginate (Zhou et al., 2007), increased bacterial cellulose production, while at the same time altering its structural properties and reducing the cellulose crystallinity. Cellulose biosynthesis is a complex bioprocess and the crystallization of bacterial cellulose is inherently complicated.

Cellulose consists of crystalline and amorphous regions. The cellulose crystallinity is defined as the cellulose crystalline mass fraction in cellulose materials (Kafle et al., 2015). There are several techniques used to measure the crystallinity indices and to characterize the crystalline cellulose structure, such as: X-ray diffraction (XRD) (Ahvenainen et al., 2016, Castro et al., 2011, Kafle et al., 2015, Oh et al., 2005, Park et al., 2010, Ruka et al., 2012, Watanabe et al., 1998), infrared (IR) spectroscopy (Castro et al., 2011, Hirai et al., 1998, Kafle et al., 2015, Oh et al., 2005, Ruka et al., 2012), and nuclear magnetic resonance (NMR) (Park et al., 2010, Watanabe et al., 1998, Yamamoto et al., 1996, Sacui et al., 2014). XRD and IR spectroscopy are prominent methods of characterizing cellulosic materials due to their non-destructive nature and wide accessibility. IR spectroscopy gives information related to the hydrogen bonding formation, elucidating polymorphic structures of cellulose I_{α} and I_{β} . Ratios of absorbance intensities obtained using IR spectroscopy is the simplest method to determine the cellulose crystallinity index. Furthermore, there are several different methods used with XRD to calculate the crystallinity index from the raw diffractograms. These methods account for peak height intensity, baseline, peak area, and fitting, and each has its own limitations and advantages (Park et al., 2010, Terinte et al., 2011).

Cellulose crystallinity is essential in many applications requiring added mechanical strength (Gea et al., 2010, Kim et al., 2009, Ruka et al., 2013). An increase in cellulose crystallinity reduces the rate of enzyme hydrolysis (Hall et al., 2010), reduces moisture absorbability of drug tablets (Awa et al., 2014), and increases the thermal stability of nanocomposites (Figueiredo et al., 2015). In addition, cellulose porosity and pore size may

be crucial for ionic or molecular adsorption (Yang et al., 2012). While it is widely known that bacterial cellulose production increases as the cultivation times increase, little is known about how cultivation times affect the crystallinity of bacterial cellulose. Bacterial cellulose cultivated in media with different carbon sources showed lower cellulose crystallinity indices when cultivated for 21 days compared to 6 days (Zeng et al., 2011).

Furthermore, there is relatively little information about the impact of mixing on cellulose crystallinity (Watanabe et al., 1998, Zeng et al., 2011). Given the immense importance of cellulose crystallinity in many applications, a fine-tuned production method is required to achieve a high yield of bacterial cellulose production with a high degree of cellulose crystallinity. The effects of mixing and length of cultivation time on the bacterial cellulose production and cellulose crystallinity are exemplified in the results presented here.

3.3 Materials and methods

3.3.1 Microorganism and culture media

Komagataeibacter xylinus (*K. xylinus*) (ATCC No. 700178), formerly known as *Gluconacetobacter xylinus*, obtained from American Type Culture Collection (ATCC) was grown in a fructose-corn steep solid solution (fru-CSS) medium (Joseph et al., 2003). The fructose-based medium used for the inoculum contained 20 g fructose, a centrifuged 20 g CSS solution, 1 g KH_2PO_4 , 3.3 g $(\text{NH}_4)_2\text{SO}_4$, 0.8 g $\text{MgSO}_4 \cdot 7\text{H}_2\text{O}$, 2.4 g trisodium citrate dehydrate, and 1.6 g citric acid dissolved in 1 litre of distilled water. Fructose, magnesium sulfate heptahydrate, ammonium sulfate, and corn steep solid (CSS) were purchased from Sigma-Aldrich, Ontario, Canada, and were used without further purification. The initial pH was adjusted to 5 by adding 2 M of NaOH. The medium was then autoclaved at 121°C for 15 minutes.

3.3.2 Preparation of stock culture

The lyophilized *K. xylinus* cells were grown in a test tube filled with 10 ml of (yeast glucose carbonate (YGC) medium as recommended by ATCC. After 7 days of incubation at 30°C in an orbital shaker incubator (New Brunswick G25-R, Edison, NJ, USA) set at 200 rpm, 5 ml of the seed culture was introduced to the 100 ml YGC medium in a 500 ml flask and

incubated for 4 days statically. After shaking the flask vigorously, 5 ml of this culture was transferred aseptically into the 100 ml fru-CSS medium and incubated for 3 days statically. The stock culture was prepared by adding the 3-day old broth to a 30% (v/v) glycerol solution with 1:1 ratio and stored in a -80°C freezer.

3.3.3 Production of cellulose in shake flasks

A total of 0.9 ml of stock culture was used to inoculate the 100 ml of fructose-CSS medium in a 500 ml flask. Following this, it was grown statically for 3 days in a 30°C incubator to make the initial cell inoculum. A fresh growth medium containing 25 g/l of fructose and a centrifuged 35 g/l of CSS with pH 4.5 was used for bacterial cellulose production described in Table 3.1. After shaking the flask vigorously, ten ml of the inoculum was transferred to 150 ml fresh growth media in 500 ml flasks with and without baffles. The flasks were kept for 1 to 10 days in a 30°C orbital shaker incubator set at 150 and 250 rpm. Bacterial cellulose fibers were produced in batch and were collected in 24 h increment up to day 5 and then at day 10. The baffled flasks had three indents designed to provide a better mixing of the solution and to improve oxygen transfer when used with an orbital shaker (Figure 3.1).

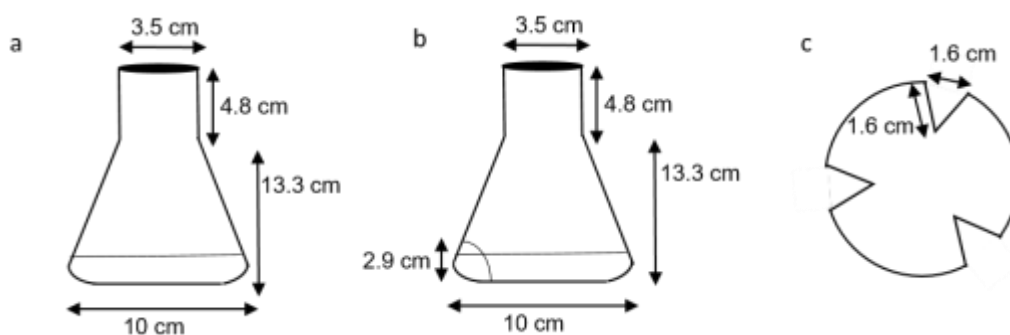


Figure 3.1 Schematic of shake flasks (a) without and (b and c) with baffles for bacterial cellulose production.

3.3.4 Measurement of bacterial cellulose and cell dry weight

The culture broth was collected and homogenized at 18,000 rpm three times for 1 min each using a Waring blender at maximum speed. A 5 ml sample was taken for bacterial cellulose

production determination and 5 ml for cell dry weight determination using the sample preparation method (Joseph et al., 2003). After the samples were centrifuged at 10,000 rpm for 10 minutes, the supernatant was kept for sugar analysis. The cellulose pellets were washed with distilled water before being centrifuged again and the washing procedure was repeated several times. The pellets were then treated with 30 ml of 0.1 M sodium hydroxide (NaOH) for 30 minutes at 90°C to lyse the cells. After being cooled in an ice bath, the sample was centrifuged and washed repeatedly with distilled water to remove excess NaOH. The pure bacterial cellulose was dried for 24 hours at 105°C and weighed. For cell dry weight determination, washed pellets from the 5 ml samples were suspended in 1 ml of 2% (v/v) cellulase (Cat # C2730, Lot # SLBH0229V, Sigma Aldrich, St. Louis, MO) solution in 0.1 M citrate buffer at pH 4.8. After a gentle inversion, the sample was incubated in a water bath at 50°C for 1 hour to hydrolyze the cellulose. The mixture was filtered using a pre-weighed 0.45 µm cellulose nitrate filter membrane, dried for 24 hours at 105°C, and weighed.

3.3.5 Measurement of sugar concentration

Fructose concentration was measured using the dinitrosalicylic acid (DNS) method (Miller, 1959). The DNS reacts with reducing sugars and forms 3-amino-5-nitrosalicylic acid which absorbs light strongly at 540 nm. One ml of the supernatant obtained from the first centrifugation was centrifuged at 10,000 rpm for 5 min. Equal volumes of supernatant sample (with proper dilution) and the DNS reagent, which were 0.5 ml each, were mixed well and placed in a boiling water bath for 5 min. After cooling in an ice bath for 5 min, the absorbance was read at 540 nm. A standard calibration curve was created using known fructose concentrations.

3.3.6 Scanning electron microscope (SEM) of bacterial cellulose fibers

Bacterial cellulose obtained after cells removal was lyophilized and was coated with a thin film of gold circa 2 nm before SEM analysis. A scanning electron microscope (SEM) Hitachi S-2600N (Hitachi High Technologies America, Inc., Schaumburg, IL, USA)

operating at 5 and 10 kV was used to examine the bacterial cells and bacterial cellulose morphology.

3.3.7 Attenuated Total Reflectance Fourier-Transform Infrared Spectroscopy (ATR-FTIR) of bacterial cellulose fibers

Freeze dried cellulose samples were scanned using a Nicolet 6700 Spectrophotometer (Thermo Scientific, Pittsburgh, PA, USA) with an attenuated total reflectance (ATR) mode equipped with a diamond crystal. Scanning was conducted from 4000-400 cm^{-1} with a scan frequency of 32 s^{-1} and resolution of 4 cm^{-1} . Using this ATR-FTIR approach, cellulose samples were pressed against the face of a single diamond crystal tip. The evanescent wave had a depth of penetration of 2 μm with an incident angle of 42 degrees. An automatic baseline correction was performed on the generated IR spectra using OMNIC software. The cellulose crystallinity indices were obtained using two methods: 1) evaluated from the ratios of the absorption intensity at wavenumber 1428 and 897 cm^{-1} ($\text{Cr}_1 = A_{1428}/A_{897}$), and 2) evaluated from the ratios of the absorption intensity at wavenumber 1372 and 2898 cm^{-1} ($\text{Cr}_2 = A_{1372}/A_{2898}$) (Oh et al., 2005, Široký et al., 2010). Avicel™ PH-101 (Sigma Aldrich, Ontario, Canada) was used for comparison.

3.3.8 X-ray Diffraction (XRD) of bacterial cellulose fibers

The cellulose crystallinity of samples was analyzed using an X-ray diffractometer Rigaku Ultima IV (Rigaku, The Woodlands, TX, USA) operating at 40 kV and 40 mA. The freeze dried samples were pressed into a thin and flat layer using glass slides, and analyzed following the method described previously (Cheng et al., 2009). Using a copper x-ray source, scans were collected at 2° per min from 10-30° 2 θ . The cellulose crystallinity index based on peak intensity is described in the following equation: $\text{Cr}_1 = (I_{200} - I_{\text{am}})/I_{200}$, where I_{002} is the overall intensity corresponding to (002) peak at 2 θ about 22.6° and I_{am} is the peak intensity of the baseline at 2 θ about 18.5°. The cellulose crystallinity index was also reported using the peak area method (Roman and Winter, 2004, Ruka et al., 2013). Peak fitting was carried out using Origin (OriginLab, Northampton, MA) Peak Analyser software. Three cellulose diffraction peaks at diffraction angles of 14.6°, 16.8°, 22.6° 2 θ , corresponding to the -101, 101, and 002 crystal planes, respectively, were fitted to a

Gaussian function. A broad peak with a maximum between 18° and 22° was fitted as the amorphous cellulose contribution. The diffraction peak position was selected within 0.2° of the literature value to represent the true peak for fitting. Cellulose crystallinity index determined by the peak area method (Cr_A) is described as a ratio of the sum of the areas under crystalline diffraction peaks to the total area under the curve between $2\theta = 10-30^\circ$. In brief, $Cr_A = A_{cr}/(A_{cr} + A_{am})$ where A_{sample} is the area under the sample intensity curve (Ahvenainen et al., 2016).

3.3.9 Data analysis

Quantitative data are presented as the averages of triplicates for bacterial cellulose production data. The error shown is the standard deviation. The significant differences of between the data sets were evaluated using two-way ANOVA and a post-hoc Tukey's test using OriginPro 2016 (OriginLab, Northampton, MA, USA) ($p < 0.05$).

3.4 Results and Discussion

3.4.1 Bacterial cellulose morphology

Cell suspension isolated from the inoculum was spread out on an agar plate. Smooth, slightly irregular, and light brown/yellowish colonies were observed after a few days, confirming the presence of pure *K. xylinus* in the inoculum (Figure 3.2a). After the inoculum was cultured statically for 2 days, a transparent cellulose biofilm was visible at the air/liquid interface, which thickened each day (Figure 3.2b). When the broth culture was kept in an orbital shaker, round balls of cellulose with a tail at the end were formed (Figure 3.2c). The sphere-like bacterial cellulose was formed because the cells attached themselves around the surface of air bubbles existing in the liquid medium. As the *G. xylinus* cells grew, the cellulose ribbons formed a more dense sphere (Czaja et al., 2004). Eventually, the constant motion and shear force from the agitation or shaker speed separated the cells from the cellulose or preventing cell-cellulose agglomerates to form, which generated a tadpole-like shape structure.

Bacterial cellulose from cultures shaken in flasks without baffles had a more defined shape and smooth surface with a few distinct agglomerations suspended in a clear growth

medium. On the other hand, bacterial cellulose from cultures shaken in flasks with baffles had more variations in shape with smaller, more reticulated, and rougher surface. The culture medium was more opaque with bacterial cellulose and cell suspended in smaller lumps compared to those grown in shake flask without baffles. The presence of baffles promoted the formation of localized eddies and enhanced the mixing and shear (Li et al., 2013) which affected the way BC assembled outside the bacterial cells (Figure 3.2d). These morphological changes were induced by changes in microstructure, such as degree of polymerization, crystallinity, and mass fraction of cellulose I_α (Watanabe et al., 1998).

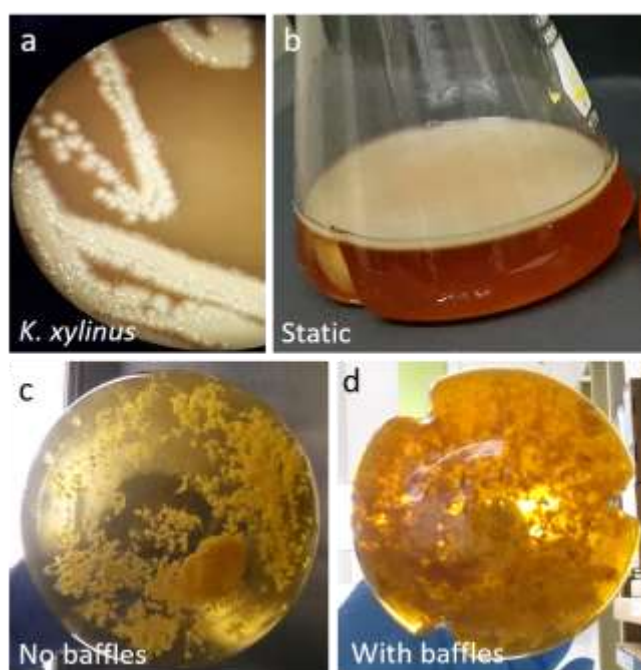


Figure 3.2 Images of *K. xylinus*, bacterial culture, and bacterial cellulose in shake flasks.

The morphology of bacterial cells and bacterial cellulose before and after purification was investigated. Figure 3.3 (a and b) shows SEM images of rod-shaped *K. xylinus* bacteria that are embedded within the bacterial cellulose network. Bacterial cells extruded thin cellulose fibers, which eventually formed a bundle of fibers and enveloped the cells. After being treated with NaOH for 30 min, bacterial cells were successfully removed from bacterial cellulose. Twisted microfibril bundles and a fine bacterial cellulose network are shown in

Figure 3.3 (c and d). *K. xylinus* had been reported to produce a twisting ribbon of cellulose made from the aggregation of microfibril bundles (Haigler et al., 1982, Hirai et al., 1997).

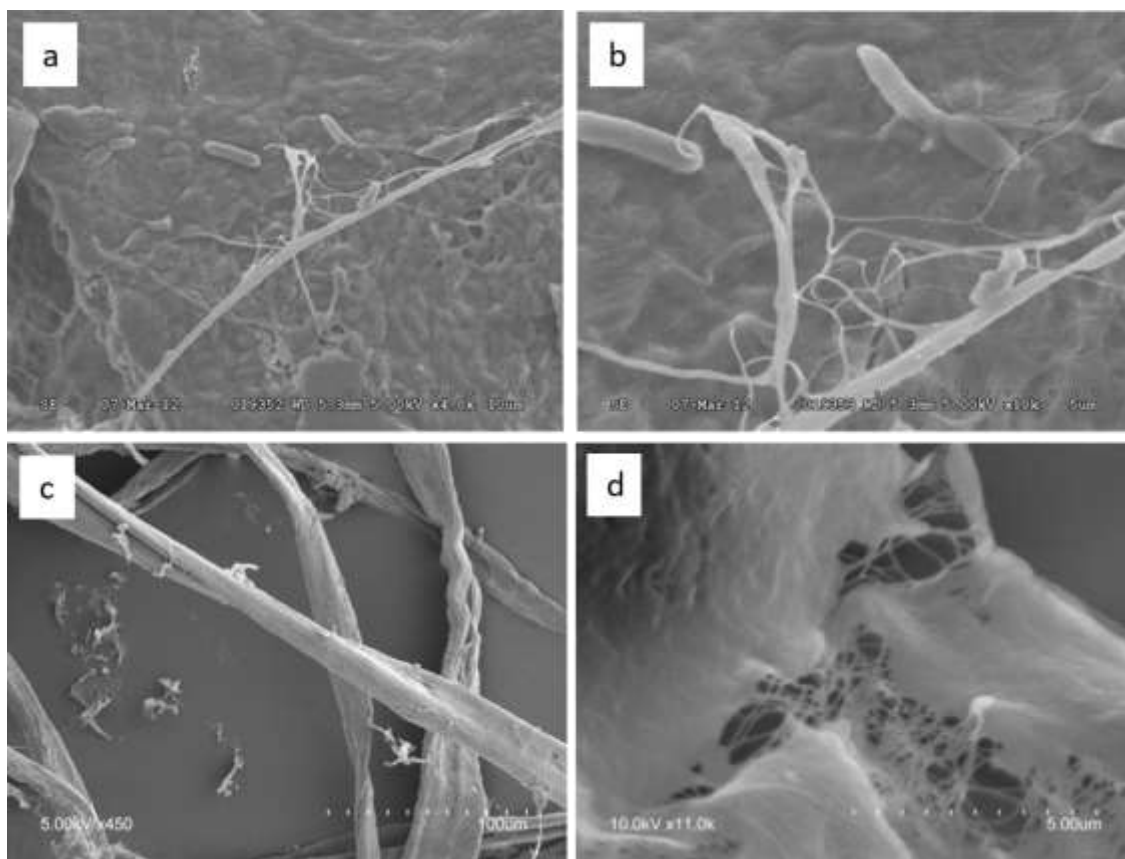


Figure 3.3 SEM images of bacterial cellulose produced by *K. xylinus* grown for 5 days in a fructose-CSS medium at 250 rpm: (a) and (b) showing bacterial cellulose being produced from the bacterial cells, (c) and (d) showing pure bacterial cellulose after being treated with 0.1 N NaOH. Scale bar for (a) and (c) is 10 μm while for (b) and (d) it is 5 μm.

This twisting of cellulose ribbons was created by the movement and rotation of *G. xylinus* around its longitudinal axis during the production of the ribbons (Brown et al., 1976). The length of bacterial cellulose microfibrils reached several micrometers in length. The determination of bacterial cellulose microfibril width was not straightforward due to the twisting of the ribbons. However, an average width could be taken by measuring them at several locations and was reported within the range of 35-70 nm (Vasquez et al., 2013). Pure bacterial cellulose from 10 day cultivations at 150 rpm were white and spongy, while

bacterial cellulose grown at 250 rpm was flakier, an obvious difference in physical appearance to the naked eye.

3.4.2 Effect of production conditions and cultivation time on bacterial cellulose fibers production

Bacterial cellulose production, cell concentration, fructose consumption, and pH medium from all shake flask culture conditions are presented in Table 3.1. Bacterial cellulose production in shake flasks with baffles achieved 2.64 g/l, which was 1.4 fold higher than in shake flasks without baffles rotated at 250 rpm. This bacterial cellulose production is in good agreement with a previous study obtaining approximately 2 g/l of bacterial cellulose after 5 days of cultivation in shake flasks without baffles at rotational speeds in the range of 90-250 rpm (Czaja et al., 2004).

Table 3.1 Bacterial cellulose (BC) production by *K. xylinus* grown in a fructose-CSS solution medium in shake flasks with fructose and CSS concentration of 25 g/l and 35 g/l, respectively. Values represent average \pm standard deviations from triplicate experiments (n=3).

Label	Culturing condition	BC ^a (g/l)	BC ^a (g/g)	BC productivity ^{a, c} (g/l/h)	BC productivity ^{b, c} (g/l/h)	Cell ^a (g/l)
A	250 rpm, no baffles	1.83 \pm 0.04	0.26 \pm 0.01	0.008	0.015	0.76 \pm 0.20
B	250 rpm, with baffles	2.64 \pm 0.01	0.25 \pm 0.08	0.011	0.022	1.05 \pm 0.04
C	150 rpm, no baffles	1.50 \pm 0.03	0.19 \pm 0.02	0.006	0.013	0.93 \pm 0.30
D	150 rpm, with baffles	1.91 \pm 0.03	0.19 \pm 0.01	0.008	0.016	0.92 \pm 0.14

^a Values obtained after 10 days of cultivation.

^b Values obtained after 5 days of cultivation.

^c The standard deviations are nearly zero within the significant digit reported

Bacterial cellulose production increased as the cultivation time increased (Figure 3.4 and Figure 3.5). Fructose was consumed more rapidly in shake flasks with baffles compared to ones without baffles. During the 10 day cultivation period, cultures grown in shake flasks

without baffles consumed 30% of the fructose in the media compared to those grown with baffles, which consumed 40% of the fructose. Higher rotational speed led to a faster depletion of fructose. There was a rapid pH increase from 4.5 to 8 at 250 rpm (Figure 3.4) and more gradual pH increase at 150 rpm (Figure 3.5). Higher speed and the presence of baffles promoted increased bacterial metabolic rates and a release of a water-soluble substance, increasing the pH. In addition, bacterial cellulose yield was calculated by dividing the bacterial cellulose production (g/l) by the amount of fructose consumed (g/l). The general trend in bacterial cellulose yield showed that the culture grown at higher shaker speeds resulted in higher yields, obtaining 0.25 g/g for 250 rpm and 0.19 g/g for 150 rpm.

The mean bacterial cellulose production harvested at day 5 was significantly different between the flasks with and without baffles ($p=0.027$) and high and low rotational speeds ($p=0.001$) according to the two-way ANOVA. We also observed a significant interaction between the rotational speed and type of flask ($p=0.018$). The means comparison performed using post-hoc Tukey analysis showed that the mean bacterial cellulose production at a rotational speed of 250 rpm with baffles is significantly different from that at a rotational speed at 250 rpm without baffles and at 150 rpm both with and without baffles.

Cell concentrations of *K. xylinus* increased immediately after inoculation and reached a stationary phase after reaching maximum sugar consumption level. Cultures grown in shake flasks with baffles rotated at 250 rpm reached the highest cell concentration of 1.05 g/l. Cell concentration was significantly affected by the presence of baffles ($p=0.013$) and the interaction of baffles and rotational speed ($p=0.011$). The presence of baffles promoted more cell production compared to those without baffles.

Mixing and baffles ensured the growth of aerobic bacteria by promoting evenly distributed dissolved oxygen in the liquid medium. The gas-liquid interface in baffled flasks was irregular and increased the interfacial area for oxygen mass transfer (Li et al., 2013). When the fluid collided with the baffles, it splashed around the baffles caused the development of cellulose biofilm on the wall of shake flasks. Rotational speed influenced the shear force developed in baffled shake flasks (Li et al., 2013). The turbulence intensity formed in the

baffled flask was much greater than in flask without baffles. Moreover, in shake flask with baffles, the velocity changed greatly and formed higher velocity gradient resulting in higher shear strain rate (Li et al., 2013). The shear strain rate increased with rotational speed and understanding the shear environment in the baffled flasks provided valuable information for design and scale-up of bioreactors to cultivate shear-sensitive biological systems.

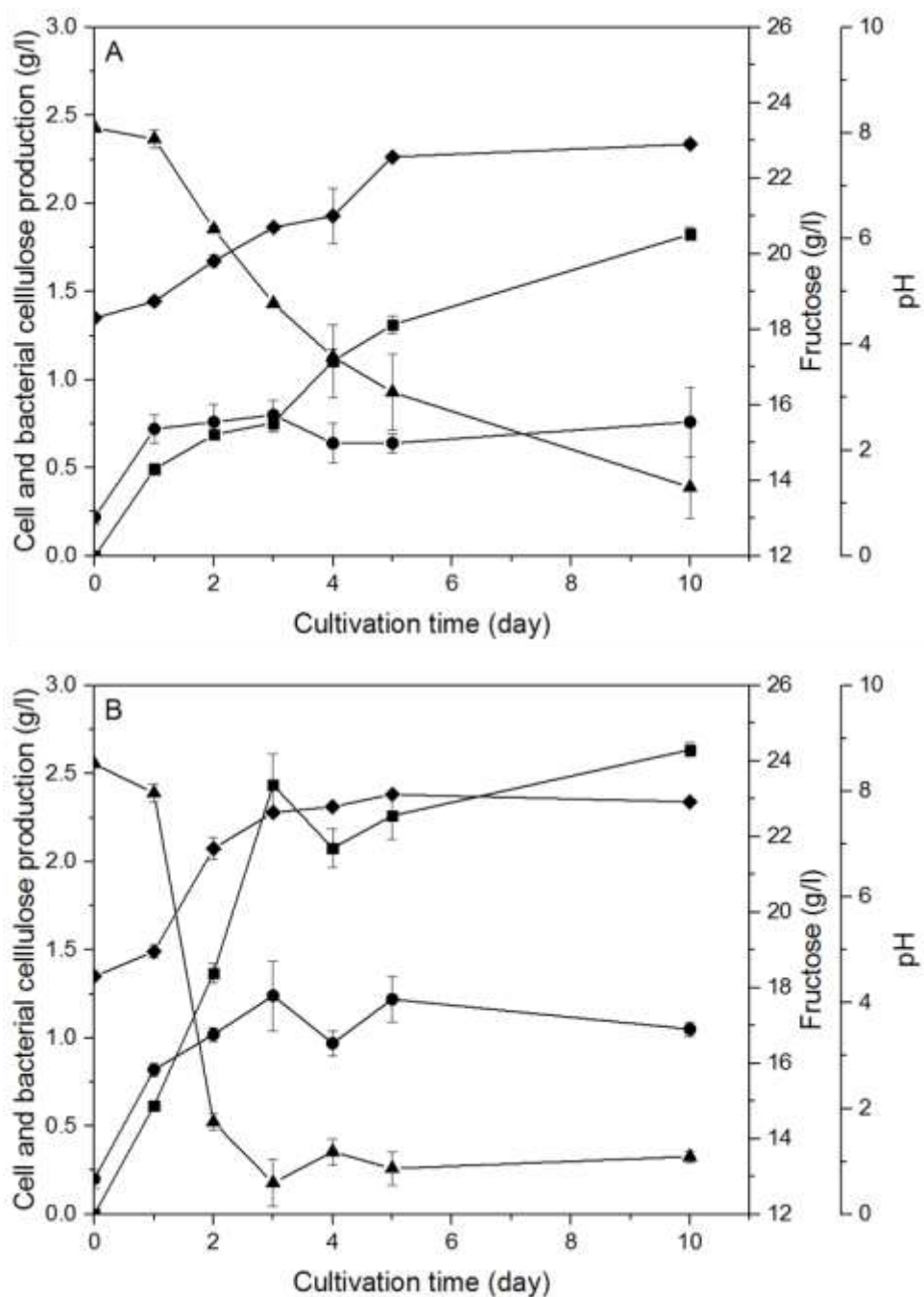


Figure 3.4 Bacterial cellulose production by *K. xylinus* in fructose-CSS medium incubated in an orbital shaker set at 30°C and with a rotational speed of 250 rpm in shake flasks (A) without baffles and (B) with baffles. Legend: ■: bacterial cellulose concentration, ●: cell concentration, ▲: fructose concentration, ◆: pH.

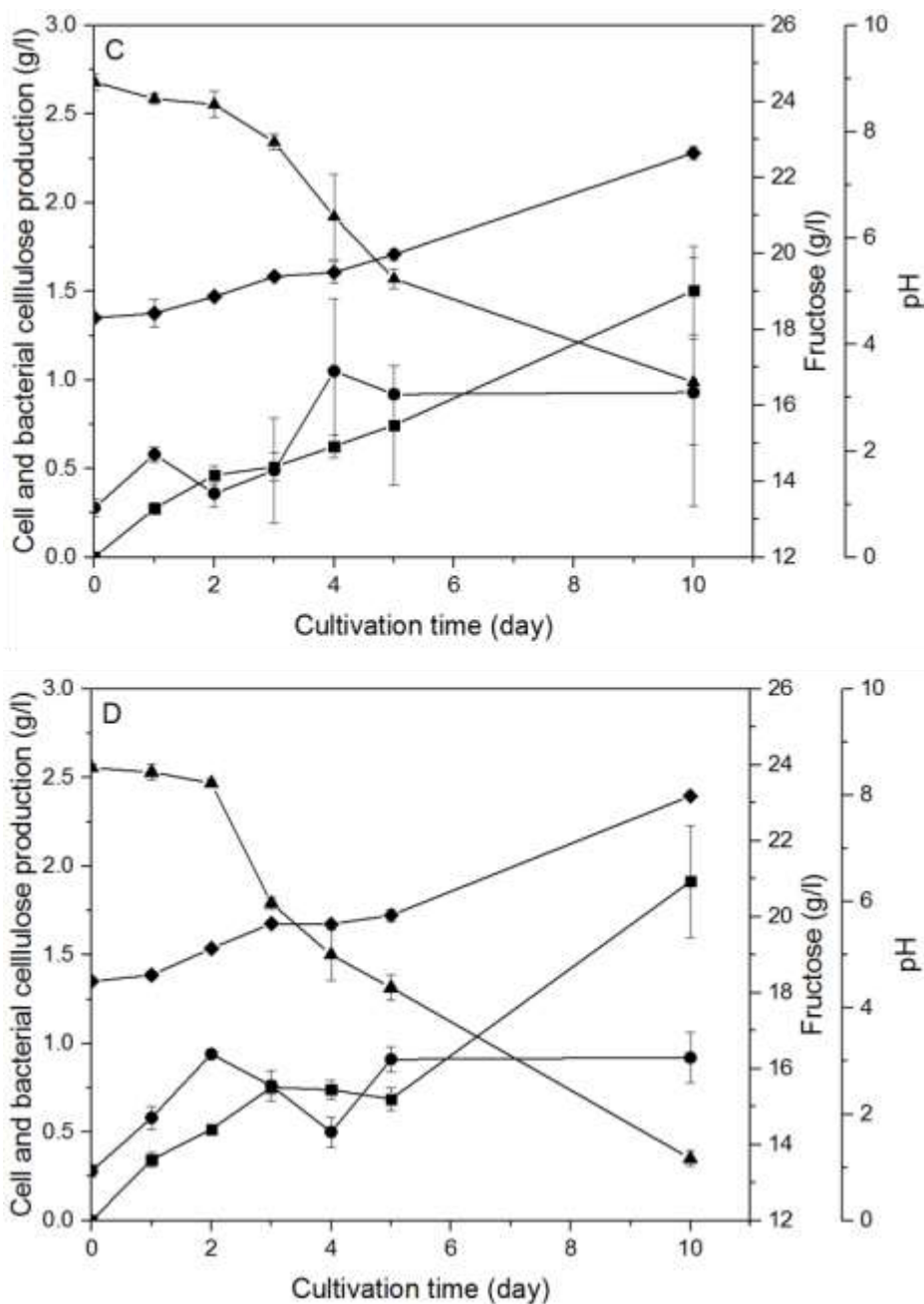


Figure 3.5 Bacterial cellulose production by *K. xylinus* in fructose-CSS medium incubated in an orbital shaker set at 30°C and with a rotational speed of 150 rpm in shake flasks (C) without baffles and (D) with baffles. Legend: ■: bacterial cellulose concentration, ●: cell concentration, ▲: fructose concentration, ◆: pH.

3.4.3 Evaluation of changes in bacterial cellulose crystallinity measured with XRD and ATR-FTIR

In this study, several methods for measuring the crystallinity indices of cellulose were investigated to give a comprehensive understanding of the effects of cultivation time and production conditions on cellulose crystallinity. ATR-FTIR accounts for the contribution of both amorphous and crystalline cellulose, while the XRD approach provides more detailed information on the crystalline features of materials (Terinte et al., 2011).

First, the crystallinity indices of the cellulose samples were determined by peak intensity and then compared to the values obtained from the peak area of XRD diffractograms. Figure 3.6 shows an X-ray diffractogram of bacterial cellulose grown for 1, 2, 3, 4, 5, and 10 days in shake flasks with and without baffles at two different rotational speeds of 250 rpm and 150 rpm. The X-ray diffractogram of bacterial cellulose shows three main characteristic peaks at the Bragg angle 2θ ($^{\circ}$) of 14.6, 16.8, and 22.6 corresponding with the crystal planes $\langle -110 \rangle$, $\langle 110 \rangle$, and $\langle 200 \rangle$, respectively (Roman and Winter, 2004). These peaks identify the structure of cellulose I (Roman and Winter, 2004). Bacterial cellulose produced by *Gluconacetobacter* consisted of two crystalline allomorphs of native cellulose, I_{α} and I_{β} (Atalla and VanderHart, 1984, Sugiyama et al., 1991). Cellulose I_{α} has a triclinic form and is metastable, which could be converted to a more stable cellulose I_{β} by heat-assisted alkali treatment (Sugiyama et al., 1991).

The ratio of cellulose I_{α} over I_{β} produced in nature depends on the source or origin of the cellulose. While cellulose from plant origin is rich in cellulose I_{β} , cellulose from bacterial origin is rich in cellulose I_{α} . Cellulose I_{α} is easily identified by a higher peak intensity at 14.6° compared to peak intensity at 16.8° (Ahvenainen et al., 2016, Kafle et al., 2015). For all bacterial cellulose samples, the peak at 14.6° decreases and becomes more broad as the cultivation time increases (Figure 3.6). Different cultivation times or the presence of baffles did not affect the type of cellulose being produced; however, when examined closely, the peak intensity of bacterial cellulose grown in 10 days is generally lower than that of bacterial cellulose grown for fewer days. A decrease in intensity and a broadening of peaks indicate a decrease in the degree of crystallinity, more amorphous formations, and/or a decrease in crystallite size (Watanabe et al., 1998). However, in order to detect subtle

changes in crystal size and cellulose crystallinity index, a high-resolution spectrum with a high signal to noise ratio is required to reduce discrepancies and increase sensitivity to crystallinity changes (Kafle et al., 2015, Park et al., 2010).

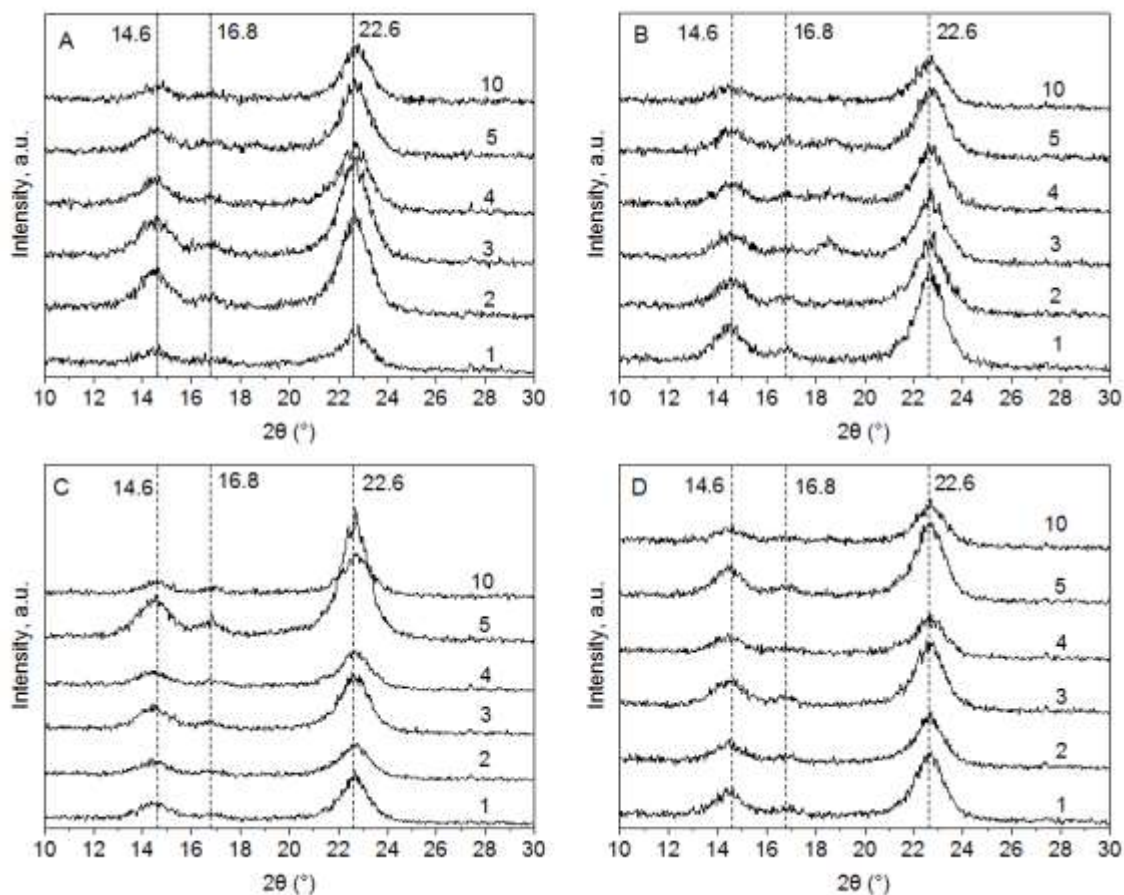


Figure 3.6 X-ray diffractogram of bacterial cellulose fibers produced by *K. xylinus* in shake flask culture using two different rotational speeds: A (250 rpm, without baffles), B (250 rpm, with baffles), C (150 rpm, with baffles), and D (150 rpm, without baffles) at different cultivation days (as labelled on the graphs).

All bacterial cellulose samples exhibited a relatively sharp peak at 14.6° while Avicel showed a broad peak between 14.6 to 16.8° (Figure 3.7). Avicel, a microcrystalline cellulose derived from wood, consists of short, densely packed cellulose I_β with a low degree of polymerization (Kafle et al., 2015, Terinte et al., 2011). Cultures grown in shake flasks without baffles at 150 rpm produced bacterial cellulose with a relatively high

intensity crystallinity peak at 22.6° compared to other bacterial cellulose samples and Avicel.

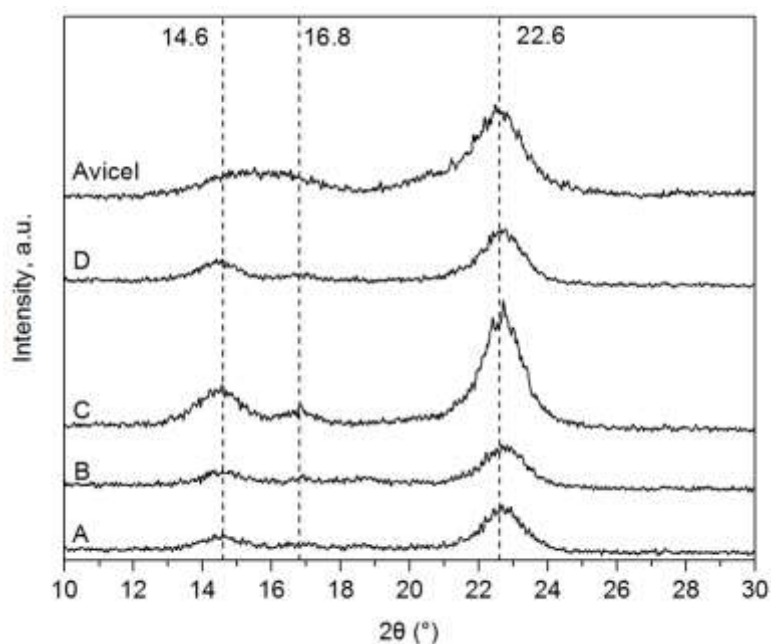


Figure 3.7 X-ray diffractogram of bacterial cellulose fibers produced by *K. xylinus* after 5 days of cultivation in an orbital shaker set at 30°C in shake flasks: A (250 rpm, without baffles), B (250 rpm, with baffles), C (150 rpm, without baffles), and D (150 rpm, with baffles). Avicel is presented for comparison.

Figure 3.8 shows the calculated cellulose crystallinity indices using both: (a) a peak area fitting (Cr_A) and (b) a peak intensity method (Cr_I). Both Cr_A and Cr_I display parallel behaviours over the whole range of process conditions and cultivation times; only the absolute value differs. The Cr_I of bacterial cellulose grown for 5 days in baffled flasks at 250 rpm is roughly 15% lower while the Cr_A is 30% lower than that grown without baffles. All bacterial cellulose samples showed Cr_I approximately 0.73 and Cr_A approximately 0.32 after 10 days of cultivation. In this study, the Cr_I of bacterial cellulose produced in shake flasks at slower rotational speeds was 0.86. This was comparable to a previously reported value of 0.88 (Terinte et al., 2011). Other growing conditions, with baffles and at high rotational speeds, produced bacterial cellulose with a Cr_I around 0.70.

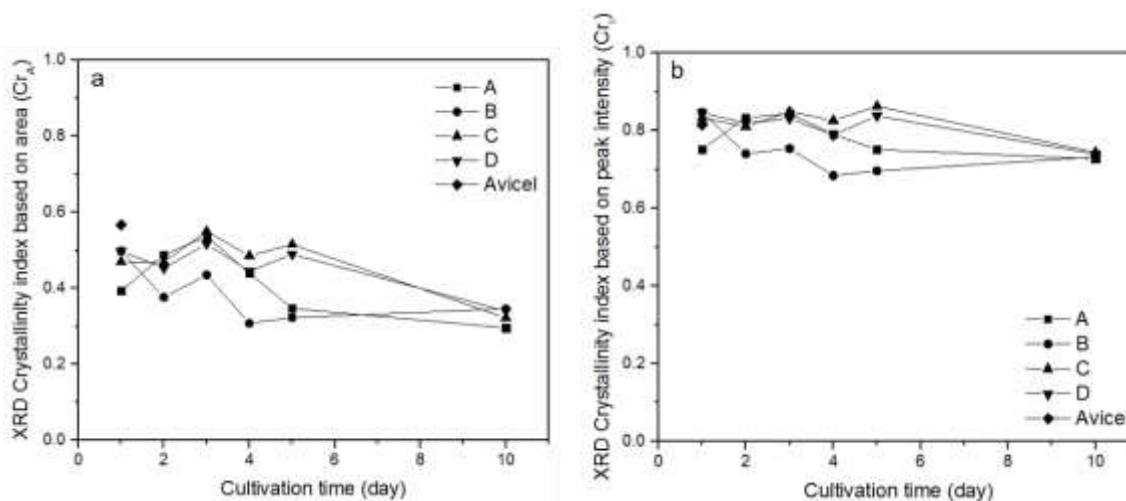


Figure 3.8 XRD crystallinity indices of bacterial cellulose fibers produced in shake flasks filled with fru-CSS medium, incubated from 1 to 10 days inside a 30°C orbital shaker set at 250 rpm (A: without baffles, B: with baffles), and at 150 rpm (C: without baffles, D: with baffles) as determined using (a) the peak area fitting method and (b) the peak intensity method.

Bacterial cellulose produced in an incubated orbital shaker at 250 rpm with baffles showed a significant decrease of cellulose crystallinity indices with cultivation time and exhibited the lowest cellulose crystallinity indices compared to other examined bacterial cellulose samples at lower speeds. After 48 h hours of cultivation, Cr_A showed approximately 25% decreased from Cr_A at 24 h. Bacterial cellulose samples grown with shaker speed of 250 rpm exhibited a substantial drop in Cr_A after 96 h of cultivation, while it took more than 5 days of cultivation for bacterial cellulose grown with shaker speed of 150 rpm. This indicates that the presence of baffles affected the crystalline arrangement of glucan chains within microfibrils and reduced the cellulose crystallinity indices even at low agitation speed. Rotational speed and agitation rate have been reported to disrupt hydrogen bonding and the organization of fibrils, resulting in a decrease in cellulose crystallinity (Czaja et al., 2004).

Moreover, the cellulose crystallinity index determination using the peak area method was thought to provide a better representation of the crystallinity index of cellulose. Although the peak intensity ratio method (Segal et al., 1959, Park et al., 2010) and ratio of area under

the curve (Park et al., 2010, Roman and Winter, 2004, Oh et al., 2005) have been used to calculate the cellulose crystallinity index, it is important to note that the measurement of the crystallinity index using XRD was method-dependent and direct comparison to values obtained from different studies needs to be carefully made.

The cellulose crystallinity index determined by the peak intensity method is generally higher than one determined by peak area fitting, which agrees with previously published results (Park et al., 2010, Ahvenainen et al., 2016, Terinte et al., 2011). The low cellulose crystallinity value obtained from Gaussian fitting may result from overestimating the amorphous cellulose contribution (Ahvenainen et al., 2016). The value of the crystallinity index determined using the peak area method is highly dependent on the selected baseline and the peak fitting. Since determining cellulose crystallinity index is method dependent, it necessitates a careful comparison with values from other published work. The Cr_A , however, can be used to qualitatively compare the differences in the cellulose crystallinity indices between samples obtained in the same study, assuming a consistent method applied throughout the study. For a much simpler process, the peak intensity method offers much more convenience. It saves time while being able to qualitatively compare different cellulose crystallinity indices of samples within the research work. Cr_I shows a positive correlation with cellulose crystallite size, thus the peak area method is recommended to determine crystallinity indices of samples with different crystallite size (Ahvenainen et al., 2016).

Figure 3.9 shows the ATR-FTIR spectra of bacterial cellulose fibers produced by *K. xylinus* after 5 days of cultivation in an orbital shaker set at 30°C in shake flasks at different conditions. The ATR-FTIR spectra show typical bands of cellulose I recorded from cellulose of bacterial origin as previously reported (Castro et al., 2011, Dayal et al., 2013). The absence of non-cellulose signature bands confirms that the bacterial cellulose samples presented in this case, are pure. A broad absorption band in the 3600-3100 cm^{-1} region is due to the OH-stretching vibrations representing the hydroxyl bonds in these cellulose samples. Signature peaks in this area are: 3455-3410, 3375-3340, and 3310-3230 cm^{-1} (Ciolacu et al., 2011). An absorption band at 2900 cm^{-1} is attributed to C-H stretching vibration, which confirms amorphous cellulose characteristics. There is a weak absorption

band in the range of 900-870 cm^{-1} and a strong band at 1430 cm^{-1} , which define the cellulose I allomorph (Nelson and O'Connor, 1964b). An absorption band at 897 cm^{-1} is assigned to C-O-C stretching at the β (1-4) linkage and indicates an amorphous cellulose absorption band. An absorption band at 1430 cm^{-1} is assigned to CH_2 symmetrical bending vibration and has been correlated to the degree of crystallinity and is also referred to as cellulose crystallinity band (Ciolacu et al., 2011).

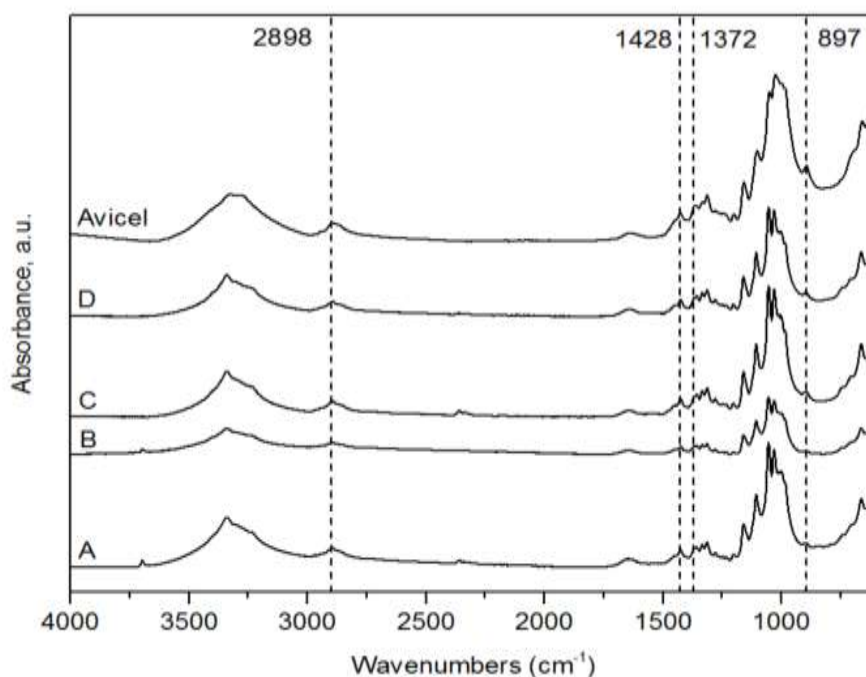


Figure 3.9 ATR-FTIR spectra of bacterial cellulose fibers produced by *K. xylinus* after 5 days of cultivation in an orbital shaker set at 30°C in shake flasks: A (250 rpm, without baffles), B (250 rpm, with baffles), C (150 rpm, without baffles), and D (150 rpm, with baffles). Avicel is presented for comparison.

An absorption band at 1420 cm^{-1} is attributed to amorphous cellulose and crystallized cellulose II (Nelson and O'Connor, 1964b). The spectra obtained in this study show the absorption band at 1428 cm^{-1} which suggests that the bacterial cellulose samples contained a mixture of crystalline cellulose I and amorphous cellulose, which is in good agreement with the XRD results. The absorption bands near 3240 and 750 cm^{-1} in the ATR-FTIR spectra of native cellulose correspond to cellulose I_α , whereas bands near 3270 and 710 cm^{-1}

¹ correspond to cellulose I_β (Yamamoto et al., 1996). The absorbance band at 1372 cm⁻¹ in the ATR-FTIR spectra is attributed to C-H bending (Oh et al., 2005).

Cellulose crystallinity indices of bacterial cellulose samples were also calculated using the absorbance intensities obtained from the ATR-FTIR spectroscopy spectra. The intensity ratio of absorbance at 1430 to 893 cm⁻¹ and the intensity ratio of absorbance at 1372 to 2900 cm⁻¹ have been previously reported for cellulose (Ciolacu et al., 2011, Nelson and O'Connor, 1964b, Nelson and O'Connor, 1964a, Široký et al., 2010, Carrillo et al., 2004). A ratio of peak intensity at a given wavenumber to that at the reference wavenumber helps to identify the changes in hydrogen-bond intensities in relation to the crystallinity index. Figure 3.10 shows the cellulose crystallinity indices determined from ATR-FTIR absorbance intensity using two ratios: Cr₁ and Cr₂. An increasing of the absorbance intensity at 1428 cm⁻¹, the designated crystalline band, leads to an increase in Cr₁. At 250 rpm, bacterial cellulose grown with or without baffles show relatively higher Cr₁ than those grown at 150 rpm, especially on days 2, 4 and 5 for cultures with baffles. A high Cr₁ indicates that bacterial cellulose grown in shake flasks with baffles at 250 rpm produced a higher yield of crystalline bacterial cellulose fiber than other conditions. The Cr₁ trends are not in agreement with the crystallinity indices results from XRD. To make a clearer comparison, Table 3.2 shows the numerical values of the cellulose crystallinity indices determined by XRD and ATR-FTIR for all bacterial cellulose samples after 5 days of cultivation and Avicel.

On the other hand, Cr₂ reveals similar trends to the crystallinity indices profile evaluated by XRD (Figure 3.10 and Table 3.2). Lower Cr₂ corresponds with higher absorbance at the amorphous band of 2900 cm⁻¹, suggesting less C-H bond stretching leading to amorphous arrangement. From analysis of the cellulose crystallinity indices using Cr₂, bacterial cellulose grown at 250 rpm showed a lower cellulose crystallinity than bacterial cellulose grown at 150 rpm and cultivation time reduced the cellulose crystallinity indices. This study demonstrates that Cr₂ is more reliable in representing cellulose crystallinity of cellulose I than Cr₁ and can be used to determine relative crystallinity of cellulose samples. This is because Cr₂ is proportional to the degree of crystallinity of the cellulose sample

while the value of Cr_1 is a useful indicator for the order of cellulose in cellulose II (Carrillo et al., 2004).

Table 3.2 Summary of cellulose crystallinity indices of bacterial cellulose produced by *K. xylinus* in shake flasks at 30°C for 5 days. Legend: A (250 rpm, without baffles), B (250 rpm, with baffles), C (150 rpm, without baffles), and D (150 rpm, with baffles). Avicel is presented for comparison.

Cellulose samples	XRD		ATR-FTIR	
	Cr. _A Based on peak area	Cr. _I Based on peak height	Cr ₁ = A ₁₄₂₈ /A ₈₉₇	Cr ₂ = A ₁₃₇₂ /A ₂₈₉₈
A	0.35	0.75	0.74	1.06
B	0.32	0.70	0.77	1.16
C	0.52	0.85	0.72	1.35
D	0.49	0.84	0.72	1.25
Avicel	0.57	0.82	0.39	1.83

ATR-FTIR spectroscopy method provides a rapid analysis, non-destructive technique, and suitable for real time online monitoring system, such as: for investigating the growth of bacterial cell in aqueous media, the development of biofilm, and changes on biofilm surfaces (Schmitt and Flemming, 1998). ATR-FTIR is versatile for detecting and measuring changes in chemical composition and cellulose structure; however, since this method detects the surface of the material, it has some limitations in detecting subtle internal structural changes. XRD is useful for studying crystal structure and atomic spacing, and is sensitive to subtle crystallinity changes. However, the usage of XRD in a real time online monitoring system is not likely. The use of both XRD and FTIR is complementary in providing a better understanding of cellulose structure and its changes.

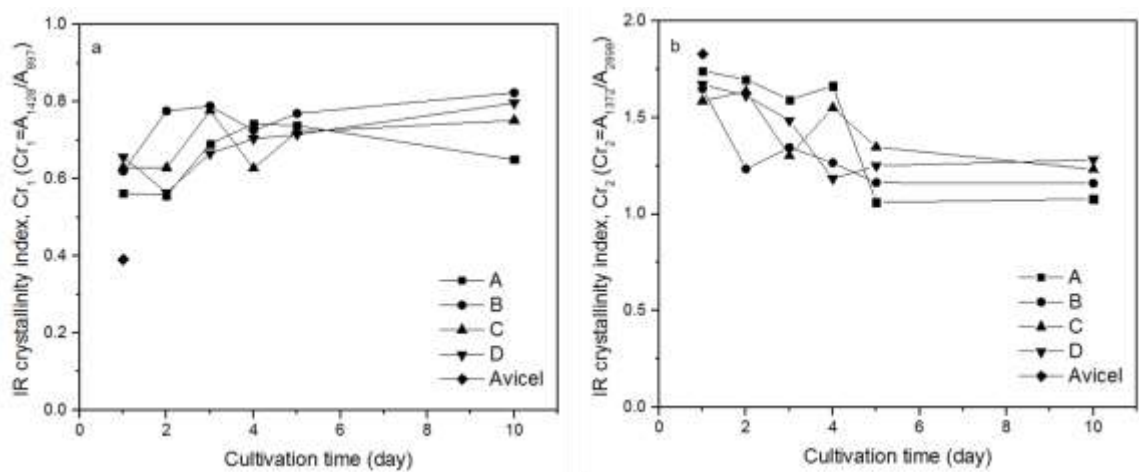


Figure 3.10 IR Cellulose crystallinity indices (a) $Cr_1 = A_{1428}/A_{897}$ and (b) $Cr_2 = A_{1372}/A_{2898}$ of bacterial cellulose fibers produced by *K. xylinus* in an orbital shaker set at 30°C in shake flasks: A (250 rpm, without baffles), B (250 rpm, with baffles), C (150 rpm, without baffles), and D (150 rpm, with baffles). Avicel is presented for comparison.

3.5 Conclusions

The shake flask has been the most commonly used bioreactor in bioprocesses because of its flexibility and great practical value. In the present study, the effect of cultivation conditions on bacterial cellulose production and the cellulose crystallinity indices were investigated using shake flasks with and without baffles at two different rotational speeds. The comparison between shake flasks with and without baffles emphasized the advantages of mixing on the bacterial cellulose production. Cultures grown at 250 rpm in shake flasks with baffles produced the maximum bacterial cellulose production of 2.6 g/l in 10 days.

Bacterial cellulose crystallinity indices decreased with increased rotational speed, presence of baffles, and cultivation time. The cellulose crystallinity indices were assessed by both XRD and ATR-FTIR spectroscopy. Crystallinity indices of cellulose indicate a change in the crystalline structure of cellulose at the molecular level. Crystallinity influences the physical, chemical, and mechanical properties of cellulose and an important feature for the use of cellulose in diverse applications. The versatility of bacterial cellulose production using different methods provides ample opportunities to tailor cellulose crystallinity during

cultivation. This work underlines the importance of the level of mixing and the length of cultivation time on bacterial cell growth, bacterial cellulose production, and bacterial cellulose crystallinity. The findings of this study provide new insights into enhancing a bioprocessing system in a scale-up bioreactor.

3.6 Reference

- Abeer, M. M., Mohd Amin, M. C. I. & Martin, C. 2014. A review of bacterial cellulose-based drug delivery systems: their biochemistry, current approaches and future prospects. *Journal of Pharmacy and Pharmacology*, 66, 1047-1061.
- Ahvenainen, P., Kontro, I. & Svedström, K. 2016. Comparison of sample crystallinity determination methods by X-ray diffraction for challenging cellulose I materials. *Cellulose*, 23, 1073-1086.
- Atalla, R. H. & Vanderhart, D. L. 1984. Native Cellulose: A Composite of Two Distinct Crystalline Forms. *Science*, 223, 283-285.
- Awa, K., Shinzawa, H. & Ozaki, Y. 2014. An Effect of Cellulose Crystallinity on the Moisture Absorbability of a Pharmaceutical Tablet Studied by Near-Infrared Spectroscopy. *Applied Spectroscopy*, 68, 625-632.
- Bae, S., Sugano, Y. & Shoda, M. 2004. Improvement of bacterial cellulose production by addition of agar in a jar fermentor. *Journal of bioscience and bioengineering*, 97, 33-8.
- Brown, R. M., Willison, J. H. M. & Richardson, C. L. 1976. Cellulose biosynthesis in *Acetobacter xylinum*: Visualization of the site of synthesis and direct measurement of the in vivo process*. *Cell Biology*, 73, 4565-4569.
- Cacicedo, M. L., Castro, M. C., Servetas, I., Bosnea, L., Boura, K., Tsafrakidou, P., Dima, A., Terpou, A., Koutinas, A. & Castro, G. R. 2016. Progress in bacterial cellulose matrices for biotechnological applications. *Bioresource Technology*, 213, 172-180.
- Carrillo, F., Colom, X., Suñol, J. J. & Saurina, J. 2004. Structural FTIR analysis and thermal characterisation of lyocell and viscose-type fibres. *European Polymer Journal*, 40, 2229-2234.
- Castro, C., Zuluaga, R., Putaux, J.-L., Caro, G., Mondragon, I. & Gañán, P. 2011. Structural characterization of bacterial cellulose produced by *Gluconacetobacter swingsii* sp. from Colombian agroindustrial wastes. *Carbohydrate Polymers*, 84, 96-102.
- Charreau, H., Foresti, M. L. & Vasquez, A. 2013. *Nanocellulose patents trends: A comprehensive review on patents on cellulose nanocrystals, microfibrillated and bacterial cellulose*, Bentham Science Publishers.

- Cheng, K. C., Catchmark, J. M. & Demirci, A. 2009. Enhanced production of bacterial cellulose by using a biofilm reactor and its material property analysis. *Journal of biological engineering*, 3, 12.
- Cheng, K. C., Catchmark, J. M. & Demirci, A. 2011. Effects of CMC addition on bacterial cellulose production in a biofilm reactor and its paper sheets analysis. *Biomacromolecules*, 12, 730-6.
- Ciolacu, D., Ciolacu, F. & Popa, V. 2011. Amorphous Cellulose - Structure and Characterization. *Cellulose Chemistry and Technology*, 45, 13-21.
- Czaja, W., Romanovicz, D. & Brown, R. M. 2004. Structural investigations of microbial cellulose produced in stationary and agitated culture. *Cellulose*, 11, 403-411.
- Dayal, M. S., Goswami, N., Sahai, A., Jain, V., Mathur, G. & Mathur, A. 2013. Effect of media components on cell growth and bacterial cellulose production from *Acetobacter aceti* MTCC 2623. *Carbohydrate Polymers*, 94, 12-16.
- Figueiredo, A. R. P., Silvestre, A. J. D., Neto, C. P. & Freire, C. S. R. 2015. In situ synthesis of bacterial cellulose/polycaprolactone blends for hot pressing nanocomposite films production. *Carbohydrate Polymers*, 132, 400-408.
- Gatenholm, P. & Klemm, D. 2010. Bacterial Nanocellulose as a Renewable Material for Biomedical Applications. *MRS Bulletin*, 35, 208-213.
- Gea, S., Reynolds, C. T., Roohpur, N., Soykeabkaew, N., Wirjosentono, B., Bilotti, E. & Peijs, T. 2010. Biodegradable Composites Based on Poly(-Caprolactone) and Bacterial Cellulose as a Reinforcing Agent. *Journal of Biobased Materials and Bioenergy*, 4, 384-390.
- Haigler, C. H., White, A. R., Brown, R. M. & Cooper, K. M. 1982. Alteration of in vivo cellulose ribbon assembly by carboxymethylcellulose and other cellulose derivatives. *Journal of Cell Biology*, 94, 64-69.
- Hall, M., Bansal, P., Lee, J. H., Reaff, M. J. & Bommaris, A. S. 2010. Cellulose crystallinity – a key predictor of the enzymatic hydrolysis rate. *FEBS Journal*, 277, 1571-1582.
- Hirai, A., Tsuji, M. & Horii, F. 1997. COMMUNICATION: Culture conditions producing structure entities composed of Cellulose I and II in bacterial cellulose. *Cellulose*, 4, 239-245.
- Hirai, A., Tsuji, M., Yamamoto, H. & Horii, F. 1998. In Situ Crystallization of Bacterial Cellulose III. Influences of Different Polymeric Additives on the Formation of Microfibrils as Revealed by Transmission Electron Microscopy. *Cellulose*, 5, 201-213.

- Huang, H.-C., Chen, L.-C., Lin, S.-B. & Chen, H.-H. 2011. Nano-biomaterials application: In situ modification of bacterial cellulose structure by adding HPMC during fermentation. *Carbohydrate Polymers*, 83, 979-987.
- Jorfi, M. & Foster, E. J. 2015. Recent advances in nanocellulose for biomedical applications. *Journal of Applied Polymer Science*, 132.
- Joseph, G., Rowe, G. E., Margaritis, A. & Wan, W. 2003. Effects of polyacrylamide-co-acrylic acid on cellulose production by *Acetobacter xylinum*. *Journal of Chemical Technology and Biotechnology*, 78, 964-970.
- Kafle, K., Shin, H., Lee, C. M., Park, S. & Kim, S. H. 2015. Progressive structural changes of Avicel, bleached softwood, and bacterial cellulose during enzymatic hydrolysis. *Scientific Reports*, 5, 15102.
- Kim, Y., Jung, R., Kim, H.-S. & Jin, H.-J. 2009. Transparent nanocomposites prepared by incorporating microbial nanofibrils into poly(l-lactic acid). *Current Applied Physics*, 9, S69-S71.
- Klemm, D., Kramer, F., Moritz, S., Lindström, T., Ankerfors, M., Gray, D. & Dorris, A. 2011. Nanocelluloses: A new family of nature-based materials. *Angewandte Chemie (International Edition)*, 50, 5438-5466.
- Klemm, D., Schumann, D., Udhardt, U. & Marsch, S. 2001. Bacterial synthesized cellulose — artificial blood vessels for microsurgery. *Progress in Polymer Science*, 26, 1561-1603.
- Lee, K.-Y., Buldum, G., Mantalaris, A. & Bismarck, A. 2014. More than meets the eye in bacterial cellulose: Biosynthesis, bioprocessing, and applications in advanced fiber composites. *Macromolecular Bioscience*, 14, 10-32.
- Li, C., Xia, J.-Y., Chu, J., Wang, Y.-H., Zhuang, Y.-P. & Zhang, S.-L. 2013. CFD analysis of the turbulent flow in baffled shake flasks. *Biochemical Engineering Journal*, 70, 140-150.
- Miller, G. L. 1959. Use of Dinitrosalicylic Acid Reagent for Determination of Reducing Sugar. *Analytical Chemistry*, 31, 426-428.
- Müller, A., Ni, Z., Hessler, N., Wesarg, F., Müller, F. A., Kralisch, D. & Fischer, D. 2013. The biopolymer bacterial nanocellulose as drug delivery system: Investigation of drug loading and release using the model protein albumin. *Journal of Pharmaceutical Sciences*, 102, 579-592.
- Nelson, M. L. & O'connor, R. T. 1964a. Relation of certain infrared bands to cellulose crystallinity and crystal lattice type. Part II. A new infrared ratio for estimation of crystallinity in celluloses I and II. *Journal of Applied Polymer Science*, 8, 1325-1341.

- Nelson, M. L. & O'connor, R. T. 1964b. Relation of certain infrared bands to cellulose crystallinity and crystal latticed type. Part I. Spectra of lattice types I, II, III and of amorphous cellulose. *Journal of Applied Polymer Science*, 8, 1311-1324.
- Oh, S. Y., Yoo, D. I., Shin, Y., Kim, H. C., Kim, H. Y., Chung, Y. S., Park, W. H. & Youk, J. H. 2005. Crystalline structure analysis of cellulose treated with sodium hydroxide and carbon dioxide by means of X-ray diffraction and FTIR spectroscopy. *Carbohydrate Research*, 340, 2376-2391.
- Oshima, T., Taguchi, S., Ohe, K. & Baba, Y. 2011. Phosphorylated bacterial cellulose for adsorption of proteins. *Carbohydrate Polymers*, 83, 953-958.
- Park, J., Hyun, S. & Jung, J. 2004. Conversion of *G. hansenii* PJK into non-cellulose-producing mutants according to the culture condition. *Biotechnology and Bioprocess Engineering*, 9, 383-388.
- Park, S., Baker, J. O., Himmel, M. E., Parilla, P. A. & Johnson, D. K. 2010. Cellulose crystallinity index: measurement techniques and their impact on interpreting cellulase performance. *Biotechnology for Biofuels*, 3, 10-10.
- Reiniati, I., Hrymak, A. N. & Margaritis, A. 2017. Recent developments in the production and applications of bacterial cellulose fibers and nanocrystals. *Critical Reviews in Biotechnology*, 37, 510-524.
- Roman, M. & Winter, W. T. 2004. Effect of Sulfate Groups from Sulfuric Acid Hydrolysis on the Thermal Degradation Behavior of Bacterial Cellulose. *Biomacromolecules*, 5, 1671-1677.
- Ruka, D. R., Simon, G. P. & Dean, K. M. 2012. Altering the growth conditions of *Gluconacetobacter xylinus* to maximize the yield of bacterial cellulose. *Carbohydrate Polymers*, 89, 613-622.
- Ruka, D. R., Simon, G. P. & Dean, K. M. 2013. In situ modifications to bacterial cellulose with the water insoluble polymer poly-3-hydroxybutyrate. *Carbohydrate Polymers*, 92, 1717-1723.
- Sacui, I. A., Nieuwendaal, R. C., Burnett, D. J., Stranick, S. J., Jorfi, M., Weder, C., Foster, E. J., Olsson, R. T. & Gilman, J. W. 2014. Comparison of the Properties of Cellulose Nanocrystals and Cellulose Nanofibrils Isolated from Bacteria, Tunicate, and Wood Processed Using Acid, Enzymatic, Mechanical, and Oxidative Methods. *ACS Applied Materials & Interfaces*, 6, 6127-6138.
- Saska, S., Barud, H. S., Gaspar, A. M. M., Marchetto, R., Ribeiro, S. J. L. & Messaddeq, Y. 2011. Bacterial Cellulose-Hydroxyapatite Nanocomposites for Bone Regeneration. *International Journal of Biomaterials*, 2011.
- Schmitt, J. & Flemming, H.-C. 1998. FTIR-spectroscopy in microbial and material analysis. *International Biodeterioration & Biodegradation*, 41, 1-11.

- Segal, L., Creely, J. J., Martin, A. E. & Conrad, C. M. 1959. An Empirical Method for Estimating the Degree of Crystallinity of Native Cellulose Using the X-Ray Diffractometer. *Textile Research Journal*, 29, 786-794.
- Shah, N., Ul-Islam, M., Khattak, W. A. & Park, J. K. 2013. Overview of bacterial cellulose composites: A multipurpose advanced material. *Carbohydrate Polymers*, 98, 1585-1598.
- Široký, J., Blackburn, R. S., Bechtold, T., Taylor, J. & White, P. 2010. Attenuated total reflectance Fourier-transform Infrared spectroscopy analysis of crystallinity changes in lyocell following continuous treatment with sodium hydroxide. *Cellulose*, 17, 103-115.
- Son, H. J., Kim, H. G., Kim, K. K., Kim, H. S., Kim, Y. G. & Lee, S. J. 2003. Increased production of bacterial cellulose by *Acetobacter sp.* V6 in synthetic media under shaking culture conditions. *Bioresource technology*, 86, 215-9.
- Sugiyama, J., Persson, J. & Chanzy, H. 1991. Combined infrared and electron diffraction study of the polymorphism of native celluloses. *Macromolecules*, 24, 2461-2466.
- Terinte, N., Ibbett, R. & Schuster, K. C. 2011. Overview on native cellulose and microcrystalline cellulose I structure studied by x-ray diffraction (WAXD): comparison between measurement techniques. *Lenzinger Berichte*, 89, 118-131.
- Vasquez, A., Foresti, M., Cerrutti, P. & Galvagno, M. 2013. Bacterial Cellulose from Simple and Low Cost Production Media by *Gluconacetobacter xylinus*. *Journal of Polymers and the Environment*, 21, 545-554.
- Watanabe, K., Tabuchi, M., Morinaga, Y. & Yoshinaga, F. 1998. Structural features and properties of bacterial cellulose produced in agitated culture. *Cellulose*, 5, 187-200.
- Yamamoto, H., Horii, F. & Hirai, A. 1996. In situ crystallization of bacterial cellulose II. Influences of different polymeric additives on the formation of celluloses Ia and Ib at the early stage of incubation. *Cellulose*, 3, 229-242.
- Yang, G., Xie, J., Hong, F., Cao, Z. & Yang, X. 2012. Antimicrobial activity of silver nanoparticle impregnated bacterial cellulose membrane: Effect of fermentation carbon sources of bacterial cellulose. *Carbohydrate Polymers*, 87, 839-845.
- Yano, H., Sugiyama, J., Nakagaito, A. N., Nogi, M., Matsuura, T., Hikita, M. & Handa, K. 2005. Optically Transparent Composites Reinforced with Networks of Bacterial Nanofibers. *Advanced Materials*, 17, 153-155.
- Zeng, X., Liu, J., Chen, J., Wang, Q., Li, Z. & Wang, H. 2011. Screening of the common culture conditions affecting crystallinity of bacterial cellulose. *Journal of Industrial Microbiology and Biotechnology*, 38, 1993-1999.

Zhou, L. L., Sun, D. P., Hu, L. Y., Li, Y. W. & Yang, J. Z. 2007. Effect of addition of sodium alginate on bacterial cellulose production by *Acetobacter xylinum*. *Journal of Industrial Microbiology and Biotechnology*, 34, 483-9.

Chapter 4

4 Kinetics of Cell Growth and Crystalline Nanocellulose Production by *Komagataeibacter xylinus*

The information presented in this Chapter is based on the paper “Kinetics of Cell Growth and Crystalline Nanocellulose Production by *Komagataeibacter xylinus*”, published online in Biochemical Engineering Journal, In Press, 22 July 2017 (<https://doi.org/10.1016/j.bej.2017.07.007>).

4.1 Abstract

The mass transfer rate of oxygen often limits the cell growth of aerobic bacteria and its product formation. Baffles and agitation increase mixing and oxygen transfer. The effects of agitation rates on the cell growth and oxygen uptake rate (OUR) of *Gluconacetobacter xylinus* (*G. xylinus*), recently named *Komagataeibacter xylinus* (*K. xylinus*), in stirred-tank bioreactors are presented in this study. Agitation rates also affected the bacterial cellulose production with yields of 1.13 and 0.54 g/l at agitation rates of 700 rpm and 500 rpm, respectively. Stirred-tank bioreactors offer a means to scale up production and result in higher production yields of bacterial cellulose. Separation and purification of bacterial cellulose was achieved in a one step process and preserved the crystalline cellulose I_α structure. This work gives insight into the conditions necessary to increase bacterial cellulose production and to alter the bacterial cellulose crystallinity during bioprocessing.

4.2 Introduction

Interest in bacterial cellulose has been increasing in past decades due to its high purity, biocompatibility, and high mechanical strength. Currently, bacterial cellulose is used in a range of applications, including nanocomposites, biomedical devices, drug delivery, environmental remediation, and materials science (Gatenholm and Klemm, 2010, Reiniati et al., 2017, Klemm et al., 2011, Shah et al., 2013, Cacicedo et al., 2016). Although

bacterial cellulose has the same chemical structure as plant cellulose, bacterial cellulose is produced free from hemicellulose, lignin, and other non-cellulosic materials. One of the advantages of bacterial cellulose is the ability to modify its physical characteristics during bioprocessing. Bacterial cellulose produced in the presence of water soluble polymers carboxymethyl cellulose exhibited smaller-size microfibrils (Haigler et al., 1982), increased rehydration ability (Chen et al., 2011, Huang et al., 2010), increased copper ions absorption capacity (Seifert et al., 2003), and decreased cellulose crystallinity (Chen et al., 2011, Huang et al., 2010). Dispersion of insoluble polymers during bacterial cellulose synthesis allowed the incorporation of polycaprolactone and poly-3-hydroxybutyrate within the cellulose network, altering the crystallinity, morphology, mechanical performance, and thermal stabilities of bacterial cellulose nanocomposites, without the use of harmful organic solvents commonly used to dissolve these polymers (Figueiredo et al., 2015, Ruka et al., 2013). In addition, cultivation methods including: static culture, shaken culture, and agitated culture, influence the arrangement and crystallization of cellulose microfibrils (Czaja et al., 2004, Krystynowicz et al., 2002). The versatility of bacterial cellulose allows it to be tailored to specific applications.

The success of building an economically viable bioprocessing method depends highly on lowering the cost of substrates, increasing the product yield, and enhancing the rate of production. The prospect of using inexpensive feedstocks as substrates makes bacterial cellulose production more attractive and feasible, which is likely to encourage future growth of bacterial cellulose production and its application in various products and industries. The production of bacterial cellulose using agricultural and industrial food wastes, including saccharified food wastes (Song et al., 2009), grape medium (Rani et al., 2011), pineapple juice (Castro et al., 2011), grape bagasse (Vaszquez et al., 2013), glycerol from biodiesel (Vaszquez et al., 2013), low quality date syrup (Moosavi-Nasab and Yousefi, 2011), and many others (Cacicedo et al., 2016) have been previously demonstrated. These media have different types of substrates, nitrogen, and proteins which affect the kinetics of cell growth and bacterial cellulose production.

The conventional method of static culture has been successful in producing bacterial cellulose; however, static culturing requires a long period of cultivation of at least 2 weeks

(Hornung et al., 2006b). Different types of bioreactors have been used to enhance the production of bacterial cellulose, including stirred tank reactors (Bae and Shoda, 2005, Cheng et al., 2009b, Kouda et al., 1997), rotating disk bioreactors (Kim et al., 2007, Krystynowicz et al., 2002), air-lift bubble reactors (Chao et al., 2000, Wu and Li, 2015), and variations of surface culture reactors (Hornung et al., 2007, Kralisch et al., 2010). These bioreactor systems provide the capability to control bioprocessing parameters, including agitation rate, aeration rate, pH, and dissolved oxygen (DO) level.

Stirred-tank bioreactors offer high volumetric mass-transfer coefficients for oxygen transfer and flexibility for commercial use. Baffles and agitation in a bioreactor facilitate nutrients and oxygen mass transfer from the liquid medium to the bacterial cells. Impellers and agitation play a role in improving the bacterial cellulose yield and production rate (Kouda et al., 1997) through rapid mixing, which disperses gas bubbles throughout the bioreactor and breaks larger bubbles into small bubbles. However, it is important to modulate stirring rates because *Gluconacetobacter* has been reported to exhibit shear sensitivity, which promotes the conversion of cellulose producing cells into non-cellulose producing cells (Park et al., 2004). The intense mixing and high shear stress in a stirred-tank bioreactor not only affect the bacterial cell growth, but also the physical and structural properties of bacterial cellulose fibers. Shaking and agitation affect the cellulose crystallinity, cellulose crystallite size, and degree of polymerization (Czaja et al., 2004, Krystynowicz et al., 2002, Watanabe et al., 1998).

The influence of mixing and shear stress on the volumetric bacterial cells oxygen uptake rate (OUR) and volumetric mass transfer coefficient (k_{La}) have not been investigated in detail. The determination of k_{La} is essential to establish aeration efficiency and to quantify the effects of operating variables on the provision of oxygen. However, the measurement of k_{La} is complex because dissolved solutes, temperature, and pressure affect the solubility of oxygen (Shuler and Kargi, 2002). During bioprocessing, the amount of dissolved solutes changes with time, imposing changes in k_{La} . Culture broth during bacterial cellulose production exhibits non-Newtonian fluid behavior (Kouda et al., 1996). The OUR and k_{La} determination during bioprocessing have not been performed previously.

There are several methods to determine the k_{LA} value (Garcia-Ochoa and Gomez, 2009). A static gassing-out method was employed to measure k_{LA} in a stirred-tank reactor with different agitators (Kouda et al., 1997) and air-lift bioreactor (Chao et al., 2001a). Since there is only suspended bacterial cellulose without living bacterial cells, this measurement method does not adequately represent the true k_{LA} during the bioprocessing. The dynamic gassing-out method is widely used to measure OUR and k_{LA} during bioprocessing, but have not yet been used on bacterial cellulose production in a stirred-tank. However, the dynamic gassing-out method has an inherent limitation when there is an increase in viscosity and cell concentration.

This study presents the behavior of *K. xylinus* growing in a turbulent liquid medium and characterizes the bacterial cellulose fibers. Production of bacterial cellulose was performed in a stirred tank bioreactor agitated by two disks of six blades of Rushton turbines at a rate of 700 and 500 rpm. A relatively low substrate concentration was used to examine the growth kinetics behavior of *K. xylinus* affected by mixing. Bacterial cellulose production, cell concentration, sugar consumption, pH and DO level from the bioreactor were reported. The morphology of bacterial cellulose fibers was observed using scanning electron microscope (SEM) to confirm the success of the purification step. This work presents the kinetics of cell growth and the oxygen uptake rate profile of *K. xylinus* cultivated in a stirred-tank bioreactor. This study provides a crucial information to promote crystalline nanocellulose production.

4.3 Materials and experimental methods

4.3.1 Microorganism

K. xylinus (ATCC No. 700178) obtained from the American Type Culture Collection (ATCC, Rockville, MD) was grown in a fructose-based medium with corn steep solid solution (fru-CSS medium).

4.3.2 Culture media

All chemicals were analytical grade and commercially available (Sigma-Aldrich, ON, Canada). For inoculum medium, the following compositions dissolved in 1 L of distilled

water: 20 g fructose, centrifuged 20 g CSS solution, 1 g KH_2PO_4 , 3.3 g $(\text{NH}_4)_2\text{SO}_4$, 0.8 g $\text{MgSO}_4 \cdot 7\text{H}_2\text{O}$, 2.4 g trisodium citrate dehydrate and 1.6 g citric acid (modified from (Joseph et al., 2003)). The initial pH was adjusted to 5 by addition of 2 M NaOH. The medium was then autoclaved at 121°C for 15 minutes. From a medium optimization study in shake flasks (data not shown), the concentrations of fructose and CSS were modified to 25 g/l and 35 g/l, respectively. The initial pH of medium was adjusted to at 4.5. The medium was poured into the 3-L bioreactor and was autoclaved for 30 min.

4.3.3 Inoculum and culture conditions

The inoculum was prepared by adding 1 ml of 30 % (v/v) glycerol stock culture stored in -80°C freezer to 100 ml of fru-CSS medium in a 500 ml flask, and was grown for 3 days in a 30°C incubator without agitation. Using a 6.25% (v/v) inoculum ratio, 10 ml of inoculum was added to 150 ml of fresh fru-CSS medium in a 500 ml baffled flask and was incubated in a rotary shaker at 250 rpm and 30°C for 27 hours. The broth was blended aseptically using a Waring blender for 1 min and was used to inoculate the bioreactor. Figure 4.1 shows the schematic diagram of production and purification of bacterial cellulose fibers. A 100 ml of the inoculum was added to 1500 ml of fru-CSS medium in a 3L bioreactor (Bioflo 110, New Brunswick Scientific) (Figure 4.2) equipped with aeration controller, pH, DO, temperature and foam probes.

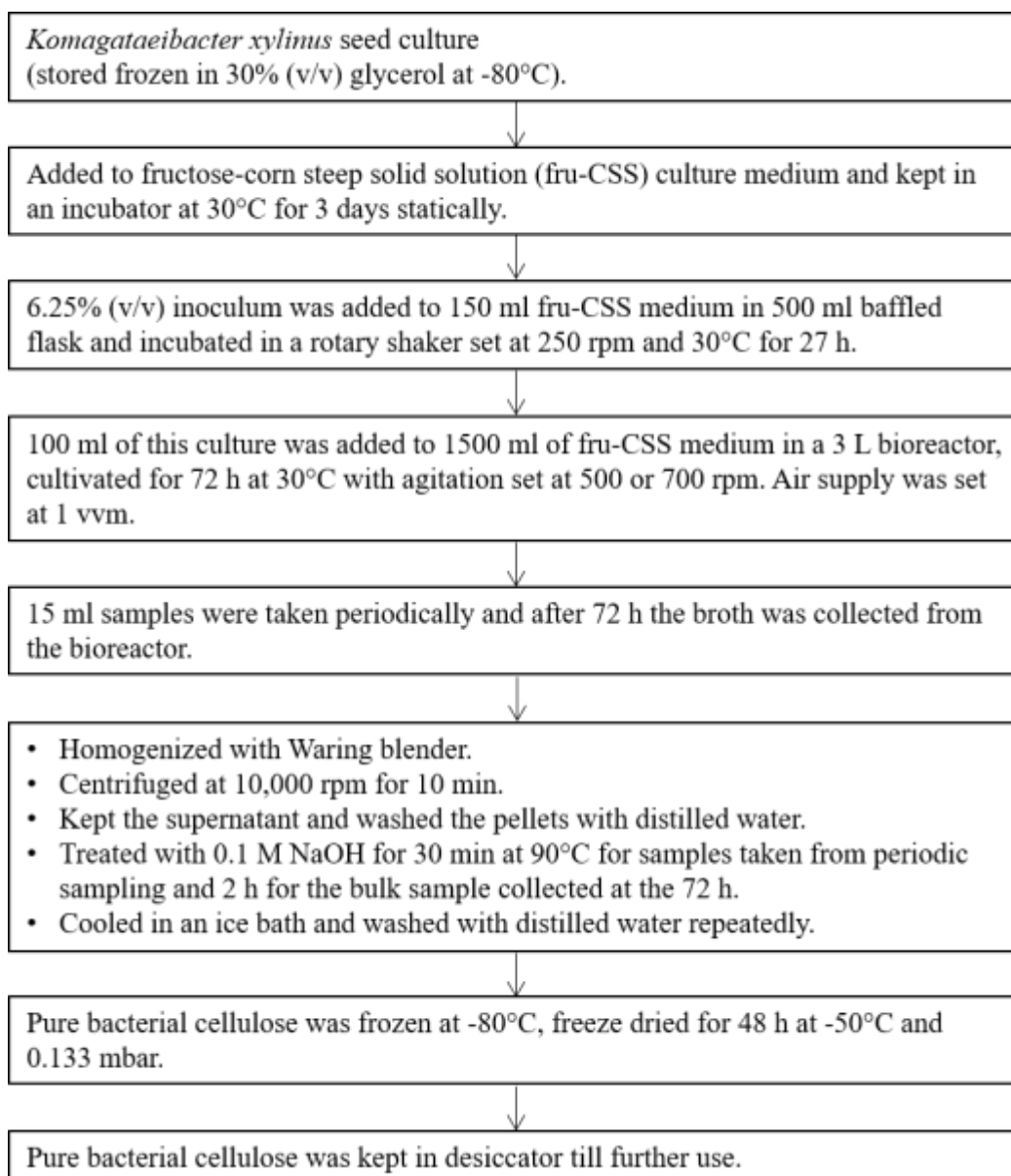


Figure 4.1. Schematic diagram of bacterial cellulose production.

4.3.4 Operational conditions

The air flow rate and temperature of culture broth were maintained at 1 vvm and 30°C, respectively. DO and pH probes were used to monitor the change in DO concentration and pH of the medium, respectively. Agitation was provided by two-disk Rushton turbine impellers set at 700 rpm and 500 rpm for 72 h with periodical sampling. Sterilized anti-

foam was added to the medium as necessary during the cultivation. After 5 min of inoculation, the first sample, $t = 0$ h, was collected. Approximately 15 ml of sample was taken out of the bioreactor periodically to construct a growth curve. DO, pH and temperature readings were recorded for each sampling time. The broth was collected, mixed, and homogenized with a Waring blender. Right after taking samples, the dynamic gassing out method was performed and the DO reading was obtained by an on-line Ingold polarographic electrode.

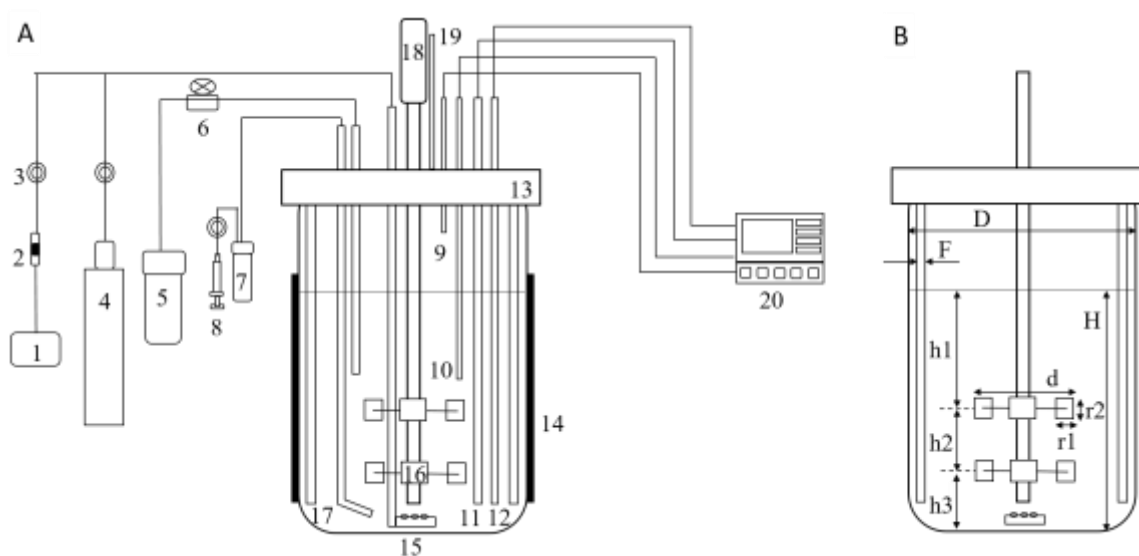


Figure 4.2. Schematic diagram of (A) a 3-L bioreactor used in batch fermentation for bacterial cellulose production (not to scale): 1) air supply, 2) flow meter, 3) air filter, 4) compressed nitrogen gas, 5) inoculum bottle, 6) peristaltic pump for inoculum feeding, 7) sampling tube, 8) syringe, 9) level probe, 10) temperature electrode, 11) pH electrode, 12) DO probe, 13) head plate, 14) strap heater, 15) air sparger, 16) Rushton turbine impeller, 17) baffles, 18) agitation motor, 19) gas outlet, 20) control panel. Legends for diagram (B): diameter of bioreactor, $D=12.5$ cm, height of liquid media, $H=17.5$ cm, baffle ($F/D=0.08$), 6-bladed Rushton-type turbine impellers ($d/D=0.44$), $H/D=1.4$, $h1/H=0.35$, $h2/H=0.39$, $h3/H=0.26$.

4.3.5 Measurement of bacterial cellulose and cell dry weight

From each 10 ml of culture broth, 5 ml were taken for measurements of bacterial cellulose and cell dry weight. Each sample was centrifuged at 10,000 rpm for 10 min and washed 5 times with 25 ml of distilled water to remove remaining nutrients. The supernatant obtained after each centrifugation was collected for protein and fructose measurement. For bacterial cellulose dry weight determination, the washed pellets were treated with 30 ml of 0.1 M NaOH for 30 min at 90°C to lyse the cells (Mikkelsen et al., 2009). The samples were washed with distilled water repeatedly to remove the alkaline solution. The pure bacterial cellulose was oven-dried for 24 h at 90°C and weighed. For cell dry weight determination, the washed pellets from the 5 ml samples were suspended in 1 ml of 2% (v/v) cellulase (Cat # C2730, Lot # SLBH0229V, Sigma Aldrich, St. Louis, MO) solution in 0.1 M citrate buffer at pH 4.8. After mixing through gentle inversion, the sample was incubated in a water bath at 50°C for 1 hour to hydrolyze the cellulose. After cooling, the mixture was filtered using a pre-weighed dried 0.45 µm cellulose nitrate filter membrane. The wet filter was then dried for 24 hours at 90°C and weighed.

4.3.6 Measurement of sugar concentration

Fructose concentration was estimated using the dinitrosalicylic acid (DNS) method (Miller, 1959). DNS reacts with reducing sugars and forms 3-amino-5-nitrosalicylic acid which absorbs light strongly at 540 nm. Briefly, one ml of sample was centrifuged in a microcentrifuge at 10,000 rpm for 5 min. Equal volume of supernatant sample and DNS reagent were mixed well and placed in a boiling water bath for 5 min. After cooling and proper dilution, the absorbance was read at 540 nm. A standard calibration curve was created using known fructose concentrations.

4.3.7 Separation and purification of bacterial cellulose fibers

BC fibers were separated from the remaining nutrients using repeated centrifugation and washing cycles. After 25 ml of homogenized culture broth was centrifuged and washed using 25 ml of distilled water for each washing cycle, the absorbance of the supernatant at a wavelength of 600 nm was read using a Genesys 10S UV-VIS spectrophotometer (Thermo Fisher Scientific, Waltham, MA, USA). After several washing cycles, the cleaned

pellets, free from nutrients, were treated with 30 ml of 0.1 M NaOH at 90°C for 30 and 60 min to lyse the cells. For bulk samples, 500 ml broth was centrifuged, washed with distilled water, and treated with 500 ml of 0.1 M NaOH for 1 h and 2 h min at 90°C to lyse the cells. The pure bacterial cellulose samples were washed repeatedly with distilled water and were frozen in a -80°C freezer. The samples were lyophilized using Savant ModulyoD freeze dryer (Thermo Fisher Scientific, Waltham, MA, USA).

4.3.8 Protein quantification

Bradford reagent (Amresco LLC., Solon, OH, USA) was diluted 4 times with distilled water. After mixing thoroughly, 100 µl of sample (supernatant from washing procedure in Section 2.5) was added to 3 ml of a diluted Bradford reagent. The binding of the proteins stabilizes the blue form of Coomassie dye in Bradford reagent. The amount of the complex exhibits different shades of blue. The absorbance at 595 nm was read within 5 min after mixing. A standard calibration curve was created using known concentrations of bovine serum albumin (BSA) (Cat# A3059, Lot# 100M1767V, Sigma Aldrich, St. Louis, MO).

4.3.9 Scanning electron microscope (SEM)

The morphology of bacterial cell and the bacterial cellulose fibers was characterized using a LEO 1540 XB Scanning Electron Microscope (SEM) (Zeiss Nano Technology Systems Division, Oberkochen, Germany) with GEMINI electron optics in the Western Nanofabrication Facility at the University of Western Ontario. The freeze-dried samples were coated with 5 nm of osmium prior to analysis.

4.3.10 Fourier-Transform Infrared Spectroscopy (FTIR)

FTIR spectra of freeze-dried bacterial cellulose samples in attenuated total reflectance (ATR) mode were recorded using a Nicolet 6700 spectrophotometer (Thermo Fisher Scientific, Waltham, MA, USA). All the spectra were acquired from 4000 to 400 cm^{-1} with a scan frequency of 32 s^{-1} and a resolution of 4 cm^{-1} . An automatic baseline correction was performed on the generated spectra using OMNICTM software. Ratios of the absorption intensities were used to represent cellulose crystallinity indices. IR cellulose crystallinity indices were obtained using two methods: 1) evaluated from the ratios of the absorption

intensity at wavenumber 1428 and 897 cm^{-1} ($\text{Cr}_1 = A_{1428}/A_{897}$), and 2) evaluated from the ratios of the absorption intensity at wavenumber 1372 and 2898 cm^{-1} ($\text{Cr}_2 = A_{1372}/A_{2898}$).

4.3.11 X-ray Diffraction (XRD)

The XRD diffractogram of samples were recorded on Rigaku Ultima IV X-ray diffractometer (Rigaku, The Woodlands, TX, USA) using copper x-ray source operating at 40 kV and 40 mA. The freeze dried bacterial cellulose samples were pressed into a thin and flat layer using glass slides, and analyzed following a method described previously (Cheng et al., 2009b). Scans were collected at 2° per min in the range of $10\text{-}30^\circ 2\theta$. The cellulose crystallinity index was reported using the peak area method (Roman and Winter, 2004, Ruka et al., 2013). Peak fitting of individual crystalline peaks to a Gaussian function was carried out using Origin (OriginLab, Northampton, MA) Peak Analyser software. A broad peak with a maximum between 18° and 22° was fitted as the amorphous cellulose contribution. The diffraction peak position was selected within 0.2° of the literature value to represent the true peak for fitting. Cellulose crystallinity index determined by the peak area method (Cr_A) is described as a ratio of the sum of the areas under crystalline diffraction peaks to the total area under the curve between $2\theta = 10\text{-}30^\circ$ or in brief, $\text{Cr}_A = A_{\text{cr}}/(A_{\text{cr}} + A_{\text{am}})$ (Ahvenainen et al., 2016).

4.3.12 Cell growth kinetics

The growth of bacterial cells is divided into five successive phases; the lag phase followed by an exponential phase growth phase, then deceleration phase, stationary and finally the death phase (Shuler and Kargi, 2002). The logistic model, derived from Monod equation, was confirmed to describe the growth of *Acetobacter* in a static surface culture (Hornung et al., 2006b, Hornung et al., 2006a). Cell growth kinetics of *K. xylinus* in a stirred tank bioreactor and air-lift bioreactor were commonly achieved using an exponential model Monod (Bae and Shoda, 2005, Chao et al., 2001a). An exponential model, Monod's growth equation (Equation 1), was the most common way to express the dependency of cell growth on the concentration of the growth-limiting substrate.

$$\mu = \frac{\mu_{\text{max}} \cdot S}{K_S + S} \quad (\text{Equation 1})$$

The maximum specific growth rate, μ_{\max} (/h), was determined from the slope of $\ln(C_X/C_{X0})$ vs. time (h) where C_{X0} (g/l) was the initial cell dry weight concentration and C_X (g/l) was the cell dry weight concentration at different time. K_s was the Monod saturation constant and was the concentration of the rate-limiting substrate when specific growth rate equals to one-half of the maximum (Shuler and Kargi, 2002). The specific growth rate of the microorganisms, μ , is dependent on several factors, such as pH, temperature, pressure, inhibitors, as well as substrate, product and biomass concentration (Shuler and Kargi, 2002). However, most of these factors (temperature, pH, and pressure) were kept constant during the cultivation, therefore, only cells, substrate, and product concentrations really matter. Further, to better describe cell growth kinetics, yield coefficients based on the amount of consumption of another substance were used. $Y_{X/S}$ (g dry weight/g substrate) was the cell growth yield and $Y_{P/S}$ (g dry weight/g substrate) was the bacterial cellulose production yield based on the substrate consumed (Shuler and Kargi, 2002). $Y_{P/X}$ (g dry weight/g dry weight) was the ratio of bacterial cellulose produced based on the cell concentration.

4.3.13 Measurement of oxygen uptake rate (OUR)

The dynamic gassing-out and gassing-in method was employed to determine the oxygen uptake rate for a bioreactor system with organisms. This method measures the respiration activity of microorganisms growing within a well-mixed system in the bioreactor (García-Ochoa et al., 2000). The DO concentration was monitored during a short period of non-aeration (gas-out) and subsequent re-aeration (gas-in) as shown in Figure 4.3. The gas-out period was short to ensure that the volumetric oxygen uptake rate was constant (Tribe et al., 1995). The DO was kept above 15%, the critical DO concentration, in order to ensure the respiration rate coefficient was constant and no cell damage due to lack of oxygen (Shuler and Kargi, 2002). The gas out-gas in method can also provide estimates of both the oxygen uptake rate of the bacterial cells and the average oxygen interfacial concentration.

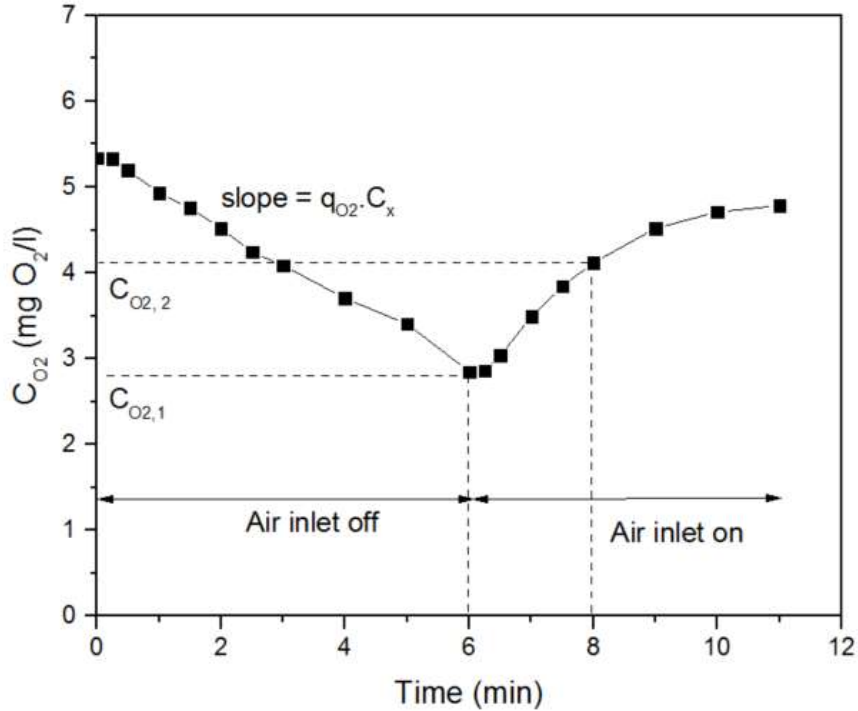


Figure 4.3. Results obtained during dynamic gassing-out for k_La and OUR determination during cultivation of *K. xylinus*.

Equation 2 describes the oxygen mass balance in batch fermentation (Shuler and Kargi, 2002). The rate of oxygen accumulation in the liquid phase (dC_{O_2}/dt (mg of DO/l-h)) is described as the difference between oxygen transfer rate (OTR) from the gas to the liquid phase and the volumetric oxygen uptake rate of microorganisms (OUR) (Shuler and Kargi, 2002).

$$\frac{dC_{O_2}}{dt} = OTR - OUR \quad (\text{Equation 2})$$

The rate of oxygen transfer from the gas to liquid phase is shown in Equation 3:

$$OTR = k_La \cdot (C^*_{O_2} - C_{O_2}) \quad (\text{Equation 3})$$

where k_La (/h) is volumetric oxygen transfer coefficient (/h), characterizing the transport from gas bubbles to liquid film, C_{O_2} (g/l) is actual DO concentration in the broth, and $C^*_{O_2}$

(g/l) is oxygen saturation concentration in the bulk liquid in equilibrium to the bulk gas phase. The rate of oxygen uptake is described in Equation 4:

$$OUR = q_{O_2} \cdot C_X \quad (\text{Equation 4})$$

where C_x (g/l) is cell dry weight concentration, and q_{O_2} (mg DO/g dry weight cell-h) is specific rate of oxygen consumption by microorganisms.

One important assumption is that the bacterial cellulose production is in a quasi-steady state between oxygen transfer and oxygen. Equation 2 reduced to Equation 5:

$$\frac{dc_{O_2}}{dt} = -q_{O_2} \cdot C_X \quad (\text{Equation 5})$$

which allows the estimation of volumetric OUR from the slope of linear regression of the change in DO concentration during gassing-out with respect to time. The oxygen saturation constant ($C^*_{O_2}$) at 30°C and 1 atm in water is 7.54 mg/l (Shuler and Kargi, 2002). The DO measurement was done at each sampling time, except when DO was near or below the DO critical level. Schematic description of the direct measuring of OTR in bioprocess by dynamic techniques is explained in detail elsewhere (Garcia-Ochoa and Gomez, 2009).

4.4 Results and Discussion

4.4.1 Bacterial cellulose formation

After cell incubation, bacterial cells adjusted to their environment and the production of bacterial cellulose did not start immediately. The culture grown in bioreactor with agitation rates of 500 rpm and 700 rpm increased in opacity within 4 hours of inoculation, indicating a rapid increase of bacterial cell and bacterial cellulose concentration. Biofilms were observed after 7 hours of cultivation on the probes and baffles close to the wall of the bioreactor. Figure 4.4 shows bacterial cellulose morphology cultivated for 7, 17, 30, and 72 h in a 3-L bioreactor with an agitation rate of 700 rpm. A thin cellulose network was formed after 7 hours and a denser fiber network was seen after 17 hours. The bacterial cells, which roughly measured approximately 2 μm , were embedded in layers of entangled cellulose fibers.

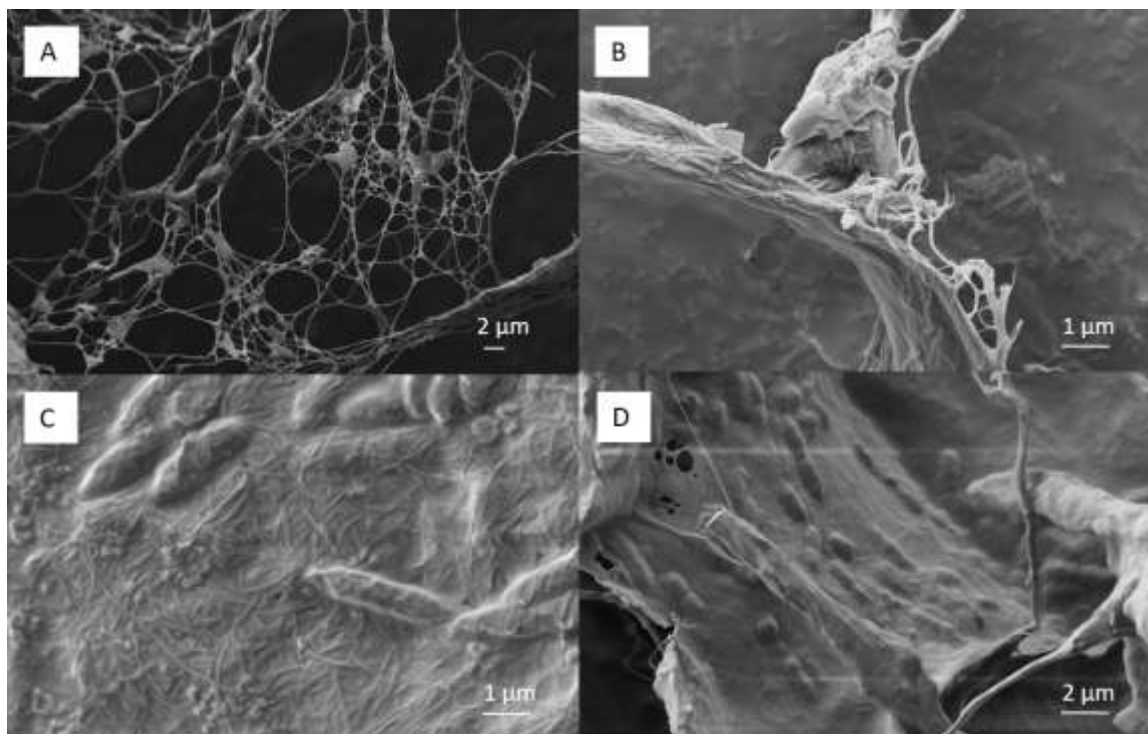


Figure 4.4. SEM images of *K. xylinus* and bacterial cellulose fibers produced in a 3-L stirred-tank bioreactor agitated at 700 rpm collected at different times: (A) 7 h, (B) 17 h, (C) 30 h, and (D) 72 h. Scale bar for (A) and (D) is 2 μm while for (B) and (C) is 1 μm .

4.4.2 Bacterial cellulose production in a stirred-tank bioreactor

Figure 4.5 and Figure 4.6 show the time course of cellular growth, bacterial cellulose production, fructose, DO concentration, and pH in a bioreactor at two different agitation rates. In both examined agitation rates, cell concentration increased slowly in the first few hours after inoculation, known as the lag phase. During this lag phase, microorganisms were adapted to new environmental conditions and the cellular biomass increased slightly. After adjusting to their new environment, the cells multiplied rapidly and cell mass increased exponentially, thus this is called the exponential growth phase. Within 7 h, cells cultivated at 500 rpm enter the exponential growth phase while it took 5 h for cells cultivated at 700 rpm. While cells grew exponentially, the DO concentration declined rapidly due to cells respiratory activities and reached minimum after 10 h for both agitation rates. In this period, fructose was consumed rapidly and depleted within 29 h and 24 h for

cells cultivated at 500 rpm and 700 rpm, respectively. Metabolic activities of cells were much faster in a bioreactor agitated at higher rates.

Once fructose was completely depleted there was no other substrate for cells to consume and thus cell growth deceleration occurred. This caused cell stress and induced cell restructuring to increase cellular survival in a hostile environment (Shuler and Kargi, 2002). Cell respiratory eventually stopped as indicated in the increased of DO concentration at 29 h and 24 h for cells cultivated at 500 rpm and 700 rpm, respectively. The stationary phase started at the end of the deceleration phase, when there was no cell growth or when the growth rate was equal to the death rate. During the stationary phase, live cells still metabolized and produced primary metabolite. The primary metabolite, i.e, bacterial cellulose, was a growth-related product. As seen in Figure 4.5A and Figure 4.6A, bacterial cellulose was still produced until the end of cultivation time of 72 h.

After 7 h of cultivation, the broth was thicker and DO was measured near a critical level of 15%. The culture broth of *K. xylinus* cultivation was non-homogeneous and showed non-Newtonian behavior with an increase in viscosity at low shear rates (Kouda et al., 1996). In addition, the pH of the growth medium increased from 4.5 to 7.1 for bioreactor agitated at 700 rpm and to pH 6 at 500 rpm by the end of cultivation time. As shown in Figure 4.5 and Figure 4.6, the pH increase occurred when the DO saturation level was at the minimum. The final DO saturation value would have returned to 100% and remained at that level as cells stopped respiration in the stationary phase.

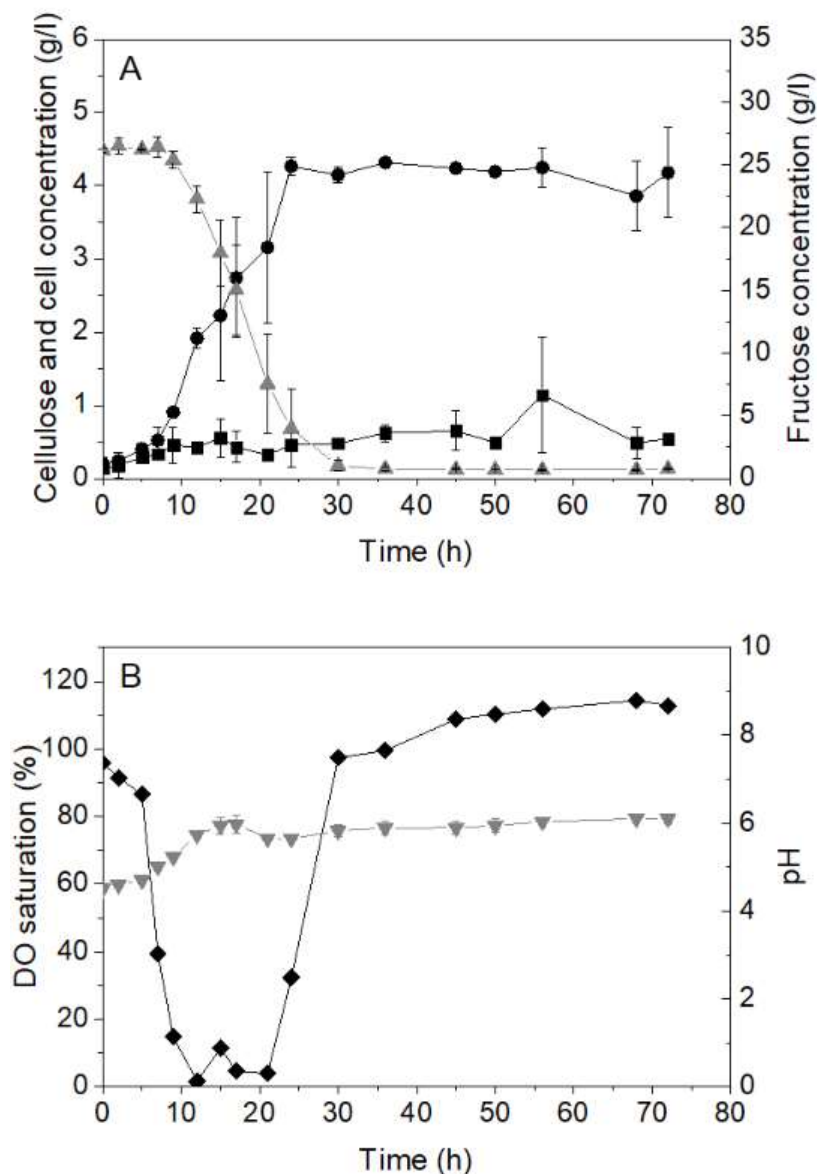


Figure 4.5 Growth kinetics of *K. xylinus* and bacterial cellulose production in a 3-L stirred-tank bioreactor with dual Rushton turbines set at agitation rates of 500 rpm (A and B), air supplied at 1 vvm, initial pH fructose-corn steep solid solution medium of 4.5 and kept at a constant temperature of 30°C. Legends: cellulose concentration (■), cell concentration (●), fructose concentration (▲), dissolved oxygen (DO) saturation (◆), and pH (▼). The values reported were obtained from duplicate runs and expressed as mean \pm standard deviation.

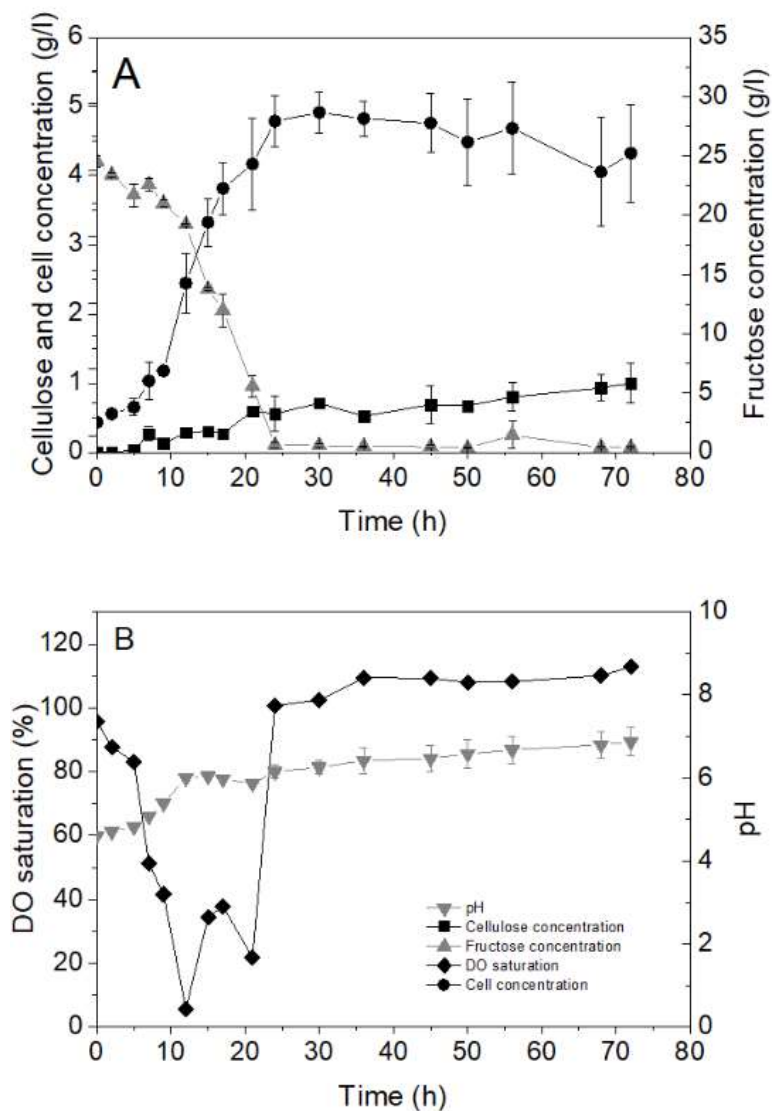


Figure 4.6 Growth kinetics of *K. xylinus* and bacterial cellulose production in a 3-L stirred-tank bioreactor with dual Rushton turbines set at agitation rates 700 rpm (A and B), air supplied at 1 vvm, initial pH fructose-corn steep solid solution medium of 4.5 and kept at a constant temperature of 30°C. Legends: cellulose concentration (■), cell concentration (●), fructose concentration (▲), dissolved oxygen (DO) saturation (◆), and pH (▼). The values reported were obtained from duplicate runs and expressed as mean \pm standard deviation.

Table 4.1 shows the process parameters and summary of results for bacterial cellulose production in a 3-L bioreactor for 72 h. Bacterial cellulose production increased steadily throughout the experiment, reaching a maximum of 1.13 g/l at 700 rpm and 0.54 g/l at 500 rpm in less than 72 h, showing 2-fold increase of bacterial cellulose production at the higher agitation rate. This indicates that the increase of agitation rate in this bioreactor promoted the bacterial cellulose production over cell growth.

Table 4.1. Process parameters for bacterial cellulose production, substrate consumption, and cell growth of *K. xylinus* in fructose-corn steep solid solution medium in a 3-L stirred-tank bioreactor at 30°C for 72 h. The values reported were obtained from duplicate runs and expressed as mean \pm standard deviation.

Process parameters	Agitation rate (rpm)	
	500	700
Bacterial cellulose production		
Bacterial cellulose (g/l)	0.54 \pm 0.00	1.13 \pm 0.10
Q _P (g/l/h)	0.01 \pm 0.00	0.02 \pm 0.00
Y _{P/S} (g/g)	0.02 \pm 0.00	0.05 \pm 0.00
Y _{P/X} (g/g)	0.13 \pm 0.02	0.27 \pm 0.07
Substrate consumption		
Fructose consumed (%)	97.58 \pm 0.52	98.27 \pm 0.21
Q _S (g/l/h)	0.35 \pm 0.00	0.33 \pm 0.01
Cell growth		
Cell (g/l)	4.18 \pm 0.62	4.25 \pm 0.74
Y _{X/S} (g/g)	0.16 \pm 0.02	0.18 \pm 0.03
μ _{max} (/h)	0.15 \pm 0.02	0.17 \pm 0.01
K _S (g/l)	7.03 \pm 2.64	18.90 \pm 1.56

Figure 4.7 shows the trend of OUR and q_{O_2} during bacterial cellulose production in a bioreactor agitated at 500 rpm and 700 rpm, respectively. The growth of bacterial cells was minimal during the lag phase, while OUR and q_{O_2} increased quickly, reaching maximum after 4 hours of cultivation in 700 rpm and after 7 hours of cultivation in 500 rpm. During this time, cells metabolized the substrate and acclimatized to the new environment. After

the lag phase ended, cells entered the cell growth phase and self replicated. During this growth phase, the OUR and q_{O_2} were not able to be measured since the DO reading fell below a critical level and gassing off was not performed. This could be because bacterial cellulose pellets or biofilm covered the DO probe, or there was a large oxygen requirement for cellular respiration. Hence, this graph represents the OUR and q_{O_2} trend during lag phase and stationary growth phase. The OUR and q_{O_2} dropped precipitously and reached a minimum after 30 hours. The tendency of OUR and q_{O_2} to drop drastically and reach a minimum at the end of stationary phase before cell death has been observed during bacterial cellulose production supplied with oxygen enriched air (Chao et al., 2001b) and xanthan gum production (García-Ochoa et al., 2000). The decline in OUR during the stationary phase can be attributed to the slowing down of active primary metabolism.

Oxygen transfer is often the rate-limiting step in aerobic bioprocesses, and the correct measurement or calculation of k_{La} is crucial in the design and scale-up of bioreactors (Garcia-Ochoa and Gomez, 2009). The k_{La} value offers a tool for scaling up fermentation strategies to provide similar aerobic growth conditions at different sizes or in different fermentation systems, and to achieve the desired product concentration at higher volumes. The magnitude of k_{La} is strongly dependent on the mixing speed used in a bioreactor system (Garcia-Ochoa and Gomez, 2009). Despite its importance, direct measuring of OTR in bioprocesses using dynamic methods is not commonly employed. Several studies obtained OTR using static gassing-out method and gas phase analysis for bacterial cellulose production (Kouda et al., 1997, Song et al., 2009). The broth culture containing four phases: liquid medium, air and carbon dioxide gas, cells, and insoluble bacterial cellulose pellets, is a complex system and an accurate calculation of k_{La} is difficult to achieve. The dynamic gassing-out and gassing-in method is less accurate when the DO concentration is very low, which occurred in this study.

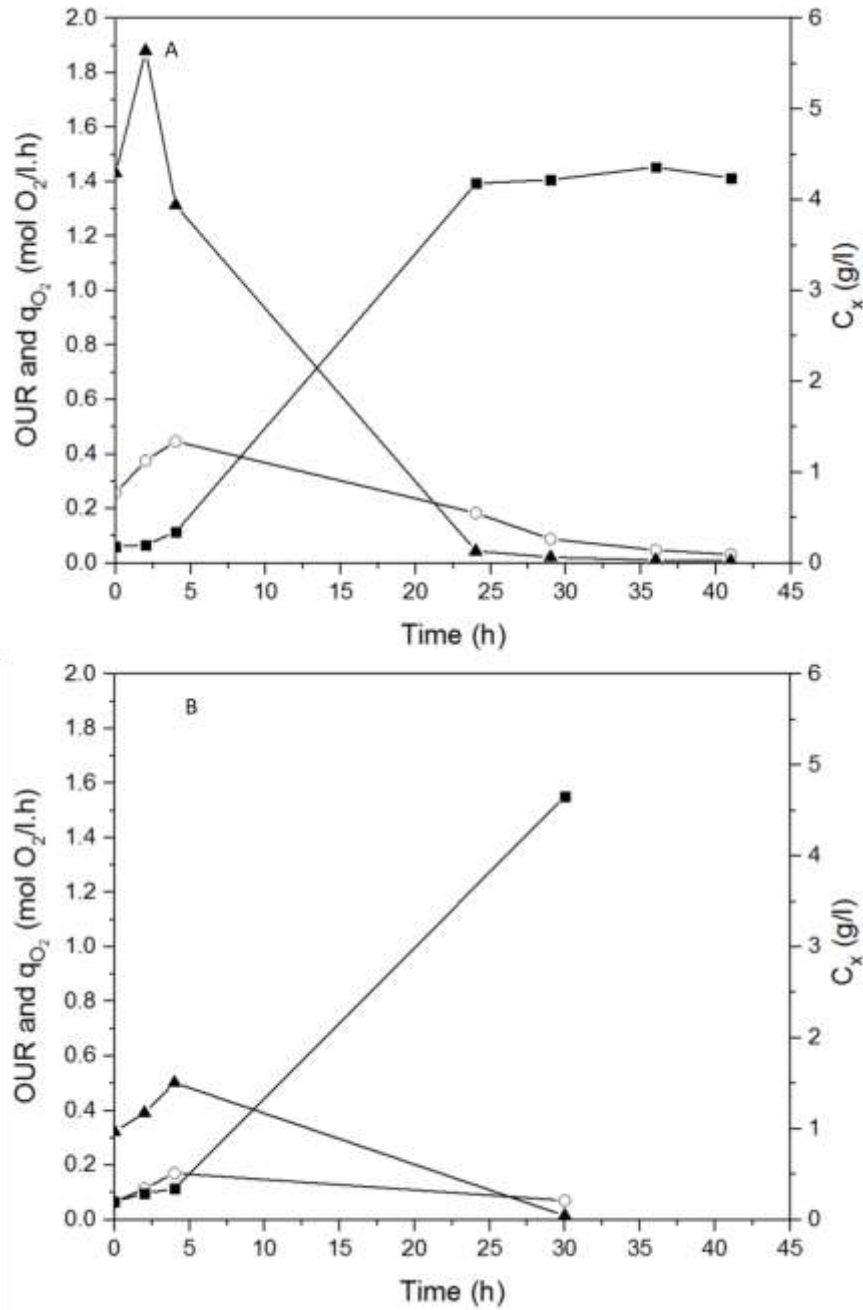


Figure 4.7. Experimental data for oxygen uptake rate (OUR), specific oxygen uptake rate (q_{O_2}), and bacterial cellulose concentration (C_x) in a bioreactor agitated at (A) 500 rpm and (B) 700 rpm. Legends: OUR (○), q_{O_2} (▲), and C_x (■).

4.4.3 Separation and purification of bacterial cellulose fibers

Separation of cell and bacterial cellulose fibers from the liquid medium was obtained by centrifugation and repeated washing cycles with distilled water. The first purification step was to separate the biomass from the liquid medium and nutrients. The absorbance of supernatant samples after each washing with distilled water decreased and eventually leveled off after 3 washes (Figure 4.8A). The protein concentration in supernatant samples from each washing cycle decreased and reached nearly zero after the fourth washing cycle (Figure 4.8B). Once the soluble nutrients were removed, samples were treated with a dilute NaOH solution to lyse the bacterial cells, generating pure bacterial cellulose fibers.

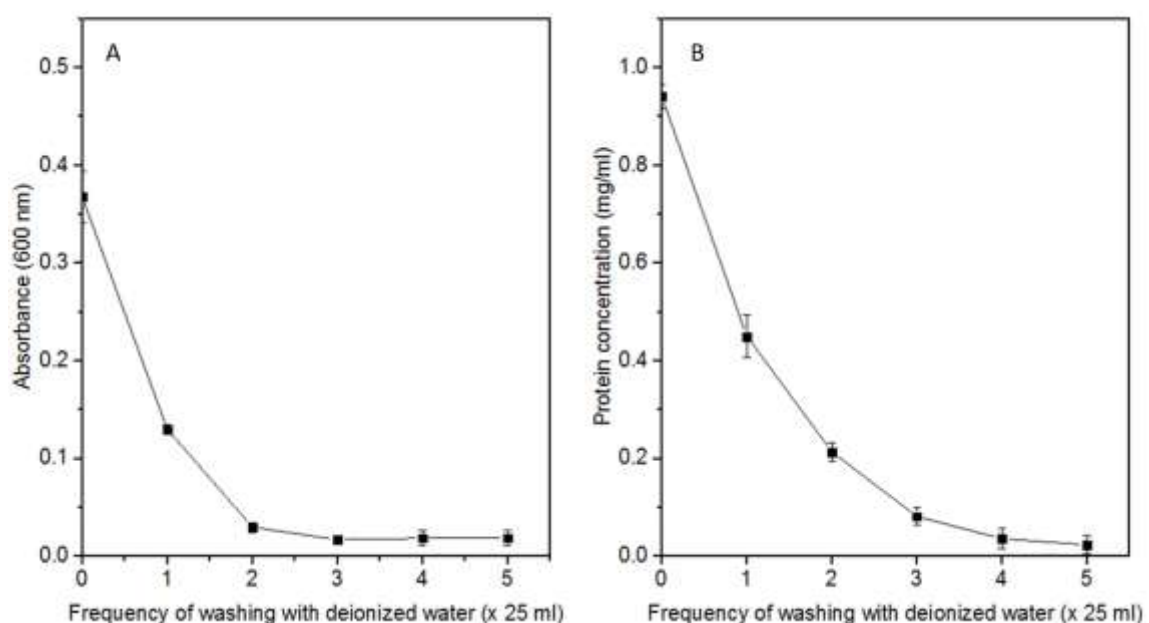


Figure 4.8. (A) Absorbance reading at 600 nm and (B) protein concentration profile of supernatant samples from each washing cycle. The mean is average of triplicates.

Figure 4.9 shows the morphology of bacterial cellulose from a small batch volume, showing pure bacterial cellulose fibers without cells and cell debris. However, the separation of cells and bacterial cellulose fibers from the broth for sample volumes of more than 500 ml, referred as the bulk sample, was more complex. In addition to repeated washing cycles, thorough mixing and treatment duration with NaOH solution were essential for bacterial cellulose fiber purification. Figure 4.10 shows that intact cells and

cell debris, which were observed on the bulk sample treated with NaOH solution for 1 h, were completely lysed and removed after being treated for 2 h. This showed that 2 h treatment with a dilute NaOH solution at 90°C was sufficient to completely lyse the bacterial cells from 500 ml of broth culture samples. For comparison, a two-step purification process was proposed earlier using a five-fold of NaOH concentration compared to that used in this study, followed by a second treatment with 2.5 wt.% NaOCl (bleaching) (Gea et al., 2011).

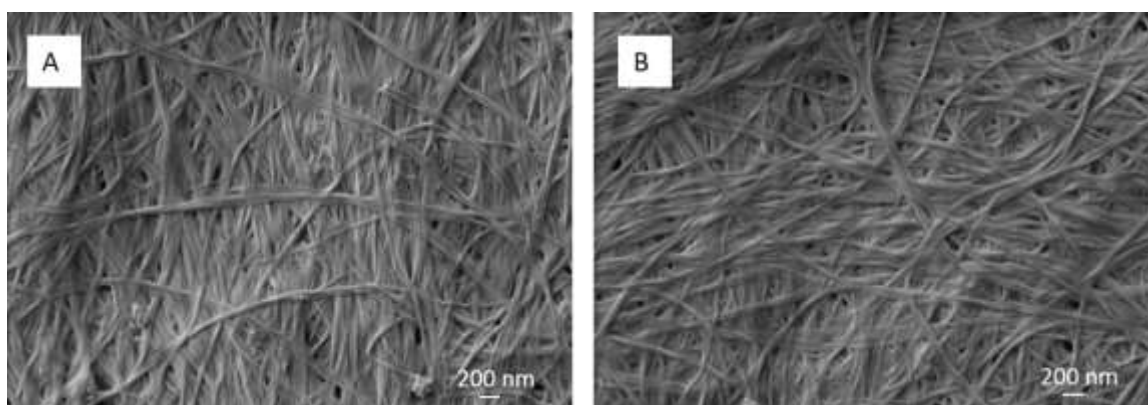


Figure 4.9. SEM images of bacterial cellulose fibers produced by *K. xylinus* in a 3-L stirred-tank bioreactor at 700 rpm after being treated with 0.1 N NaOH solution at 90°C for (A) 30 min and (B) 1 h in a small batch (25 ml sample size). Scale bar is 200 nm.

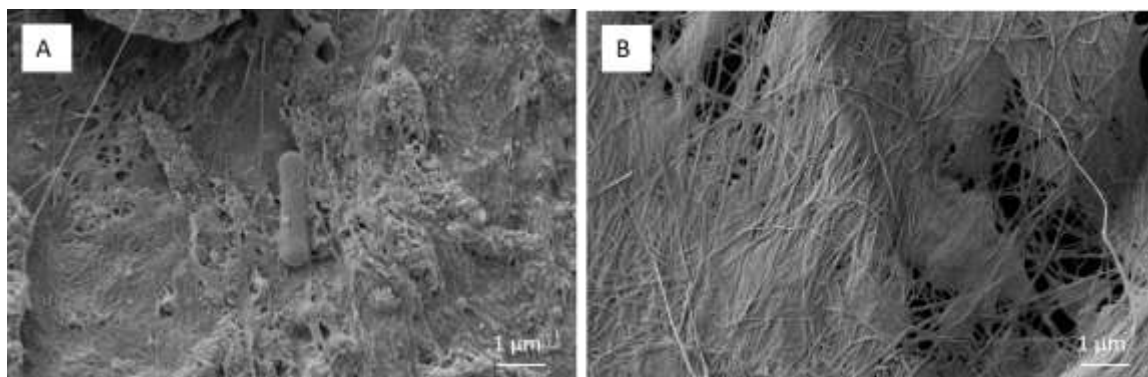


Figure 4.10. SEM images of bacterial cellulose fibers from 500 ml broth culture after purification treatment with 0.1 M NaOH solution at 90°C: (A) bacterial cellulose fibers, *K. xylinus* cell, and cell debris after 1 h treatment, (B) pure bacterial cellulose fibers after 2 h treatment. Scale bar is 1 µm.

4.4.4 Cellulose crystallinity

Naturally produced crystalline cellulose has two distinct allomorphs of cellulose I, I_{α} with a triclinic unit cell and I_{β} with a monoclinic unit cell (Atalla and VanderHart, 1984). The source of origin influences the crystalline type of cellulose and the mass fraction of each cellulose allomorph (Atalla and VanderHart, 1984). While cellulose from higher plants and tunicin were purely I_{β} , cellulose produced by bacteria and *Valonia* algae consisted of a cellulose I_{α} and I_{β} mixture (Sugiyama et al., 1991).

Figure 4.11 shows the x-ray diffractogram of bacterial cellulose produced in baffled shake flasks with a rotational speed of 250 rpm and in a bioreactor with agitation rate of 700 rpm. The x-ray diffractogram of bacterial cellulose shows three signature peaks at the Bragg's angle 2θ (°) of 14.6°, 16.8°, 22.6° corresponding with the crystal planes $\langle -101 \rangle$, $\langle 101 \rangle$, and $\langle 002 \rangle$ crystal planes of a native cellulose I allomorph, respectively (Castro et al., 2011, Watanabe et al., 1998). A broad peak at the minimum 19.5° 2θ was accounted for by amorphous cellulose scattering (Roman and Winter, 2004). Cellulose I_{α} , such as produced in this experiment, is easily identified by a higher peak intensity at 14.6° compared to peak intensity at 16.8° (Kafle et al., 2015).

Cellulose crystallinity refers to the mass fraction of crystalline cellulose among the total cellulosic content. Table 4.2 shows cellulose crystallinity indices of bacterial cellulose produced in a bioreactor obtained by peak area fitting of XRD diffractograms (Cr_A) and ratios of cellulose crystallinity (Cr_1 and Cr_2) of ATR-FTIR absorption bands. In our study, Cr_A , determined by peak area method, was found to be 0.37. Depending on the peak area integration method, others have reported different values for Cr_A for bacterial cellulose produced in shaken flasks culture varying from 0.50 to 0.95 (Ruka et al., 2012, Czaja et al., 2004).

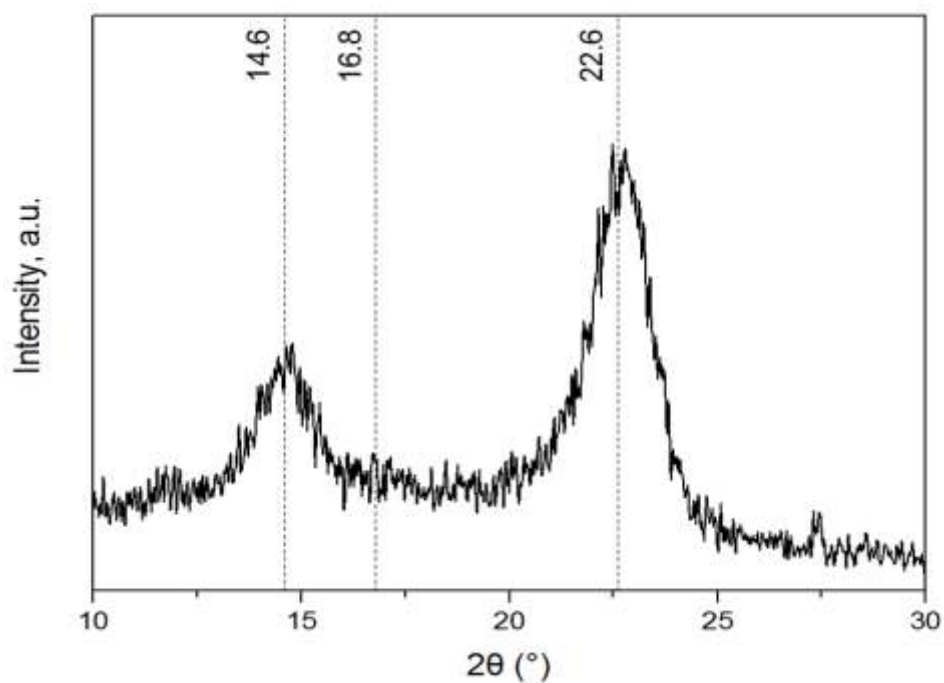


Figure 4.11. X-ray diffractogram of pure bacterial cellulose fibers produced in a 3-L stirred-tank bioreactor agitated at 700 rpm for 72 h.

Table 4.2. Crystallinity indices of bacterial cellulose fibers produced in a 3-L bioreactor agitated at 700 rpm for 72 h, measured using XRD and ATR-FTIR.

Bacterial cellulose production method	Cellulose crystallinity indices		
	Cr _A ^a	Cr ₁ ^b	Cr ₂ ^c
Bioreactor at 700 rpm	0.37	0.56	1.40

^aCr_A is the ratio of the sum under the crystalline diffraction peaks to the total area under the curve between $2\theta = 10-28^\circ$ obtained by XRD.

^bCr₁ is the ratio of the absorption intensity at wavenumber 1428 and 897 cm^{-1} ($\text{Cr}_1 = A_{1428}/A_{897}$) obtained by ATR-FTIR.

^cCr₂ is the ratio of the absorption intensity at wavenumber 1372 and 2898 cm^{-1} ($\text{Cr}_2 = A_{1372}/A_{2898}$) obtained by ATR-FTIR.

There has been a substantial discussion on comparisons between XRD cellulose crystallinity analysis methods (Ahvenainen et al., 2016, Park et al., 2010, Terinte et al., 2011). Since XRD analysis is method-dependent and there is no established standard method to determine cellulose crystallinity from XRD data, comparing results from different literature sources is challenging. IR spectroscopy, specifically ATR-FTIR, offers a complimentary method in providing information on chemical compounds and hydrogen bonding characteristics to confirm the XRD findings.

Figure 4.12 shows the ATR-FTIR spectra of bacterial cellulose fibers produced in a bioreactor. These spectra show typical bands of cellulose from bacterial origin as reported earlier (Castro et al., 2011, Dayal et al., 2013, Gea et al., 2011). A broad absorption band in the 3600-3100 cm^{-1} region is due to the OH-stretching vibrations representing the hydroxyl bonds (Ciolacu et al., 2011). The spectra of bacterial cellulose produced in shake flasks showed a strong peak at 3340 cm^{-1} and the intensity of this O-H stretching band was higher than bacterial cellulose produced in the bioreactor. Bands centered near 2900 cm^{-1} are C-H stretching vibration bands which confirms amorphous cellulose characteristics (Ciolacu et al., 2011). An absorption band at 897 cm^{-1} is assigned to C-O-C stretching at

the β (1-4) linkage of glucose polymers and indicates an amorphous cellulose absorption band (Castro et al., 2011). An absorption band at 1430 cm^{-1} is assigned to CH_2 symmetrical bending vibrations and has been correlated to the degree of cellulose crystallinity and is also referred to as cellulose crystallinity band (Ciolacu et al., 2011). The absorbance band at 1372 cm^{-1} is attributed to C-H bending (Oh et al., 2005).

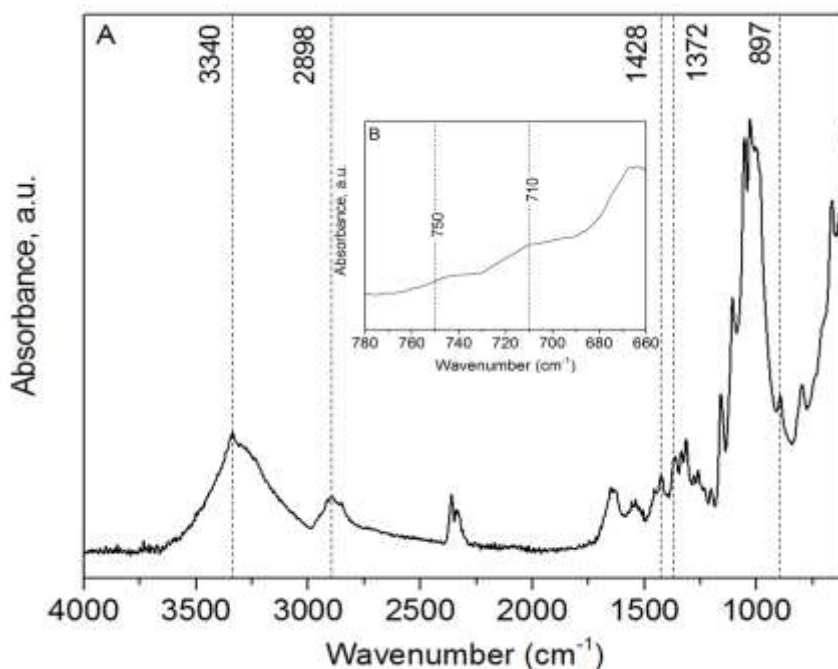


Figure 4.12. ATR-FTIR spectra of pure bacterial cellulose fibers produced by *K. xylinus* for 72 h at 30°C in a 3-L stirred-tank bioreactor agitated at 700 rpm: (A) full spectrum; (B) absorption bands at 750 and 710 cm^{-1} correspond to cellulose I_α and I_β , respectively.

A weak absorption band around $900\text{--}870\text{ cm}^{-1}$ and a strong band at 1430 cm^{-1} define the cellulose I allomorph. The absorption bands near 3240 and 750 cm^{-1} in the ATR-FTIR spectra of native cellulose correspond to cellulose I_α , whereas bands near 3270 and 710 cm^{-1} correspond to cellulose I_β (Yamamoto et al., 1996, Sugiyama et al., 1991). The presence of these bands confirmed that both triclinic cellulose I_α and monoclinic cellulose I_β phase were present in these bacterial cellulose fibers. Moreover, bacterial cellulose produced in an agitated culture displayed a broader peak and lower intensity at 750 cm^{-1} , compared to

bacterial cellulose produced in a static culture, indicating lower cellulose I_{α} contribution (Czaja et al., 2004).

The reduction of absorption band intensity at 3240 cm^{-1} implied weaker inter-molecular hydrogen bonds, a lower cellulose crystallinity, and a lower I_{α} content (Sugiyama et al., 1991). Thermal treatment of cellulose I_{α} with 0.1 M NaOH at 260°C converted the cellulose sample to cellulose I_{β} as indicated by the disappearance of an absorption band intensity at 3240 cm^{-1} and the appearance at 3270 cm^{-1} (Sugiyama et al., 1991). Cellulose I_{α} and cellulose I_{β} have closely related molecular conformations to each other and mainly differ in hydrogen bonding networks (Kim et al., 2013). The conversion from cellulose I_{α} to cellulose I_{β} affected the OH stretching frequencies due to hydrogen bond reorganization (Sugiyama et al., 1991). In our study, the thermal treatment with 0.1 M NaOH was set at 90°C and did not convert the crystalline structure of bacterial cellulose.

The ratios of cellulose crystallinity determined from ATR-FTIR absorption bands are the ratio of the absorption intensity at wavenumber 1428 and 897 cm^{-1} (Cr_1) and the ratio of the absorption intensity at wavenumber 1372 and 2898 cm^{-1} (Cr_2) (Ciolacu et al., 2011, Dayal et al., 2013). These ratios of cellulose crystallinity had been previously used and agreed with XRD findings. There was no direct comparison of cellulose crystallinity index of bacterial cellulose produced in a stirred-tank bioreactor against other type of bioreactors, however, Cr_A and cellulose crystallinity indices obtained by ATR-FTIR for bacterial cellulose produced in shaken flasks culture were found to be lower than bacterial cellulose produced in a stationary culture (Czaja et al., 2004).

Baffles increased the mixing and shear which affected the organization and crystallization of bacterial cellulose (Li et al., 2013). The extent of mixing and shear experienced by the cells producing bacterial cellulose fibers in a bioreactor was intensified. These altered the cellulose arrangement and decreased the cellulose crystallinity. As reported previously, production methods, involving shaking and agitation, altered bacterial cellulose crystallinity, mass fraction of the I_{α} allomorph, and degree of polymerization (Krystynowicz et al., 2002, Watanabe et al., 1998). In addition, bacterial cellulose from agitated culture showed smaller crystallite sizes of microfibrils (Czaja et al., 2004), similar

phenomenon caused by the addition of carboxymethyl cellulose (CMC) (Hirai et al., 1998, Yamamoto et al., 1996). The presence of CMC in the growth medium (Cheng et al., 2009a, Haigler et al., 1982) and other polysaccharides in agro-industrial waste (Castro et al., 2011) have been reported to hinder the aggregation of cellulose chains into microfibrils. These polysaccharides adhered to the surface of the fibrils extruded by the microorganisms and influenced cellulose crystallization (Yamamoto et al., 1996, Haigler et al., 1982). Modification of bacterial cellulose properties can be performed *in-situ* during bioprocessing, which provides many opportunities to create desirable bacterial cellulose characteristics for different applications.

4.5 Conclusion

Stirred-tank bioreactors are often used in bioprocessing scale-up production, especially for biomanufacturing that requires consistent mixing. In the present work, the effects of agitation rates on the cell growth kinetics and the OUR of *K. xylinus* were presented. Agitation promoted rapid growth of bacterial cells and a higher agitation rate produced more bacterial cellulose fibers. The OUR and q_{O_2} trend during lag phase and stationary growth phase at two agitation rates were presented. During exponential growth phase, the OUR and q_{O_2} were not measured since the DO reading fell below a critical level and gassing off was not performed. The use of a stirred-tank bioreactor system allows the monitoring and the controlling of process parameters during cultivation. This provides a platform for increased economies of scale relative to shake flask bioreactors.

Purification of bacterial cellulose fibers from a larger sample volume was achieved with a thermal treatment using dilute NaOH solution for 2 h and without changing the cellulose I_α to I_β . The findings of this study provide new insights into the behavior of *K. xylinus* growing in a stirred-tank bioreactor at different agitation rates and the production of bacterial cellulose fibers. This work provides a platform to scale-up bacterial cellulose production and to alter bacterial cellulose crystallinity during bioprocessing.

4.6 References

- Ahvenainen, P., Kontro, I. & Svedström, K. 2016. Comparison of sample crystallinity determination methods by X-ray diffraction for challenging cellulose I materials. *Cellulose*, 23, 1073-1086.
- Atalla, R. H. & Vanderhart, D. L. 1984. Native Cellulose: A Composite of Two Distinct Crystalline Forms. *Science*, 223, 283-285.
- Bae, S. O. & Shoda, M. 2005. Production of bacterial cellulose by *Acetobacter xylinum* BPR2001 using molasses medium in a jar fermentor. *Applied microbiology and biotechnology*, 67, 45-51.
- Cacicedo, M. L., Castro, M. C., Servetas, I., Bosnea, L., Boura, K., Tsafrakidou, P., Dima, A., Terpou, A., Koutinas, A. & Castro, G. R. 2016. Progress in bacterial cellulose matrices for biotechnological applications. *Bioresource Technology*, 213, 172-180.
- Castro, C., Zuluaga, R., Putaux, J.-L., Caro, G., Mondragon, I. & Gañán, P. 2011. Structural characterization of bacterial cellulose produced by *Gluconacetobacter swingsii* sp. from Colombian agroindustrial wastes. *Carbohydrate Polymers*, 84, 96-102.
- Chao, Y., Ishida, T., Sugano, Y. & Shoda, M. 2000. Bacterial cellulose production by *Acetobacter xylinum* in a 50-L internal-loop airlift reactor. *Biotechnology and bioengineering*, 68, 345-52.
- Chao, Y., Mitarai, M., Sugano, Y. & Shoda, M. 2001a. Effect of Addition of Water-Soluble Polysaccharides on Bacterial Cellulose Production in a 50-L Airlift Reactor. *Biotechnology Progress*, 17, 781-785.
- Chao, Y., Sugano, Y. & Shoda, M. 2001b. Bacterial cellulose production under oxygen-enriched air at different fructose concentrations in a 50-liter, internal-loop airlift reactor. *Applied microbiology and biotechnology*, 55, 673-9.
- Chen, H.-H., Chen, L.-C., Huang, H.-C. & Lin, S.-B. 2011. In situ modification of bacterial cellulose nanostructure by adding CMC during the growth of *Gluconacetobacter xylinus*. *Cellulose*, 18, 1573-1583.
- Cheng, K.-C., Catchmark, J. M. & Demirci, A. 2009a. Effect of different additives on bacterial cellulose production by *Acetobacter xylinum* and analysis of material property. *Cellulose*, 16, 1033-1045.
- Cheng, K. C., Catchmark, J. M. & Demirci, A. 2009b. Enhanced production of bacterial cellulose by using a biofilm reactor and its material property analysis. *Journal of biological engineering*, 3, 12.
- Ciolacu, D., Ciolacu, F. & Popa, V. 2011. Amorphous Cellulose - Structure and Characterization. *Cellulose Chemistry and Technology*, 45, 13-21.

- Czaja, W., Romanovicz, D. & Brown, R. M. 2004. Structural investigations of microbial cellulose produced in stationary and agitated culture. *Cellulose*, 11, 403-411.
- Dayal, M. S., Goswami, N., Sahai, A., Jain, V., Mathur, G. & Mathur, A. 2013. Effect of media components on cell growth and bacterial cellulose production from *Acetobacter aceti* MTCC 2623. *Carbohydrate Polymers*, 94, 12-16.
- Figueiredo, A. R. P., Silvestre, A. J. D., Neto, C. P. & Freire, C. S. R. 2015. In situ synthesis of bacterial cellulose/polycaprolactone blends for hot pressing nanocomposite films production. *Carbohydrate Polymers*, 132, 400-408.
- García-Ochoa, F., Castro, E. G. & Santos, V. E. 2000. Oxygen transfer and uptake rates during xanthan gum production. *Enzyme and Microbial Technology*, 27, 680-690.
- Garcia-Ochoa, F. & Gomez, E. 2009. Bioreactor scale-up and oxygen transfer rate in microbial processes: An overview. *Biotechnology Advances*, 27, 153-176.
- Gatenholm, P. & Klemm, D. 2010. Bacterial Nanocellulose as a Renewable Material for Biomedical Applications. *MRS Bulletin*, 35, 208-213.
- Gea, S., Reynolds, C. T., Roohpour, N., Wirjosentono, B., Soykeabkaew, N., Bilotti, E. & Peijs, T. 2011. Investigation into the structural, morphological, mechanical and thermal behaviour of bacterial cellulose after a two-step purification process. *Bioresource technology*, 102, 9105-9110.
- Haigler, C. H., White, A. R., Brown, R. M. & Cooper, K. M. 1982. Alteration of in vivo cellulose ribbon assembly by carboxymethylcellulose and other cellulose derivatives. *Journal of Cell Biology*, 94, 64-69.
- Hirai, A., Tsuji, M., Yamamoto, H. & Horii, F. 1998. In Situ Crystallization of Bacterial Cellulose III. Influences of Different Polymeric Additives on the Formation of Microfibrils as Revealed by Transmission Electron Microscopy. *Cellulose*, 5, 201-213.
- Hornung, M., Ludwig, M., Gerrard, A. M. & Schmauder, H. P. 2006a. Optimizing the production of bacterial cellulose in surface culture: Evaluation of product movement influences on the bioreaction (Part 2). *Engineering in Life Sciences*, 6, 546-551.
- Hornung, M., Ludwig, M., Gerrard, A. M. & Schmauder, H. P. 2006b. Optimizing the production of bacterial cellulose in surface culture: Evaluation of substrate mass transfer influences on the bioreaction (Part 1). *Engineering in Life Sciences*, 6, 537-545.
- Hornung, M., Ludwig, M. & Schmauder, H. P. 2007. Optimizing the production of bacterial cellulose in surface culture: A novel aerosol bioreactor working on a fed batch principle (Part 3). *Engineering in Life Sciences*, 7, 35-41.

- Huang, H.-C., Chen, L.-C., Lin, S.-B., Hsu, C.-P. & Chen, H.-H. 2010. In situ modification of bacterial cellulose network structure by adding interfering substances during fermentation. *Bioresource Technology*, 101, 6084-6091.
- Joseph, G., Rowe, G. E., Margaritis, A. & Wan, W. 2003. Effects of polyacrylamide-co-acrylic acid on cellulose production by *Acetobacter xylinum*. *Journal of Chemical Technology and Biotechnology*, 78, 964-970.
- Kafle, K., Shin, H., Lee, C. M., Park, S. & Kim, S. H. 2015. Progressive structural changes of Avicel, bleached softwood, and bacterial cellulose during enzymatic hydrolysis. *Scientific Reports*, 5, 15102.
- Kim, S. H., Lee, C. M. & Kafle, K. 2013. Characterization of crystalline cellulose in biomass: Basic principles, applications, and limitations of XRD, NMR, IR, Raman, and SFG. *Korean Journal of Chemical Engineering*, 30, 2127-2141.
- Kim, Y.-J., Kim, J.-N., Wee, Y.-J., Park, D.-H. & Ryu, H.-W. 2007. Bacterial cellulose production by *Gluconacetobacter sp.* PKY5 in a rotary biofilm contactor. *Applied Biochemistry and Biotechnology*, 137-140, 529-537.
- Klemm, D., Kramer, F., Moritz, S., Lindström, T., Ankerfors, M., Gray, D. & Dorris, A. 2011. Nanocelluloses: A new family of nature-based materials. *Angewandte Chemie (International Edition)*, 50, 5438-5466.
- Kouda, T., Yano, H. & Yoshinaga, F. 1997. Effect of agitator configuration on bacterial cellulose productivity in aerated and agitated culture. *Journal of Fermentation and Bioengineering*, 83, 371-376.
- Kouda, T., Yano, H., Yoshinaga, F., Kaminoyama, M. & Kamiwano, M. 1996. Characterization of non-newtonian behavior during mixing of bacterial cellulose in a bioreactor. *Journal of Fermentation and Bioengineering*, 82, 382-386.
- Kralisch, D., Hessler, N., Klemm, D., Erdmann, R. & Schmidt, W. 2010. White biotechnology for cellulose manufacturing—The HoLiR concept. *Biotechnology and Bioengineering*, 105, 740-747.
- Krystynowicz, A., Czaja, W., Wiktorowska-Jeziarska, A., Gonçalves-Miśkiewicz, M., Turkiewicz, M. & Bielecki, S. 2002. Factors affecting the yield and properties of bacterial cellulose. *Journal of Industrial Microbiology and Biotechnology*, 29, 189-195.
- Li, C., Xia, J.-Y., Chu, J., Wang, Y.-H., Zhuang, Y.-P. & Zhang, S.-L. 2013. CFD analysis of the turbulent flow in baffled shake flasks. *Biochemical Engineering Journal*, 70, 140-150.
- Mikkelsen, D., Flanagan, B. M., Dykes, G. A. & Gidley, M. J. 2009. Influence of different carbon sources on bacterial cellulose production by *Gluconacetobacter xylinus* strain ATCC 53524. *Journal of Applied Microbiology*, 107, 576-583.

- Miller, G. L. 1959. Use of Dinitrosalicylic Acid Reagent for Determination of Reducing Sugar. *Analytical Chemistry*, 31, 426-428.
- Moosavi-Nasab, M. & Yousefi, A. 2011. Biotechnological production of cellulose by *Gluconacetobacter xylinus* from agricultural waste. *Iran J Biotechnol*, 9, 94-101.
- Oh, S. Y., Yoo, D. I., Shin, Y., Kim, H. C., Kim, H. Y., Chung, Y. S., Park, W. H. & Youk, J. H. 2005. Crystalline structure analysis of cellulose treated with sodium hydroxide and carbon dioxide by means of X-ray diffraction and FTIR spectroscopy. *Carbohydrate Research*, 340, 2376-2391.
- Park, J., Hyun, S. & Jung, J. 2004. Conversion of *G. hansenii* PJK into non-cellulose-producing mutants according to the culture condition. *Biotechnology and Bioprocess Engineering*, 9, 383-388.
- Park, S., Baker, J. O., Himmel, M. E., Parilla, P. A. & Johnson, D. K. 2010. Cellulose crystallinity index: measurement techniques and their impact on interpreting cellulase performance. *Biotechnology for Biofuels*, 3, 10-10.
- Rani, M. U., Udayasankar, K. & Appaiah, K. a. A. 2011. Properties of bacterial cellulose produced in grape medium by native isolate *Gluconacetobacter sp.* *Journal of Applied Polymer Science*, 120, 2835-2841.
- Reiniati, I., Hrymak, A. N. & Margaritis, A. 2017. Recent developments in the production and applications of bacterial cellulose fibers and nanocrystals. *Critical Reviews in Biotechnology*, 37, 510-524.
- Roman, M. & Winter, W. T. 2004. Effect of Sulfate Groups from Sulfuric Acid Hydrolysis on the Thermal Degradation Behavior of Bacterial Cellulose. *Biomacromolecules*, 5, 1671-1677.
- Ruka, D. R., Simon, G. P. & Dean, K. M. 2012. Altering the growth conditions of *Gluconacetobacter xylinus* to maximize the yield of bacterial cellulose. *Carbohydrate Polymers*, 89, 613-622.
- Ruka, D. R., Simon, G. P. & Dean, K. M. 2013. In situ modifications to bacterial cellulose with the water insoluble polymer poly-3-hydroxybutyrate. *Carbohydrate Polymers*, 92, 1717-1723.
- Seifert, M., Hesse, S., Kabrelian, V. & Klemm, D. 2003. Controlling the water content of never dried and reswollen bacterial cellulose by the addition of water-soluble polymers to the culture medium. *Journal of Polymer Science Part A: Polymer Chemistry*, 42, 463-470.
- Shah, N., Ul-Islam, M., Khattak, W. A. & Park, J. K. 2013. Overview of bacterial cellulose composites: A multipurpose advanced material. *Carbohydrate Polymers*, 98, 1585-1598.

- Shuler, L. M. & Kargi, F. 2002. *Bioprocess Engineering: Basic Concepts*, Upper Saddle River, NJ 07458, Prentice-Hall, Inc.
- Song, H.-J., Li, H., Seo, J.-H., Kim, M.-J. & Kim, S.-J. 2009. Pilot-scale production of bacterial cellulose by a spherical type bubble column bioreactor using saccharified food wastes. *Korean Journal of Chemical Engineering*, 26, 141-146.
- Sugiyama, J., Persson, J. & Chanzy, H. 1991. Combined infrared and electron diffraction study of the polymorphism of native celluloses. *Macromolecules*, 24, 2461-2466.
- Terinte, N., Ibbett, R. & Schuster, K. C. 2011. Overview on native cellulose and microcrystalline cellulose I structure studied by x-ray diffraction (WAXD): comparison between measurement techniques. *Lenzinger Berichte*, 89, 118-131.
- Tribe, L. A., Briens, C. L. & Margaritis, A. 1995. Determination of the volumetric mass transfer coefficient (kLa) using the dynamic “gas out–gas in” method: Analysis of errors caused by dissolved oxygen probes. *Biotechnology and Bioengineering*, 46, 388-392.
- Vaszquez, A., Foresti, M., Cerrutti, P. & Galvagno, M. 2013. Bacterial Cellulose from Simple and Low Cost Production Media by *Gluconacetobacter xylinus*. *Journal of Polymers and the Environment*, 21, 545-554.
- Watanabe, K., Tabuchi, M., Morinaga, Y. & Yoshinaga, F. 1998. Structural features and properties of bacterial cellulose produced in agitated culture. *Cellulose*, 5, 187-200.
- Wu, S.-C. & Li, M.-H. 2015. Production of bacterial cellulose membranes in a modified airlift bioreactor by *Gluconacetobacter xylinus*. *Journal of bioscience and bioengineering*, 120, 444-449.
- Yamamoto, H., Horii, F. & Hirai, A. 1996. In situ crystallization of bacterial cellulose II. Influences of different polymeric additives on the formation of celluloses I α and I β at the early stage of incubation. *Cellulose*, 3, 229-242.

Chapter 5

5 Bacterial cellulose nanocrystals by *Komagataeibacter xylinus*: yield and drug adsorption capacity

5.1 Abstract

Factors affecting the production of bacterial cellulose (BC) fibers and the yield of bacterial cellulose nanocrystals (BCNs) were investigated using a fractional factorial design. Rotational speed significantly affected the production of BC fibers and yield of BCNs. Run 5 resulted in the highest BC production, which was 1.65 g of BC fibers l⁻¹, but showed the lowest BCNs yield, which was 0.33 g BCNs g⁻¹ BC fibers. Conversely, when considering the total amount of BCNs per volume of cultivation medium, the run that produced the highest BC production generated the maximum total mass of BCNs. The optimal medium to achieve the largest amount of BCNs contained 25 g of fructose l⁻¹ and 35 g of CSS l⁻¹ at a pH of 4.5 when cultivated in a rotary shaker incubator at 250 rpm. After 6 hours of adsorption, both pH and rotational speed did not significantly affect the adsorption capacity of BCNs for the antibiotic, tetracycline hydrochloride (TCH), reaching a maximum of 54.5 mg of TCH g⁻¹ of BCNs at 25°C and pH 3. This integrated approach relates the cultivation conditions applied during BC fiber production to the yield of BCNs. Modifying the BC fibers production parameters can increase the yield of BCNs.

5.2 Introduction

Nanocellulose has attracted considerable scientific attention in the past couple of decades, taking advantage of its wide availability as an abundant biopolymer and the growing needs for renewable and biodegradable materials. This attention has precipitated a number of recent studies about its preparation methods, characterization, properties, and emerging applications (George and Sabapathi, 2015, Habibi et al., 2010, Lin et al., 2012, Sunasee et al., 2016).

Among many types of nanocellulose, bacterial cellulose (BC) has been the subject of intense research for biomedical applications (Sulaeva et al., 2015). Different cultivation methods including static culture, shaken culture, and agitated culture not only affect the BC yield, but also result in different morphologies and influence the crystallization of cellulose microfibrils (Czaja et al., 2004). When cellulose fibers were treated with strong acid solutions, nano-sized, rod-like biomaterials consisting of crystalline structures, called cellulose nanocrystals (CNs) were created. Since strong acids hydrolyzed a significant amount of cellulose into sugars, this led to low CNs yields, between 22-67% (Dong et al., 2016, Hamad and Hu, 2010, Mascheroni et al., 2016). In general, stronger acid concentrations, longer reaction times, and higher temperatures typically resulted in shorter CNs and lower CNs yields (Guo et al., 2016, Hamad and Hu, 2010).

CNs applications include nano-reinforcement materials (George and Siddaramaiah, 2012), emulsion stabilizers (Kalashnikova et al., 2011), and biomedical applications (Sunasee et al., 2016). CNs were reported to have the ability to penetrate cells with no indication of cytotoxicity against cell lines, irrespective of different CNs sizes and surface charges, making it suitable as a nanocarrier in drug delivery applications (Hanif et al., 2014, Mahmoud et al., 2010). Jackson and colleagues demonstrated the first use of pristine CNs as a pharmaceutical excipient for water soluble drugs such as tetracycline and doxorubicin (Jackson et al., 2011). Furthermore, surface modification of CNs using cetyl trimethylammonium bromide (CTAB) generated CNs that could carry and release hydrophobic cancer drugs such as docetaxel, paclitaxel, and etoposide in a controlled manner. A different surface modification of oxidized CNs with chitosan oligosaccharide showed a higher binding efficiency of imipramine hydrochloride and released in a controlled manner over 2 h (Akhlaghi et al., 2014). Furthermore, CNs had been demonstrated to remove cationic organic dyes from water via adsorption, proving their suitability as an alternative adsorbent to activated carbon in this application (Batmaz et al., 2014). Despite great potential for these various applications, there is limited information on processes resulting in high BCN yields. As a result, their large-scale production remains a challenge.

After doing a thorough literature investigation, we found that information on the effects of cultivation methods on BCN yields was not readily available. Additionally, there was no report available on the effect of these cultivation parameters on the surface characteristics of BCNs. The aim of this study is to investigate: 1) if a cultivation method that produces a high amount of BC fibers also necessarily produces a high yield of BCNs and 2) whether different cultivation methods result in different surface characteristics. Firstly, BC fibers were produced in shake flasks with varying carbon and nitrogen concentrations, initial medium pHs, and rotational shaker speeds to optimize BC fiber production. Then, the yield of BCNs obtained after acid hydrolysis was calculated. This is the first report we are aware of that addresses the yield of BCNs in relation to the amount of BC fibers produced under different cultivation conditions. Surface characteristic was determined using zeta potential and the adsorption of water soluble, ionizable antibiotic drug TCH was measured.

5.3 Materials and methods

5.3.1 Microorganism and culture media

Komagataeibacter xylinus, *K. xylinus*, (ATCC No. 700178) from the American Type Culture Collection (Rockville, MD) was used to produce BC fibers. The following ingredients were dissolved in a litre of distilled water: 20 g fructose, centrifuged 20 g corn steep solid (CSS) solution, 1 g KH_2PO_4 , 3.3 g $(\text{NH}_4)_2\text{SO}_4$, 0.8 g $\text{MgSO}_4 \cdot 7\text{H}_2\text{O}$, 2.4 g trisodium citrate dehydrate, and 1.6 g citric acid. Cellulase from *Trichoderma Reesei* and all the chemicals were purchased from Sigma-Aldrich and used without further purification. The initial pH was adjusted to 5 by the addition of 2 M NaOH but was not controlled during cultivation.

5.3.2 Shake flask experiment for one-factor-at-a-time optimization approach

An inoculum was prepared by adding 0.9 ml of the seed culture to 100 ml of a fructose-CSS solution (fru-CSS) medium, in a 500 ml flask and was grown for 3 days at a 30 °C temperature in a controlled incubator (New Brunswick G25-R, Edison, NJ). The BC was produced in 500 ml Erlenmeyer flasks with baffles containing 150 ml growth medium with various concentrations of fructose and CSS as shown in Table 5.1. After being inoculated with 6.25% (v/v), the shake flasks were incubated for 5 days at 30°C in a rotary shaker at different rotational speeds.

Table 5.1 Factors assigned at different levels for one-factor-at-a-time optimization method.

Variables	Symbols	Actual levels of coded factors		
		(-)	0	(+)
Fructose concentration (g fructose l ⁻¹)	X ₁	20	40	60
Corn steep solid concentration (CSS) (g CSS l ⁻¹)	X ₂	20	40	60
pH medium	X ₃	4	5	6
Rotational speed (rpm)	X ₄	150	275	375

5.3.3 Experimental design

The fractional factorial design was used with four parameters to identify factors that significantly influence BC production. Table 5.2 shows the parameters examined for BC fiber production using *K. xylinus* in shake flasks. These are: a) fructose concentration (X₁), b) CSS concentration (X₂), c) initial pH (X₃), and d) rotational speed (X₄). Two factor levels, low (-) and high (+) were selected per result from the one-factor-at-a-time optimization approach. In the 8-run fractional factorial design with 3 replicates, each row represents an experiment and each column represents an independent variable (Table 5.3).

Table 5.2 Factors and their levels in fractional factorial design for bacterial cellulose (BC) production in a rotary shaker incubator.

Factors	Symbols	Lower level (-)	Higher level (+)
Fructose concentration (g l ⁻¹)	X ₁	15	25
Corn steep solid concentration (CSS) (g CSS l ⁻¹)	X ₂	35	45
pH medium	X ₃	4.5	5.5
Rotational speed (rpm)	X ₄	150	250

Table 5.3 Fractional factorial design of experiments to study the effects of the culture process parameters on bacterial cellulose (BC) fiber production and bacterial cellulose nanocrystals (BCNs) yield.

Run	Factors			
	X ₁	X ₂	X ₃	X ₄
1	-	-	+	+
2	+	+	-	-
3	-	-	-	-
4	-	+	-	+
5	+	-	-	+
6	+	+	+	+
7	-	+	+	-
8	+	-	+	-

5.3.4 Analytical methods

After 5 days of cultivation, the culture broth was collected and homogenized using a Waring blender. To determine the dry weight of BC, 25 ml broth samples were centrifuged at 10,000 rpm for 10 minutes to remove the remaining nutrients and proteins. The supernatant samples were kept for sugar analysis and the cellulose pellets were washed with distilled water. This washing and centrifugation cycle was repeated several times. The

pellets were then treated with 30 ml of 0.1 M sodium hydroxide (NaOH) solution for 30 minutes at 90°C to lyse the cells. After the samples were centrifuged and washed with distilled water to remove the excess NaOH, the pure BC fibers were dried for 24 hours at 105°C and weighed. To determine the dry weight of the cells, washed pellets from the 5 ml samples were suspended in 1 ml of 2% (v/v) cellulase solution with a 0.1 M citrate buffer and a pH of 4.8. After mixing through gentle inversion, samples were incubated in a water bath at 50°C for 1 hour, to hydrolyze bacterial cellulose fibers. The mixture was filtered using a dried and pre-weighed 0.45 µm cellulose nitrate filter membrane. The wet filter was then dried for 24 hours at 105°C and weighed. Fructose concentration in a broth was measured using a dinitrosalicylic acid (DNS) method (Miller, 1959). Briefly, one ml of the supernatant obtained from the first centrifugation was centrifuged at 10,000 rpm for 5 min. Equal volumes of the diluted supernatant sample and DNS reagent were mixed well and placed in a boiling water bath for 5 min. After cooling, the absorbance of the sample was read at 540 nm. A standard calibration curve was created using known fructose concentrations.

5.3.5 Bacterial cellulose nanocrystals (BCNs) preparation

Figure 5.1 shows a schematic diagram of BCN production. After the BC fibers were washed and purified using NaOH, they were freeze dried at 0.133 mbar for 48 h at -52°C (using the Thermo Fischer Scientific ModulyoD Freeze Dryer, Waltham, MA). Freeze dried BC fibers were added to a 50 ml flask containing a 64 wt% sulfuric acid solution preheated to 45°C and with an acid to pulp ratio 100 ml:1 g was stirred with a magnetic stirring bar at 200 rpm, for 3 h. The hydrolysis reaction was then quenched by a 5-fold dilution, in cold deionized water and centrifuged at 10,000 rpm for 10 min. The supernatant sample containing an excess of sulfuric acid was discarded. The opaque/ivory suspension was placed in a Spectrum Spectra /Por regenerated cellulose dialysis membrane with a molecular weight cut off of 12,000 – 14,000 Da (Spectrum Laboratories Inc., Houston, TX). It was dialyzed against deionized water until the pH of the water stabilized to a pH of approximately 6. The resulting suspension was sonicated using a tip-sonicator at 60% power output, for 10 min while maintaining low temperature with an ice bath, and was passed through a 1.2 µm glass fiber filter to remove large particles. BCNs suspensions were

freeze dried, and were kept in a desiccator until analysis. BCNs yields were calculated by dividing the BCNs freeze dried weight after acid hydrolysis by the initial freeze-dried weight of BC fibers.

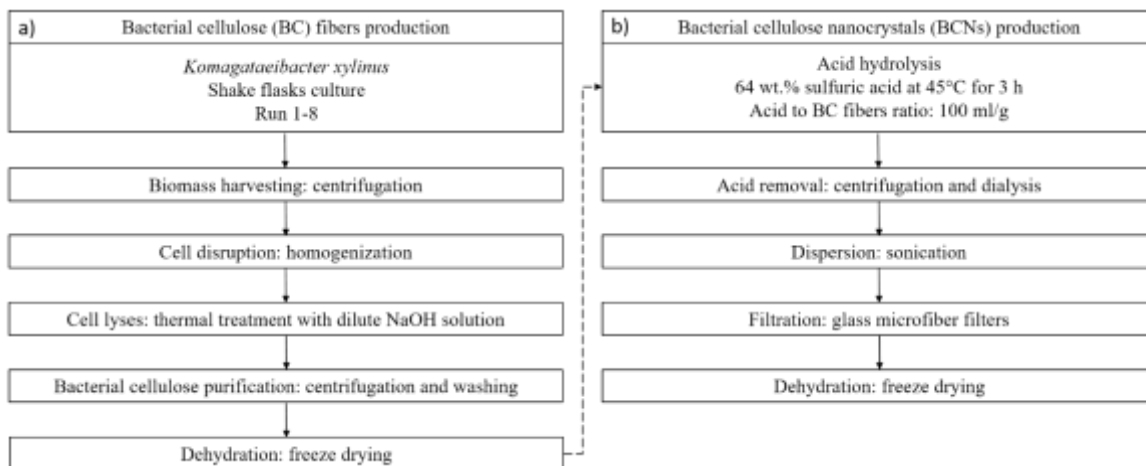


Figure 5.1. Schematic diagram of a) bacterial cellulose (BC) fibers production and b) bacterial cellulose nanocrystals production.

5.3.6 Adsorption of tetracycline hydrochloride (TCH)

Five ml of 1 mg/ml of TCH at pH 3 was added to ten mg of BCNs in 5 ml of deionized water. After mixing thoroughly using vortex, the samples were sonicated in a water bath for 10 minutes and kept in an rotational incubator shaker at 25°C and 150 rpm for 2 and 6 hours. The amount of TCH adsorbed at equilibrium, q_e (mg/g), was calculated from the difference in TCH concentrations in the aqueous phase before (C_0 , mg/L) and after adsorption (C_e , mg/L), per Equation 1.

$$q_e = \frac{(C_0 - C_e)V}{m} \quad \text{Equation 1.}$$

Where V is the volume of TCH solution (L) and m is the mass of bacterial cellulose nanocrystals (g).

The binding of TCH on BCNs was described previously (Jackson et al., 2011). One ml of samples was transferred to 2 ml centrifuge tube and was centrifuged for 20 min at 18,000

g. After the supernatant was properly diluted, it was placed in a Quartz cell and absorbance was read at 364 nm using a Genesys 10S UV-VIS spectrophotometer (Thermo Fisher Scientific, Waltham, MA, USA). The TCH concentration remaining in the solution was determined using a pre-established calibration curve.

5.3.7 Zeta potential measurements

The zeta (ζ) potential measurements of samples were measured by electrophoretic light scattering using a ZetaPlus Zeta Potential Analyzer (Brookhaven Instrument Corporation, Holtsville, NY, USA) with a 30 mV solid state laser beam at 659 nm wavelength. All samples were maintained at 0.04 wt.% at pH 3. The measurements were performed at 25 ± 1 °C, shortly after sonication in a water bath (output: 60 Watts). The Smoluchowski model was used to convert electrophoresis mobility to zeta potential and the reported values were an average of 5 measurements.

5.3.8 Data analysis

Statistical experimental design (ANOVA) was generated and analyzed using ‘Minitab 17’ (Minitab Inc., State College, PA). All experiments were carried out independently, in triplicates. The average values are presented with their standard error.

5.4 Results and Discussion

5.4.1 Effect of culture conditions on BC production using one-factor-at-a-time approach

Results from a one-factor-at-a-time optimization method on the effects of the four factors on BC production, cell production, and yield of BC are shown in Figure 5.2. The BC yield (g g^{-1}) was a ratio of the amount of BC produced over the amount of fructose consumed during the cultivation. In this optimization approach, when the effect of one factor was examined, the other three factors were kept constant. First, fructose concentration was optimized with a CSS concentration of 20 g l^{-1} , a pH of 5, and a rotational speed at 150 rpm. BC production reached 1.05, 0.98, and 1.36 g l^{-1} when 20, 40, and 60 g l^{-1} of fructose were used, respectively. At 20 g of fructose l^{-1} , the cell concentration was 0.75 g l^{-1} and it increased by 25% at 40 g of fructose l^{-1} and almost 100% at 60 g of fructose l^{-1} . However,

the BC yield was the lowest at 60 g of fructose l⁻¹ indicating a substrate inhibition and an inefficient use of the substrate. Furthermore, the CSS concentration was optimized in the range of 20-60 g l⁻¹ with the optimal fructose concentration being at 20 g l⁻¹, with a pH of 5, and a rotational speed at 150 rpm. At 40 g l⁻¹ of CSS, BC production and BC yield were the highest, with these being at 1.96 g l⁻¹, and 0.28 g g⁻¹ respectively. When increased to 60 g l⁻¹ of CSS, it showed a similar result. The lower concentration of CSS at 40 g l⁻¹ was selected for economic benefits. Moreover, pH did not considerably affect the BC production. In contrast, certain conditions promoted more bacterial cell growth than BC production, such as when the pH of the medium was 4. A higher rotational speed led to an increase in BC production but not to an augmentation of the BC yield. This indicates that increased mixing promoted bacterial cell growth and rapid fructose consumption.

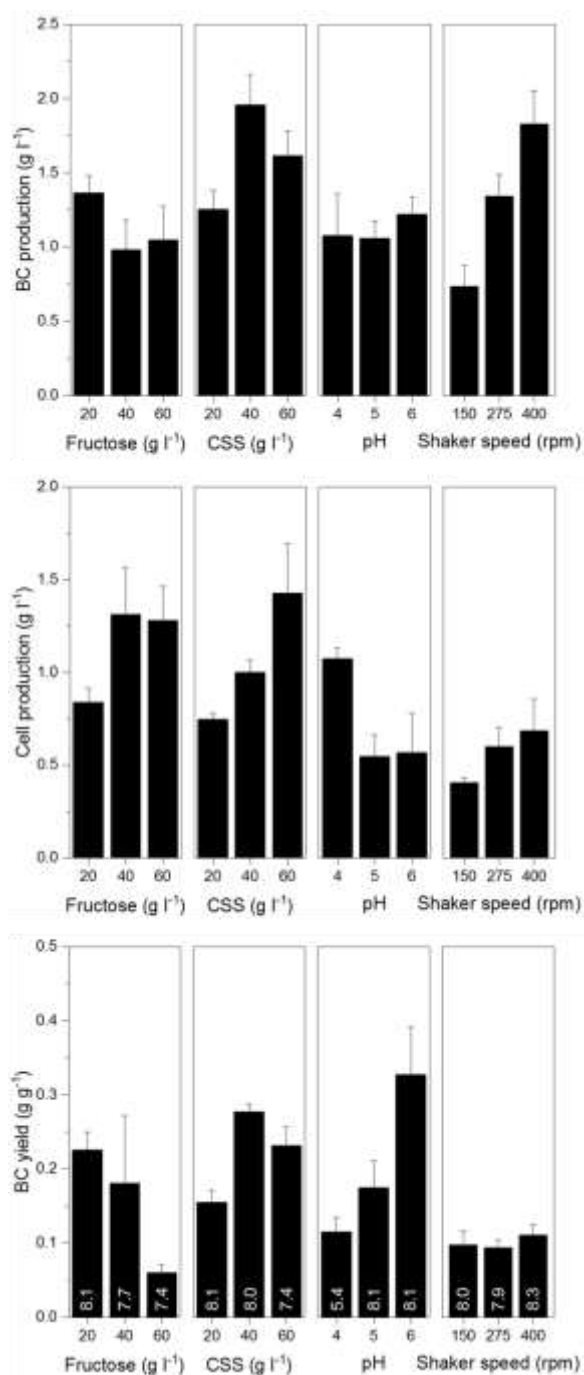


Figure 5.2. Effect of fructose concentration, CSS concentration, pH medium, and shaker speed on bacterial cellulose (BC) production, cell production, BC yield, and pH of broth (numerical values are presented at the bottom graph). Results are the mean of three replicates \pm standard error.

The pH of the medium was measured after autoclaving and was consistent with the initial pH level, confirming that autoclaving did not change the pH of the medium. Except for the media cultivated at the initial pH of 4, all fermentations reached a pH above 7.4 after 5 days of cultivation. This was significantly higher than the normal optimum pH of 5 for *K. xylinus*. The increase of the pH was suspected to have occurred due to the low buffering capacity of the media. The concentrations of trisodium citrate and citric acid were doubled in order to examine the effects of these two compounds on BC production. It was found that doubling the concentrations of trisodium citrate and citric acid did not change the pH profile and BC fibers production (data not shown). Thus, the rest of the experiment used the original buffer concentration, without doubling it. The information acquired from this investigation was used to provide a basis for a screening experiment performed with the purpose of improving BC production.

5.4.2 Screening of factors using fractional factorial design

Results from the one-factor-at-a-time approach were incorporated in this screening experiment to narrow the range of the examined parameters. Figure 5.3 shows the results from the 8-run fractional factorial design and their influence on factors affecting BC production and BCNs yields. Runs 1, 4, 5, and 6, which were grown in shake flasks rotated at 250 rpm, resulted in an exceptionally higher BC production compared to cultures grown in shake flasks rotated at 150 rpm (Figure 5.3). The three highest BC productions were 1.74 g l^{-1} from run 4, 1.71 g l^{-1} from run 6 and, 1.60 g l^{-1} from run 5. BC production increased with an increase in shaker speed.

Statistical analysis showed that fructose concentration, CSS concentration, and the initial pH of the medium did not significantly affect the BC production indicated by p value greater than 0.05. On the other hand, the shaker speed significantly affected BC production with $p < 0.05$. This could be attributed to the turbulent flow created by the baffles and a higher rotational speed which promoted rapid mixing leading to better oxygen and nutrient transfer (Li et al., 2013). However, higher rotational speeds in baffle shake flasks have been shown to promote cell mutation creating non-cellulose producing cells (Valla and Kjosbakken, 1982).

Figure 5.3 shows that a higher rotational speed leads to more BC production and a rotational lower speed increases BCNs yield. The culture grown in shake flasks and rotated at 150 rpm resulted in higher BCNs yields than the culture rotated at 250 rpm. These BCN yields were determined by calculating a ratio of freeze dried weight of BCNs over a freeze-dried weight of initial BC fibers. The total amount of BCNs in 1 L of medium was calculated by multiplying the BC fibers production by BCNs yield. For example, run 5 produced 1.65 g of BC fibers l^{-1} and resulted in 0.33 g BCNs g^{-1} BC fibers. This translates to 0.54 g of BCNs produced per 1 L of medium. On the other hand, run 8 produced 0.64 g of BC l^{-1} and resulted in 0.54 g BCNs g^{-1} BC fibers. This translates to 0.34 g of BCNs produced per 1 L of medium. This means that although the culture grown with a slower rotational speed produced a higher BCN yield, the run that resulted in higher BC fibers produces more BCNs in the end. This paper is, as far as we are aware, the first effort to relate methods producing a high amount of BC fibers to the yield of BCNs. For comparison, a CNs yield of 30% (of initial weight) was obtained from microcrystalline cellulose (Taheri and Mohammadi, 2015).

Different preparation conditions as well as post-treatment filtration methods can contribute to varying CNs yields found in the literature (Mascheroni et al., 2016). A direct assessment of the CNs yields is clearly more complex than comparing numerical values since these yield values are related to specific lab-scale production processes. However, in this study, the same preparation conditions, post-treatment filtration and drying method were applied. Thus, the differences in BCNs yields correspond to the variations in the proportions of the crystalline domains of the BC fibers under different cultivation conditions. Although it is important to employ a process resulting in a high yield of BCNs, other costs attributed to production processes need to be considered. One of the tradeoffs is the increased cost of separating the BC fibers from the broth, which involves substantial washing and centrifuging of the BC fibers.

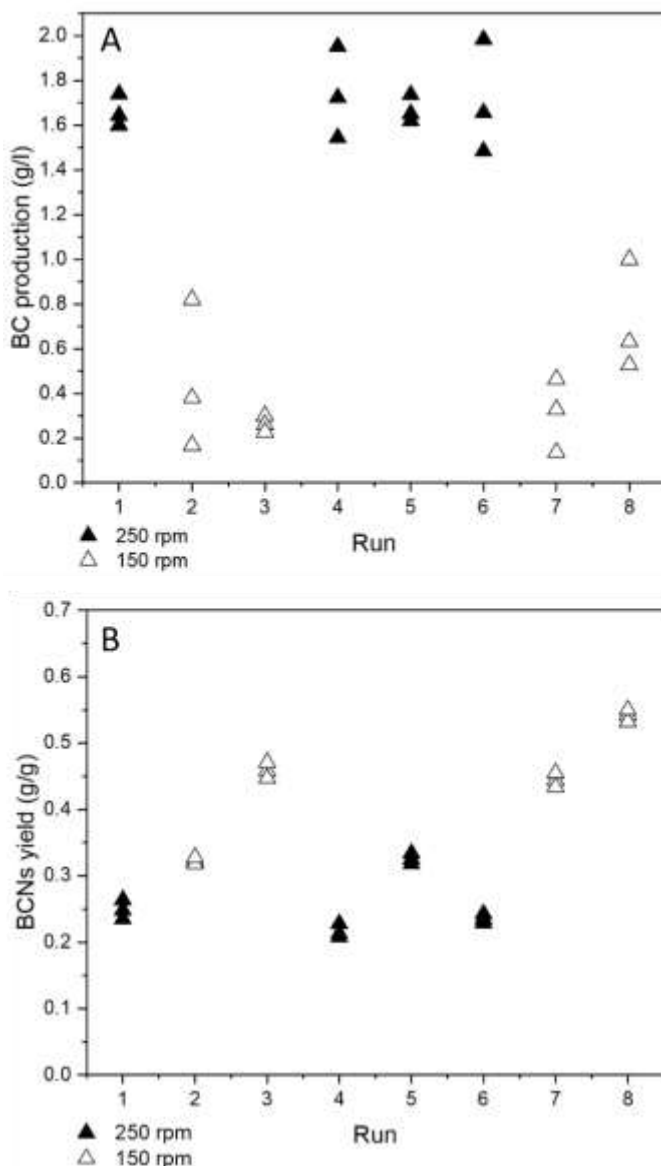


Figure 5.3 (A) Bacterial cellulose (BC) produced by *Komagataeibacter xylinus* in baffled shake flasks kept in an orbital incubator shaker at 30°C at 250 rpm and 150 rpm. (B) Bacterial cellulose nanocrystals (BCNs) yield was calculated by dividing a final freeze-dried weight of BCNs (g) after acid hydrolysis by an initial freeze-dried weight of BC fibers (g). The run numbers refer to experimental conditions described in Table 5.3. Legend: ■: BC production, ●: cell production, ▲: BCNs yield. Results show the data spread of three replicates.

5.4.3 Adsorption study

Freeze-dried BCNs were dispersed in deionized water and sonicated prior to mixing with TCH solution (Figure 5.4). While rotational speed was found to influence the yield of BCNs, the question remained whether pH and rotational speed influenced the BCNs surface characteristics. Since the acid hydrolysis treatment was applied to all samples, the differences found was due to the different surface characteristics. Table 5.4 shows the adsorption capacity of TCH on BCNs surfaces and the zeta potential of the samples. The q_e after 2 h of adsorption, ranging from 19.5 to 37.3 mg g⁻¹, showed lower values compared to q_e after 6 h, ranging from 45.5 to 54.9 mg g⁻¹. These q_e values of BCNs as TCH adsorbent were much higher compared to q_e of nanocellulose reported previously of 7.7 mg g⁻¹ (Rathod et al., 2015). This could be attributed by the lower initial TCH concentration used in Rathod and colleagues' work since higher initial TCH concentration prompted a higher q_e values (Rathod et al., 2015).

Evaluated after 2 h of adsorption, it showed that rotational speed significantly affected the q_e values (p value < 0.05) while pH did not. However, when evaluated after 6 h of adsorption, the rotational speed did not affect the q_e values significantly. The adsorption capacity is directly proportional to the exposed surface area and this showed that after 6 hours, both pH and rpm did not significantly affect the adsorption capacity. The presence of sulfate ester groups (OSO_3^-) on the surface of the BCNs resulted in negative zeta potential ranging from -9.5 to -15.5 mV. This was significantly lower compared to pristine CNs derived from wood with zeta potential values ranging from -33.1 to -35.7 mV (Akhlaghi et al., 2014, Mahmoud et al., 2010). It is important to note that all parameters (i.e. pH, rpm, and length of adsorption) did not significantly affect the zeta potentials of samples. Thus, the difference in q_e values could be attributed to the adsorption time needed to allow all the BCNs surface exposed to the TCH drugs.

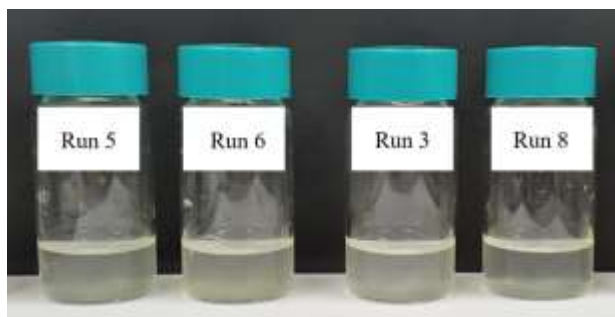


Figure 5.4. BCNs dispersion in deionized water.

Table 5.4 Adsorption capacity of TCH onto BCNs and zeta potentials of BCNs and TCH mixture after 2 and 6 hours of adsorption in deionized water at pH 3 at ambient temperature of 25°C. The mean values are average of triplicates and are presented with standard error.

BCNs from	obtained	Adsorption capacity (mg/g)	Zeta potential (mV)	Adsorption capacity (mg/g)	Zeta potential (mV)	
Run	pH	rpm	After 2 h adsorption	After 6 h adsorption		
5	4.5	250	33.4 ± 2.9	-9.5 ± 4.8	48.7 ± 0.9	-10.1 ± 2.7
6	5.5	250	37.3 ± 2.9	-15.5 ± 5.0	54.9 ± 7.1	-7.5 ± 7.8
3	4.5	150	23.7 ± 5.5	-12.1 ± 7.2	45.5 ± 2.6	-12.0 ± 3.1
8	5.5	150	19.5 ± 5.5	-13.9 ± 1.3	44.8 ± 1.3	-11.1 ± 0.7
p value	pH	0.97	0.43	0.50	0.72	
	rpm	0.01	0.92	0.14	0.58	

Acid hydrolysis properly removed the amorphous domains of cellulose while crystalline cellulose domains remained. A few rapid characterizations were often employed on these CNs to determine its particle size, particle size distribution, surface charge, surface area, and degree of crystallinity of cellulose (Boluk et al., 2011, Brinkmann et al., 2016, Hamad and Hu, 2010). Thus, with the increased interest and potential of creating new applications for CNs, there is a need for a robust production process yielding high amounts of BCNs, with consistent desired characteristics. With a proper adsorption time, BCNs from different cultivation conditions resulted in BCNs with similar surface characteristic, indicated by zeta potential values. The adsorption of TCH onto the BCNs were not affected by the different pH and rpm applied during the cultivation of BC fibers. The success of BCNs in industry is contingent upon: a) an economical BCNs production cost, b) the ability to consistently produce desired characteristics, and c) inexpensive and rapid characterization method for quality control purposes.

5.5 Conclusion

We report here for the first time that BC fibers production parameters affected the yield of BCNs. Among the evaluated BC fiber cultivation method parameters, the rotational shaker speed plays a significant role in affecting the production of BC fibers and in determining the yield of BCNs. The post-processing treatments done on the BC fibers included homogenization and acid hydrolysis treatment. Since all BC fiber samples underwent the same homogenization and sulfuric acid hydrolysis treatment conditions, the BCNs yields are strictly affected by the different BC fibers cultivation conditions. A higher BCNs yield is analogous to a higher proportion of the crystalline domains of the BC fibers. In this study, the BC fiber production was optimized using one-factor-at-a-time and fractional factorial design method. When the total amount of BCNs obtained per run was calculated, shake flasks rotated at 250 rpm were shown to produce more BCNs per L of medium than shake flasks rotated at 150 rpm. It is shown, on the basis of Run 5, having 25 g of fructose and 35 g of CSS per L, at a pH of 4.5, cultivated in an orbital shaker incubator at 250 rpm, produced the highest amount of BC fibers at 1.65 g of BC l⁻¹, yielding 0.33 g of BCNs, the largest BCNs mass. These results aid in the understanding of the process to enhance bacterial cellulose nanocrystals production. The BCNs produced are envisioned for drug

delivery and pharmaceutical related applications. After a proper adsorption time, BCNs obtained from different pH and rotational speed resulted in similar adsorption capacity values.

5.6 Reference

- Akhlaghi, S. P., Tiong, D., Berry, R. M. & Tam, K. C. 2014. Comparative release studies of two cationic model drugs from different cellulose nanocrystal derivatives. *European Journal of Pharmaceutics and Biopharmaceutics*, 88, 207-215.
- Batmaz, R., Mohammed, N., Zaman, M., Minhas, G., Berry, R. M. & Tam, K. C. 2014. Cellulose nanocrystals as promising adsorbents for the removal of cationic dyes. *Cellulose*, 21, 1655-1665.
- Boluk, Y., Lahiji, R., Zhao, L. & Mcdermott, M. T. 2011. Suspension viscosities and shape parameter of cellulose nanocrystals (CNC). *Colloids and Surfaces A*, 377, 297-303.
- Brinkmann, A., Chen, M., Couillard, M., Jakubek, Z. J., Leng, T. & Johnston, L. J. 2016. Correlating Cellulose Nanocrystal Particle Size and Surface Area. *Langmuir*, 32, 6105-6114.
- Czaja, W., Romanovicz, D. & Brown, R. M. 2004. Structural investigations of microbial cellulose produced in stationary and agitated culture. *Cellulose*, 11, 403-411.
- Dong, S., Bortner, M. J. & Roman, M. 2016. Analysis of the sulfuric acid hydrolysis of wood pulp for cellulose nanocrystal production: A central composite design study. *Industrial Crops and Products*, 93, 76-87.
- George, J. & Sabapathi, S. N. 2015. Cellulose nanocrystals: synthesis, functional properties, and applications. *Nanotechnology, Science and Applications*, 8, 45-54.
- George, J. & Siddaramaiah 2012. High performance edible nanocomposite films containing bacterial cellulose nanocrystals. *Carbohydrate Polymers*, 87, 2031+.
- Guo, J., Guo, X., Wang, S. & Yin, Y. 2016. Effects of ultrasonic treatment during acid hydrolysis on the yield, particle size and structure of cellulose nanocrystals. *Carbohydrate Polymers*, 135, 248-255.
- Habibi, Y., Lucia, L. A. & Rojas, O. J. 2010. Cellulose nanocrystals: chemistry, self-assembly, and applications. *Chemical Reviews*, 110, 3479-3500.
- Hamad, W. Y. & Hu, T. Q. 2010. Structure–process–yield interrelations in nanocrystalline cellulose extraction. *Canadian Journal of Chemical Engineering*, 88, 392-402.

- Hanif, Z., Ahmed, F. R., Shin, S. W., Kim, Y.-K. & Um, S. H. 2014. Size- and dose-dependent toxicity of cellulose nanocrystals (CNC) on human fibroblasts and colon adenocarcinoma. *Colloids and Surfaces B: Biointerfaces*, 119, 162-165.
- Jackson, J. K., Letchford, K., Wasserman, B. Z., Ye, L., Hamad, W. & Burt, H. M. 2011. The use of nanocrystalline cellulose for the binding and controlled release of drugs. *International Journal of Nanomedicine*, 6, 321-330.
- Kalashnikova, I., Bizot, H., Cathala, B. & Capron, I. 2011. New Pickering emulsions stabilized by bacterial cellulose nanocrystals. *Langmuir*, 27, 7471-7479.
- Li, C., Xia, J.-Y., Chu, J., Wang, Y.-H., Zhuang, Y.-P. & Zhang, S.-L. 2013. CFD analysis of the turbulent flow in baffled shake flasks. *Biochemical Engineering Journal*, 70, 140-150.
- Lin, N., Huang, J. & Dufresne, A. 2012. Preparation, properties and applications of polysaccharide nanocrystals in advanced functional nanomaterials: a review. *Nanoscale*, 4, 3274-3294.
- Mahmoud, K. A., Mena, J. A., Male, K. B., Hrapovic, S., Kamen, A. & Luong, J. H. T. 2010. Effect of Surface Charge on the Cellular Uptake and Cytotoxicity of Fluorescent Labeled Cellulose Nanocrystals. *ACS Applied Materials & Interfaces*, 2, 2924-2932.
- Mascheroni, E., Rampazzo, R., Ortenzi, M. A., Piva, G., Bonetti, S. & Piergiovanni, L. 2016. Comparison of cellulose nanocrystals obtained by sulfuric acid hydrolysis and ammonium persulfate, to be used as coating on flexible food-packaging materials. *Cellulose*, 23, 779+.
- Miller, G. L. 1959. Use of Dinitrosalicylic Acid Reagent for Determination of Reducing Sugar. *Analytical Chemistry*, 31, 426-428.
- Rathod, M., Haldar, S. & Basha, S. 2015. Nanocrystalline cellulose for removal of tetracycline hydrochloride from water via biosorption: Equilibrium, kinetic and thermodynamic studies. *Ecological Engineering*, 84, 240-249.
- Sulaeva, I., Henniges, U., Rosenau, T. & Potthast, A. 2015. Bacterial cellulose as a material for wound treatment: Properties and modifications. A review. *Biotechnology Advances*, 33, 1547-1571.
- Sunasee, R., Hemraz, U. D. & Ckless, K. 2016. Cellulose nanocrystals: a versatile nanoplatform for emerging biomedical applications. *Expert Opinion on Drug Delivery*, 1-14.
- Taheri, A. & Mohammadi, M. 2015. The Use of Cellulose Nanocrystals for Potential Application in Topical Delivery of Hydroquinone. *Chemical Biology & Drug Design*, 86, 102-106.

Valla, A. & Kjosbakken 1982. Cellulose-negative Mutants of *Acetobacter xylinum*.
Journal of General Microbiology, 128, 1401-1408.

Chapter 6

6 Adsorption of model drug tetracycline hydrochloride on bacterial cellulose nanocrystals

6.1 Abstract

Applications of cellulose nanocrystals depend highly on the physical and chemical characteristics of the material. In this work, bacterial cellulose nanocrystals (BCNs) obtained from sulfuric acid hydrolysis were used as an adsorbent for the ionizable antibiotic tetracycline hydrochloride (TCH) from concentrated aqueous suspension. The size distribution and crystallinity of BCNs was reported. Furthermore, the influence of pH on adsorption capacity was evaluated since the pH of solution affects the protonation and deprotonation of drug species and so influences the adsorption capacity. The adsorption kinetics data for two different BCNs doses were fitted to a pseudo-second order kinetic model. This study demonstrates that bacterial-derived cellulose nanocrystals is an effective adsorbent for drug delivery excipient in an aqueous system.

6.2 Introduction

Bacterial cellulose has gained great interest in recent years for its biocompatibility, non-toxic nature, and its vast potential in nanotechnology. While bacterial cellulose fibers have achieved success in biomedical applications such as wound dressing and strengthening of nanocomposite materials, there are many more possible applications of bacterial cellulose. Bacterial cellulose nanocrystals (BCNs), obtained from treating the bacterial cellulose fibers produced by *Komagataebacter xylinus* (*K. xylinus*) using sulfuric acid hydrolysis have unique properties compared to its fiber form. After the removal of amorphous regions in cellulose fibers via acid hydrolysis, rigid, rod-like, nanoscale materials were generated (Habibi et al., 2010). Few characteristics of CNs are its high aspect ratio, large surface area, high mechanical strength, and hydrophilicity (Peng et al., 2011).

Recent developments in the use of functionalized and modified cellulose nanocrystals (CNs) in biologically relevant applications, such as enzyme immobilization, antimicrobial material, biosensors, and drug delivery have been reviewed (Lam et al., 2012). CNs hydrophilicity, which occurs due to the presence of hydroxyl groups on its surface, could support the binding and release of hydrophobic drugs (Jackson et al., 2011). When CNs were grafted with γ -aminobutyric acid which then attached to syringing alcohol, CNs acted as nano-carrier molecules for controlled delivery of enzymes, proteins and amine-containing drug molecules (Dash and Ragauskas, 2012). Fundamental studies of pristine and modified CNs have generated a crucial understanding necessary for the development of novel functional systems. The establishment of larger scale production facilities in North America supports the growth of CNs adoption in product formulations, such as in consumer and personal care system, wastewater treatment, coatings, and biomedical engineering (Tang et al., 2017).

Adsorption of several drugs to wood-based cellulose nanocrystals has been reported previously (Jackson et al., 2011). TCH is a water-soluble antibiotic used to treat a number of bacterial infections and is usually administered according to the level of infections. TCH has a planar structure consisting of three functional groups. The pK_a values of TCH in water at 25°C are reported to be 3.30, 7.68, and 9.69, assigned as pK_{a1} , pK_{a2} , pK_{a3} , respectively (Ali, 1984). The pH of solution can influence the protonation and deprotonation of the participating drug molecules. The adsorption of TCH on BCNs has not been reported previously.

In this study, adsorption kinetics of tetracycline hydrochloride (TCH) has been accomplished using bacterial derived CNs. The release of drug molecules from CNs was rapid which may be contributed by the ion-exchange between the ions in the release medium and the surfaces of CNs (Jackson et al., 2011). This rapid release systems is necessary for delivery of local anesthetics and analgesics or treatment in periodontal infection (Lee et al., 2016).

This study aims at investigating the applicability of bacterial cellulose nanocrystals (BCNs) as a biosorbent. The BCNs were prepared from acid hydrolysis of bacterial cellulose (BC)

fibers and used to bind TCH from aqueous solution. This adsorption study provides insight in its usage as drug carriers for controlled drug delivery as well as for pollutant removal. In this study, the effect of pH, BCNs dose, and contact time on adsorption of TCH to bacterial cellulose nanocrystals were studied. The adsorption kinetics data set fitted to pseudo-second order was presented to investigate the sorption mechanism of TCH onto BCNs.

6.3 Materials and experimental methods

6.3.1 Bacterial cellulose (BC) production

K. xylinus (ATCC No. 700178) obtained from the American Type Culture Collection (ATCC, Rockville, MD) was grown in a fructose-based medium with corn steep solid solution (fru-CSS medium). BC was produced in a 1500 ml fructose-corn steep solid solution medium with 6.25 (v/v)% inoculum in 2800 ml baffled Fernbach flask and incubated at 30°C for 5 days in a rotary incubator set at 250 rpm. The following compositions were dissolved in 1 L of distilled water: 25 g fructose, centrifuged 35 g CSS solution, 1 g KH_2PO_4 , 3.3 g $(\text{NH}_4)_2\text{SO}_4$, 0.8 g $\text{MgSO}_4 \cdot 7\text{H}_2\text{O}$, 2.4 g trisodium citrate dehydrate and 1.6 g citric acid. The initial pH was adjusted to 4.5 by the addition of 2 M sodium hydroxide (NaOH). The medium was then autoclaved at 121°C for 15 minutes. All chemicals were analytical grade and commercially available (Sigma-Aldrich, ON, Canada).

6.3.2 Preparation of bacterial cellulose nanocrystals (BCNs)

After 5 days, the broth was centrifuged at 5000 rpm for 10 min to separate BC fibers from the liquid medium. After repeated washing with distilled water, BC was homogenized using a Waring blender. The washed BC was treated with 1500 ml of 0.1 M NaOH for 2 hours at 90°C. After repeated washing with deionized water, the pure BC fibers were frozen in a -80°C freezer and lyophilized using Savant ModulyoD freeze dryer (Thermo Fisher Scientific, Waltham, MA, USA). Freeze-dried BC fibers were acid hydrolyzed with a 64 % (w/w) sulphuric acid (H_2SO_4) solution under constant mixing. BC fibers with acid to pulp ratio 100 ml:1 g was placed in a round bottle neck flask and immersed in a 45°C water bath for 3 hours. The slurry was diluted 5 times with ice cold deionized water. After 10

min centrifugation at 10,000 rpm, the BCNs paste was placed in a regenerated cellulose dialysis membrane with a molecular cut off of 12-14 kDa Spectra/Por® (Spectrum Laboratories Inc., Houston, TX) with daily water change until the pH reached 6. The suspension was sonicated for 10 min using a tip-sonicator at 60% power output and was passed through a 1.2 μm glass fiber filter to remove large particles. The suspensions were lyophilized and were kept in a desiccator until analysis.

6.3.3 Scanning electron microscope (SEM)

The morphology of TCH was characterized using a LEO 1540 XB Scanning Electron Microscope (SEM) (Zeiss Nano Technology Systems Division, Oberkochen, Germany) with GEMINI electron optics in the Western Nanofabrication Facility at the University of Western Ontario. TCH powder samples were deposited on stubs and coated with 5 nm of osmium prior to analysis.

6.3.4 Transmission electron microscope (TEM)

TEM images of BCNs were recorded using a Philips CM 10 Transmission Electron Microscope (Philips Electron Optics, Eindhoven, The Netherlands) operating at an accelerating voltage of 80 kV. A drop of dilute aqueous suspension of samples were deposited on Formvar/carbon-coated electron microscope 400 mesh copper grids for 10 min, and the excess liquid was removed by blotting with a filter paper. The grids were dried by evaporation at ambient temperature. The BCNs' length and distribution (approximately 150-200 BCNs for each sample) were evaluated by an image analyzer, ImageJ (<http://rsbweb.nih.gov/ij/>).

6.3.5 X-ray diffraction (XRD)

The XRD diffractogram of samples were recorded on Rigaku Ultima IV X-ray diffractometer (Rigaku, The Woodlands, TX, USA) using copper x-ray source operating at 40 kV and 40 mA. The freeze dried bacterial cellulose samples were pressed into a thin and flat layer using glass slides, and analyzed following a method described previously (Cheng et al., 2009). Scans were collected at 2°/min in the range of 10-30° 2 θ . The cellulose crystallinity index was reported using the peak area method (Roman and Winter, 2004,

Ruka et al., 2013). Peak fitting of individual crystalline peaks to a Gaussian function was carried out using Origin (OriginLab, Northampton, MA) Peak Analyser software. A broad peak with a maximum between 18° and 22° was fitted as the amorphous cellulose contribution. The diffraction peak position was selected within 0.2° of the literature value to represent the true peak for fitting. Cellulose crystallinity index was determined by the peak area method (Cr.A) as a ratio of the sum of the areas under crystalline diffraction peaks to the total area under the curve between $2\theta = 10\text{-}30^\circ$ or in brief, $\text{Cr.A} = A_{\text{cr}} / (A_{\text{cr}} + A_{\text{am}})$ (Ahvenainen et al., 2016).

6.3.6 Zeta potential measurements

The zeta (ζ) potential measurements of samples at various pH levels were measured by electrophoretic light scattering using a ZetaPlus Zeta Potential Analyzer (Brookhaven Instrument Corporation, Holtsville, NY, USA) with a 30 mV solid state laser beam at a wavelength of 659 nm. All samples were maintained at 0.01 wt.% and measurements were taken at $25 \pm 1^\circ\text{C}$, shortly after sonication in a water bath (output: 60 Watts). The reported values are an average of 5 measurements.

6.3.7 Effect of pH on TCH adsorption

The adsorption of TCH onto BCNs, with TCH solutions at pH levels ranging from 3 to 7, was evaluated in triplicates. All suspensions were prepared using deionized water. Ten ml of 0.1 mg/ml TCH solution at a specified pH was added to 5 mg of freeze-dried BCN samples in glass vials. pH adjustment was carried out by adding 0.1 M NaOH and 0.1 M HCl. The samples were mixed thoroughly and kept in an orbital incubator for 2 h at 150 rpm and 25°C . Supernatant collected after centrifuging the sample at $10,000 \times g$ for 10 min was diluted with a proper dilution. The diluted supernatant samples were placed in a Quartz cell and absorbance was read at 364 nm using Genesys 10S UV-VIS spectrophotometer (Thermo Fisher Scientific, Waltham, MA, USA). Concentration of TCH was calculated using a calibration curve constructed using TCH solutions of different concentrations. Blank experiments without the addition of BCNs were also conducted to confirm that no adsorption occurred on the centrifuge tubes wall.

6.3.8 Adsorption kinetics of TCH on BCNs

Fifteen ml of 0.1 mg/ml of TCH solution in 10 mM phosphate buffered saline (PBS) at pH 7.4 was added to 5 ml of 2 mg/ml BCNs suspension. At each predetermined time, 0.5 ml of samples was taken out and centrifuged at 10,000 x g for 10 min. The absorbance of the supernatant was measured as mentioned on the previous section. An equal volume of fresh PBS was added to the adsorption samples. This buffer addition was done after each sampling time. For the duration of the kinetics experiment, TCH solution was covered by aluminum foil to prevent probable photo degradation of tetracycline (Wammer et al., 2011).

6.3.9 Drug release kinetics

The BCNs suspension was kept for 4 hours prior to mixing with the TCH solution. TCH was bound to BCNs for a release study by incubating a 1000 µg/ml TCH solution (at pH 3) containing 2 mg of BCNs. The suspension was centrifuged at 10000 x g for 10 min. The final mass of TCH bound to BCNs for the release studies was 150.5 ± 6.6 µg. The drug loaded BCNs samples were resuspended in 2 ml of phosphate buffered saline (PBS) followed by incubation at 37°C in a water bath. Sampling was performed at designated times. The suspensions were centrifuged and the concentration of TCH in supernatant was measured by UV-Vis as previously described.

6.4 Results and Discussion

6.4.1 TCH morphology and BCNs crystallinity

The SEM images of the TCH powder in different magnification show the bulk distribution of the drug and that proper mixing is needed to make sure that the TCH is well dispersed and dissolved in an aqueous solution (Ali, 1984). The drug solution concentration in this research work was well below the reported TCH solubility in water at 28°C which was 10.9 mg/ml (Ali, 1984).

The X-ray diffraction pattern of BCNs was characterized by three signature peaks at 2θ (°) of 14.6, 16.8, and 22.7 (Figure 6.2a). BCNs especially exhibit an intense and significant crystalline peak located at 22.7°. The crystallinity index of the BCNs samples were

calculated using peak area method and peak intensity method found to be 0.86 and 0.94, respectively. This is in agreement with that of wood-derived cellulose nanocrystals (Jackson et al., 2011). The SEM image of the BCNs suspension shows rod-like morphology of individual BCN nanocrystallites (Figure 6.2b).

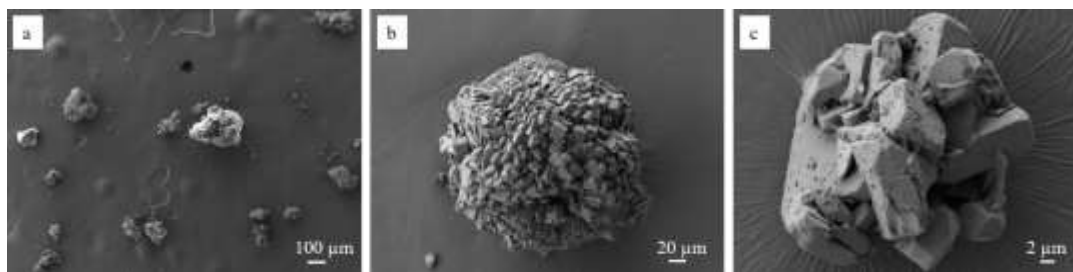


Figure 6.1 Scanning electron micrograph of tetracycline hydrochloride (TCH) powder as received.

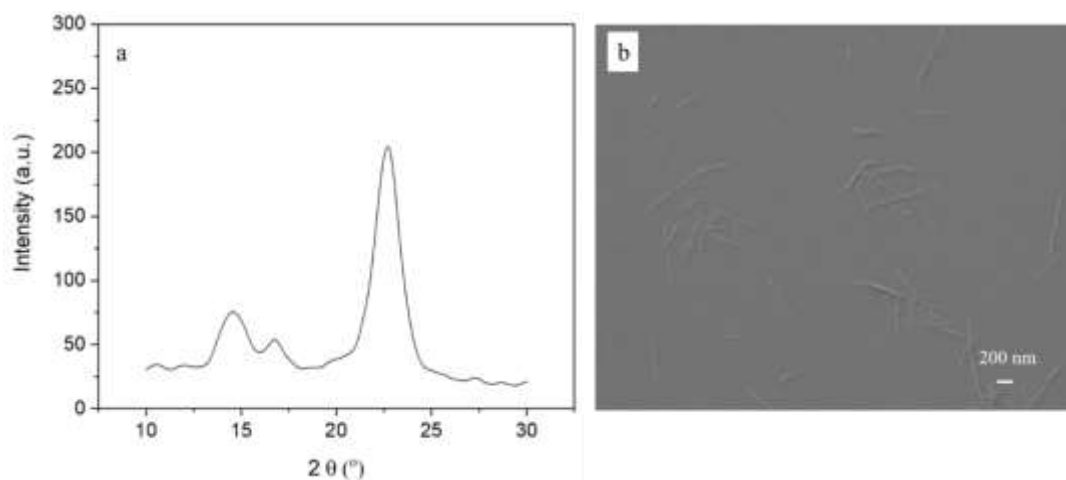


Figure 6.2. a) X-ray diffraction pattern on freeze-dried bacterial cellulose nanocrystals (BCNs). Prominent peaks at 2θ ($^{\circ}$) of 14.6, 16.8, and 22.7 indicated cellulose I. b) Scanning electron micrograph of BCNs in deionized distilled water.

6.4.2 Size distribution of BCNs

The length of about 200 individual BCNs was measured directly from TEM images. The width was defined as the largest dimension along the nanocrystals, perpendicular to its long axis (Elazzouzi-Hafraoui et al., 2008). BCNs have a wide distribution of length with most length between 100-400 nm (Figure 6.3). This is similar to CNs length reported in the literature which is in the range of 100-300 nm in length and 4-8 nm in diameter (Dash and Ragauskas, 2012).

While the width distribution of cellulose nanocrystals (CNs) was found to be relatively narrow, with mean average of 5.9 nm wide for wood-derived CNs and 14 nm wide for bacterial-derived CNs, it was not the case with the length distribution of CNs (Sacui et al., 2014). Sacui and co-workers reported that wood-derived CNs length was round 130 ± 67 nm while BCNs was 1103 ± 698 nm (Sacui et al., 2014). The substantial difference in length is reflected in CNs aspect ratio.

When comparing these values, it is important to note that CNs sources, extraction methods and treatment conditions result in CNs with different length and width distributions. Furthermore, the reporting of these CNs sizes can differ when one took into account the measurement of one particle constituted of several crystallites in opposed to single crystallite (Elazzouzi-Hafraoui et al., 2008). The size of nanocrystals plays an important role in BCNs applications. Kalashnikova and co-workers reported that CNs size directly influences the droplets coverage ratio in Pickering emulsion system (Kalashnikova et al., 2013). This physical characteristic in particular can greatly affect the adsorption process similar to its effect on stabilizing emulsions.

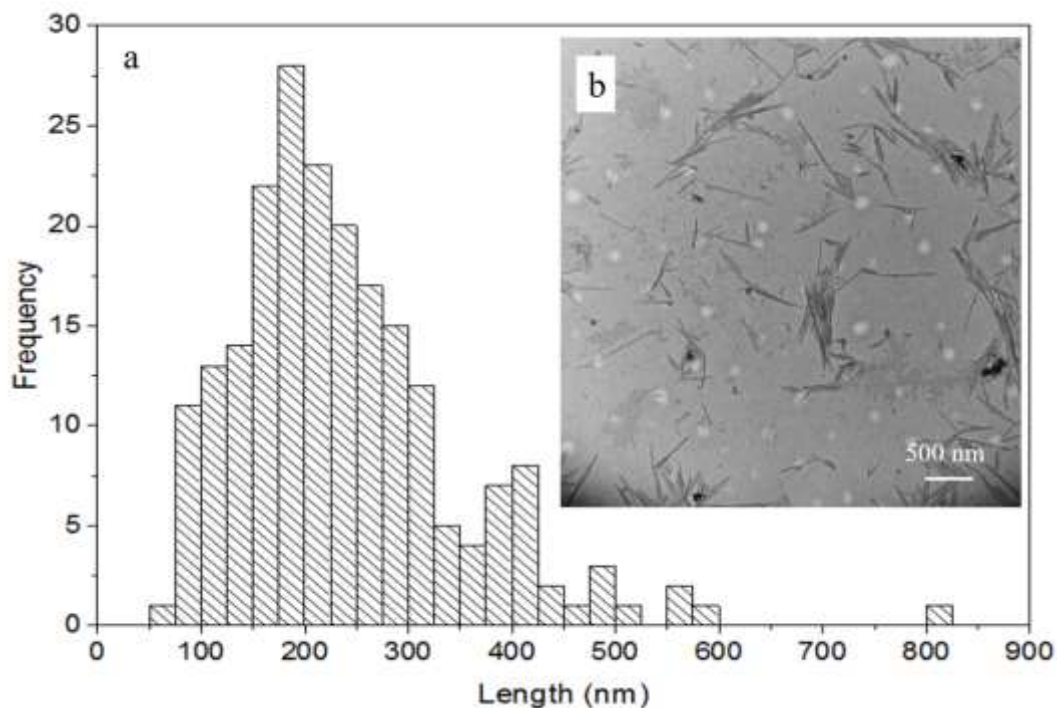


Figure 6.3 The length distribution of BCNs (a) obtained from TEM images and morphology of BCNs (b).

6.4.3 Effect of solution pH

The pH of the solution is a crucial parameter that can affect the amount of TCH adsorbed by altering the protonation and deprotonation of participating molecules. The interaction between BCNs and TCH and the zeta potentials of BCNs as a function of pH were characterized and shown in Figure 6.5. The negative charges on the surface of BCNs are due to the presence of sulfur ester functional groups from sulfuric acid hydrolysis. The zeta potentials of BCNs in water are ranging from -27.31 to -35.95 mV. It was hypothesized that the interaction between BCNs and TCH is electrostatic in nature between the positive charges on the surface of TCH and the negatively charged BCNs.

Table 6.1 Zeta potentials of bacterial cellulose nanocrystals (BCNs) in deionized water (H₂O) at 25°C and different pH. Zeta potential values are expressed as an average of three measurements.

Zeta-potential (mV)	pH 2	pH 3	pH 4	pH 5	pH 6	pH 7	pH 8
BCNs in H ₂ O	-29.04 (2.62)	-32.89 (1.22)	-27.71 (1.23)	-32.43 (1.19)	-27.49 (2.19)	-34.12 (1.14)	-35.95 (1.29)

TCH is zwitterionic and has variable charges with three functional groups. The pK_a values of TCH in water at 25°C are reported to be 3.30, 7.68, and 9.69, assigned as pK_{a1}, pK_{a2}, pK_{a3}, respectively in Figure 6.4 (Ali, 1984). The most acidic value is attributed to the β-tricarbonyl system. The middle pK_a is associated to the vinylogous acidic β-dicarbonyl system, and the highest pK_a is due to the protonated dimethylamino function at C₄. Depending on the pH of a solution, the three groups of tetracycline can undergo protonation and deprotonation reactions. However, the measurement of zeta potential for small molecules are not accurate.

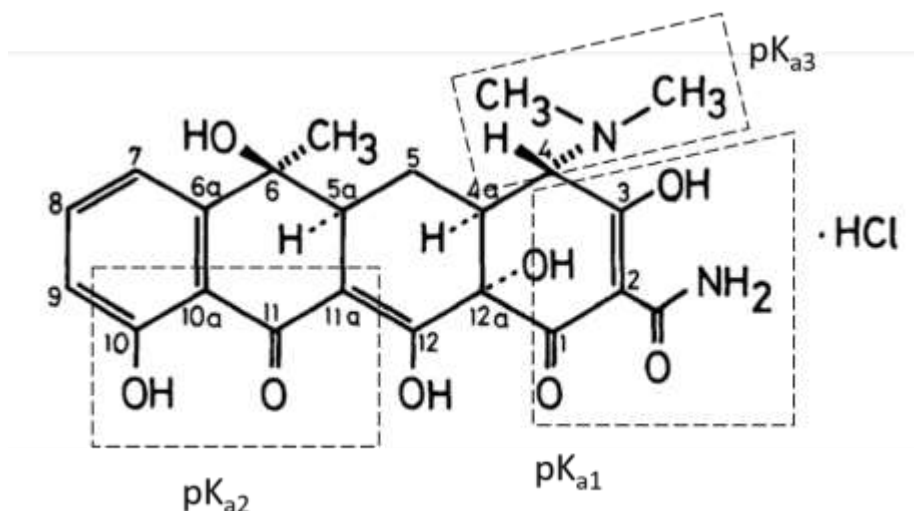


Figure 6.4. Molecular structure and functional groups of tetracycline hydrochloride (adapted from (Ali, 1984).

BCNs were mixed with TCH drug solution at different pH levels to investigate the BCNs' adsorption capacities (Figure 6.5). After 2 hours of incubation time, the adsorption capacity was determined. The adsorption capacity was the highest at pH 3 and 4, approximately 20 mg/g, while pH 5, 6, and 7 resulted in less than 12 mg/g. This agreed with the literature, indicating that TCH forms cationic species at pH <4, zwitterionic species at pH 3.5 and 7.5, and anionic species at pH >7.5 TCH (Rathod et al., 2015). In order to ensure that all the adsorption sites were completely saturated, the adsorption incubation was continued.

After 24 hours of incubation time, pH 3 and 4 samples showed a slightly lower q_e while pH 5 and 6 showed a 43% increase in q_e , approximately. The pH 7 sample appeared a slightly darker orange/yellow compared to other pH samples and showed a 53% increase in q_e compared to samples measured after 2 hours of incubation time. The absorbance of all TCH solutions without BCNs were measured and were observed to retain its absorbance value, even after 24 h. This indicated that the examined TCH solutions at all pH levels did not degrade within the observation period and the difference in sorption capacity could be attributed to the length of contact time with BCNs. This means that pH plays a more significant role on adsorption over shorter contact times.

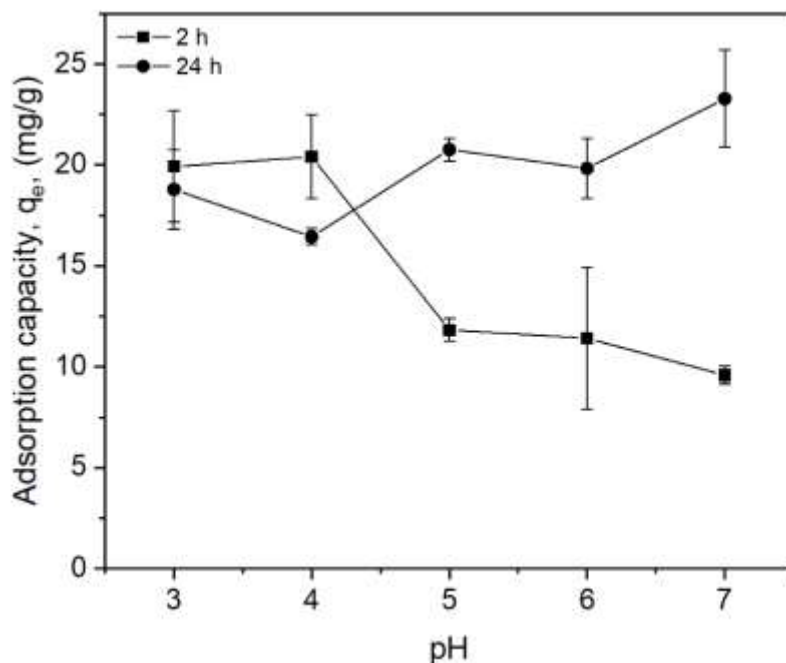


Figure 6.5. Effect of initial pH on biosorption of TCH to BCNs in deionized water (initial TCH concentration: 100 $\mu\text{g/ml}$; volume: 10 ml; BCNs: 10 mg; temperature: 25°C; agitation rate: 150 rpm; incubation time: 2 h).

6.4.4 Effect of BCNs dosage on TCH adsorption kinetics

The dose of adsorbent has an impact on adsorption properties during the adsorption process. Two different BCN concentrations were used to investigate the effect of adsorbent amount. The adsorption experiments were carried out using 0.5 and 1.0 mg BCNs/ml solution.

The adsorption kinetics study shows that the adsorption capacity is drastically enhanced in the first 30 min and gradually reached the equilibrium within 17 h (Figure 6.6). The adsorption kinetic data were analyzed by fitting the pseudo-first-order model (Equation 1) and pseudo-second-order model (Equation 2). The linear plots are shown Figure 6.7a-d.

Pseudo-first order model is expressed as follows (Equation1):

$$\log(q_e - q_t) = \log q_e - (k_1 t) \quad (1)$$

where q_t and q_e are the amount of sorbate sorbed at time t (mg/g) and sorption capacity at equilibrium (mg/g), respectively. k_1 is the pseudo-first order rate constant (/min) and t is the contact time (min). The values of q_e and k_1 of TCH in BCNs are determined from the plot of $\log(q_e - q_t)$ against t .

Pseudo-second order model is expressed as follows (Equation 2):

$$\frac{t}{q_t} = \frac{1}{k_2 q_e^2} + \frac{1}{q_e} t \quad (2)$$

Using Equation 2, the adsorption rate constant (k_2) and adsorption capacity (q_e) were calculated from the slopes and intercepts of the plot t/q_t against t .

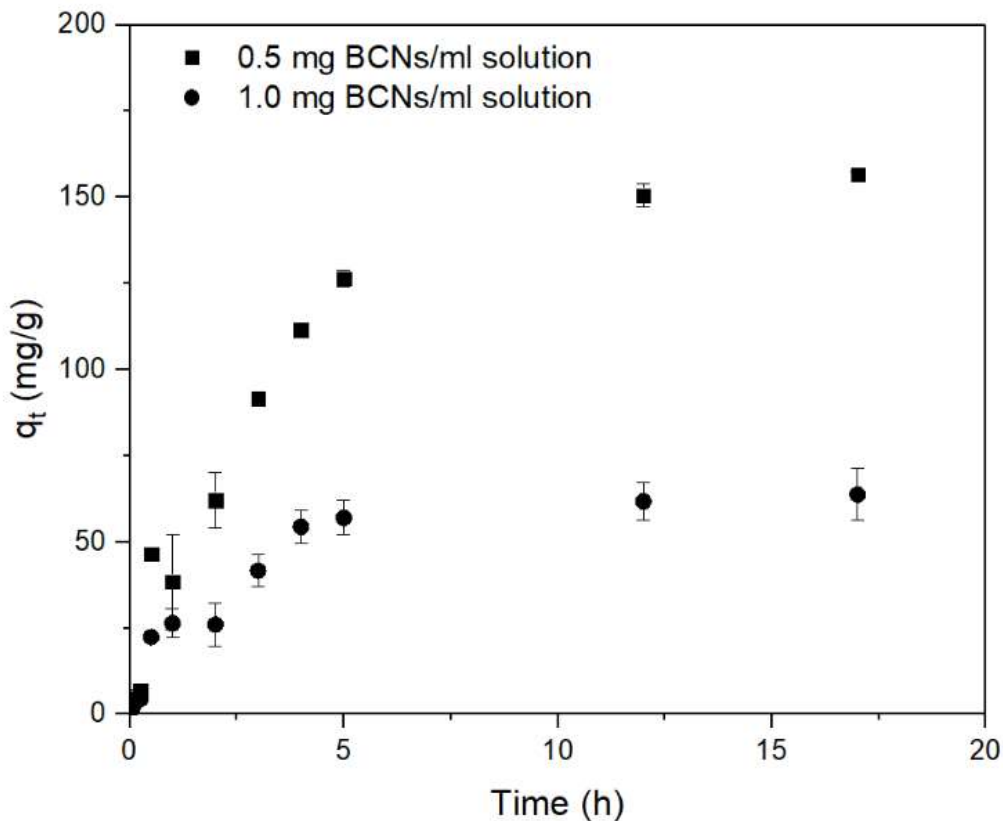


Figure 6.6. Adsorption kinetics of TCH to BCNs in water (initial pH: 3; TCH concentration: 1000 μ g/ml; volume: 2 ml; BCNs: 1 and 2 mg; temperature: 25°C).

Adsorption capacity of TCH dosed with 0.5 mg BCNs/ml solution was 157 ± 1 mg/g, nearly 2.5 times the adsorption capacity of TCH dosed with 1.0 mg BCNs/ml solution, calculated to be 64 ± 8 mg/g. Previous work reported a maximum of 251 μ g of TCH was bound when 1000 μ g of TCH was added to 2 mg of BCNs, indicating an adsorption capacity of TCH of 125.5 mg/g (Jackson et al., 2011).

The kinetic parameters calculated from the pseudo-first-order model and pseudo-second-order model are given in Table 6.2. The pseudo-second-order model showed a relatively better fit to experimental data regardless the BCN dosage. However, adsorption process in samples with BCN-0.5 mg/ml appeared to apply well to pseudo-first-order, where the calculated q_e value is similar to that of the experimental value. This could occur when the concentration of the drug is in excess and remain almost constant, thus, the rate dependence on the BCNs can be eliminated isolated. The results could also be explained by the effect of a boundary layer in the initial stages of sorption (Boudrahem et al., 2009).

When the BCNs dose was 1 mg/ml, the pseudo-second-order adsorption kinetics model represented the calculated q_e values well. This agreed with literature reports on TCH adsorption kinetics with CNs (Rathod et al., 2015).

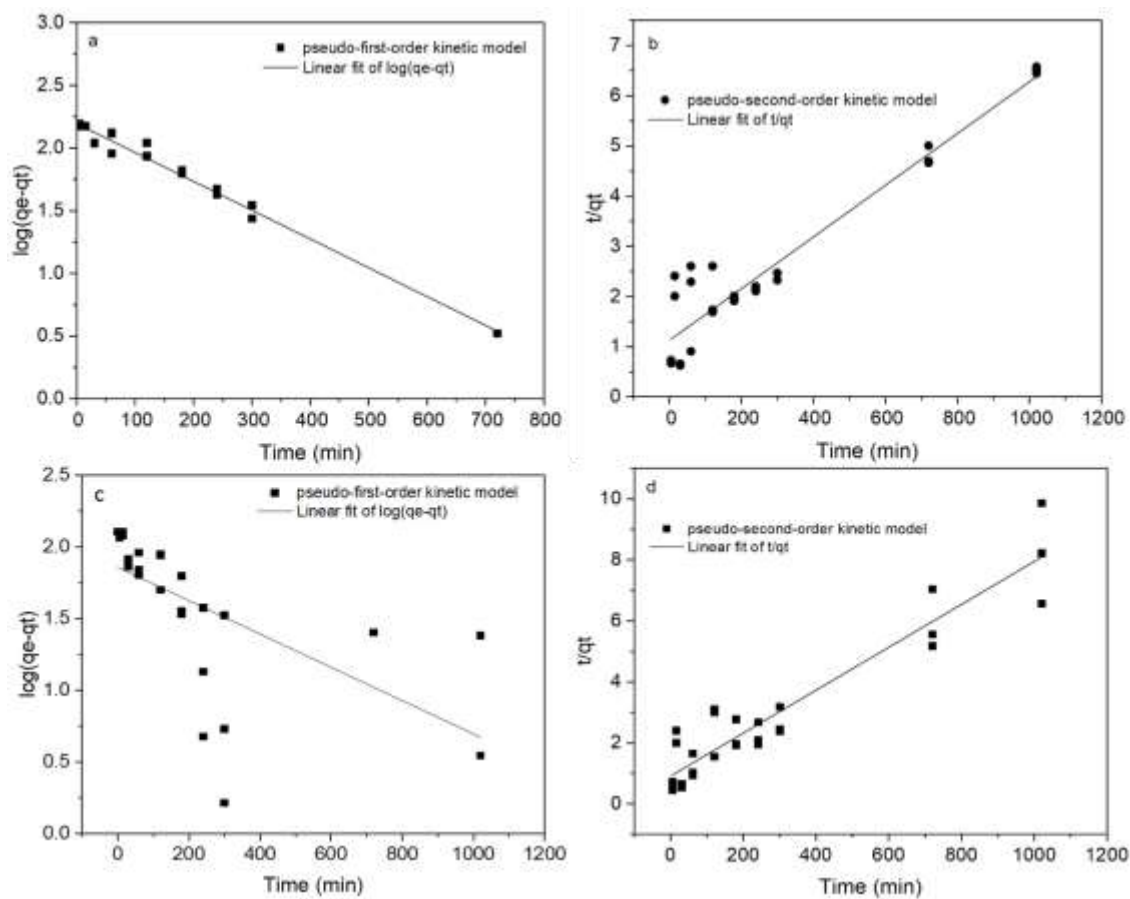


Figure 6.7. Linear regression adsorption kinetics of TCH of 0.5 mg BCNs/ml solution (a & b) and 1 mg BCNs/ml solution (c & d) following pseudo-first-order model and pseudo-second-order model.

Table 6.2. Kinetic parameters of TCH adsorption on BCNs in deionized water at 25°C.

Model	Parameters	BCNs-0.5 mg/ml	BCNs-1 mg/ml
Pseudo-first-order	C_0 (mg/l)	1000	1000
	$q_{e,exp}$ (mg/g)	156.6	64.0
	k_1 (min^{-1})	0.0023	0.0017
	$q_{e,cal}$ (mg/g)	156.5	72.1
	R^2	0.978	0.357
Pseudo-second-order	k_2 (g/mg min)	3.63E-05	6.75E-05
	$q_{e,cal}$ (mg/g)	194.2	142.0
	R^2	0.910	0.893

6.4.5 Drug release kinetics

TCH adsorbed to the BCNs surfaces was instantaneously released once suspended in PBS, reaching nearly 70% release of TCH within the first hour and reached a maximum release of 79% of TCH in 3 hours (Figure 6.8). Previous work on CNs reported 93% TCH drug released within 24 h (Jackson et al., 2011). The control TCH solution, without BCNs, was kept in a water bath at 37°C and the absorbance measurement was periodically performed. This was to ensure that TCH degradation did not occur during the experimental period. After two hours the percent released decreased, which could be due to the interaction between the ionic species of TCH as well as re-adsorption onto the BCNs surfaces.

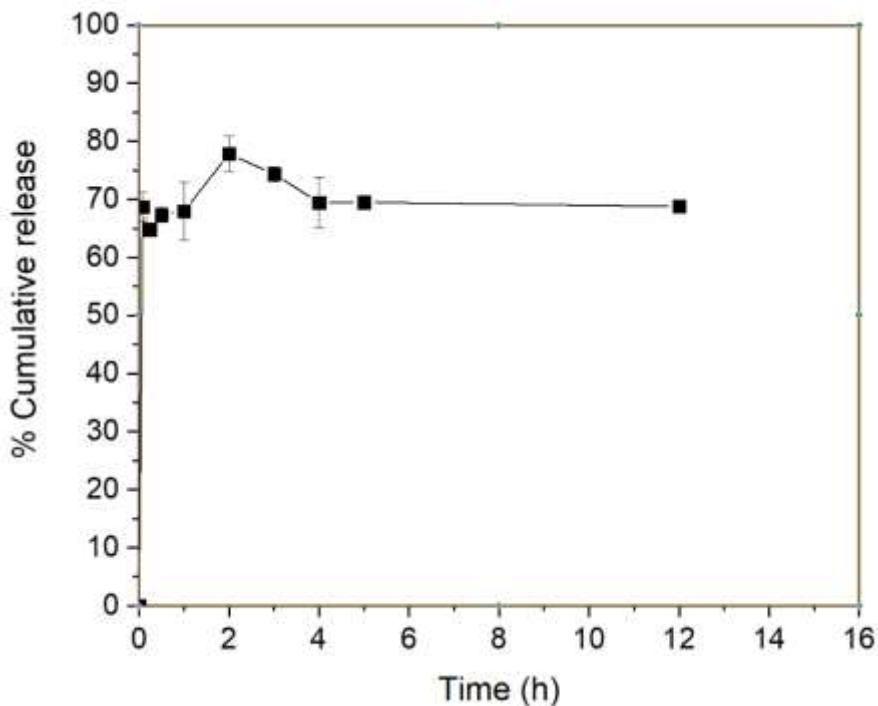


Figure 6.8. The release kinetics of tetracycline hydrochloride (TCH) from bacterial cellulose nanocrystals (BCNs) in 10 mM phosphate buffered saline at 37°C (initial TCH concentration: 1000 µg/ml; volume: 2 ml; BCNs: 2 mg; temperature: 37°C)

6.5 Conclusion

In this study, we investigated the size distribution and morphology of BCNs, demonstrated a potential application of BCNs as an alternative drug delivery carrier molecule. The pH of the solution was shown to affect the protonation and deprotonation of drug species, which influenced the adsorption capacity. At short adsorption incubation time of 2 h, the highest adsorption capacity was achieved at pH 3 of TCH solution where TCH was in the cationic form. After 24 hours of incubation time, pH 7 showed significantly higher adsorption capacity than at pH 3. BCNs are capable of binding ionizable water soluble antibiotic tetracycline hydrochloride and rapidly release this drug in PBS in less than 3 hours. The amount of TCH adsorbed to BCNs was comparable to that adsorbed by wood-cellulose derived CNs. The adsorption kinetics of TCH on BCNs appeared to follow pseudo-second order kinetic model with a better fit on higher BCNs doses.

6.6 Reference

- Ahvenainen, P., Kontro, I. & Svedström, K. 2016. Comparison of sample crystallinity determination methods by X-ray diffraction for challenging cellulose I materials. *Cellulose*, 23, 1073-1086.
- Ali, S. L. 1984. Tetracycline Hydrochloride. *Analytical Profiles of Drug Substances*, 13, 597-653.
- Boudrahem, F., Aissani-Benissad, F. & Aït-Amar, H. 2009. Batch sorption dynamics and equilibrium for the removal of lead ions from aqueous phase using activated carbon developed from coffee residue activated with zinc chloride. *Journal of Environmental Management*, 90, 3031-3039.
- Cheng, K. C., Catchmark, J. M. & Demirci, A. 2009. Enhanced production of bacterial cellulose by using a biofilm reactor and its material property analysis. *Journal of biological engineering*, 3, 12.
- Dash, R. & Ragauskas, A. J. 2012. Synthesis of a novel cellulose nanowhisker-based drug delivery system. *RSC Advances*, 2, 3403-3409.
- Elazzouzi-Hafraoui, S., Nishiyama, Y., Putaux, J.-L., Heux, L., Dubreuil, F. & Rochas, C. 2008. The shape and size distribution of crystalline nanoparticles prepared by acid hydrolysis of native cellulose. *Biomacromolecules*, 9, 57-65.
- Habibi, Y., Lucia, L. A. & Rojas, O. J. 2010. Cellulose nanocrystals: chemistry, self-assembly, and applications. *Chemical Reviews*, 110, 3479-3500.
- Jackson, J. K., Letchford, K., Wasserman, B. Z., Ye, L., Hamad, W. & Burt, H. M. 2011. The use of nanocrystalline cellulose for the binding and controlled release of drugs. *International Journal of Nanomedicine*, 6, 321-330.
- Kalashnikova, I., Bizot, H., Bertoncini, P., Cathala, B. & Capron, I. 2013. Cellulosic nanorods of various aspect ratios for oil in water Pickering emulsions. *Soft Matter*, 9, 952-959.
- Lam, E., Male, K. B., Chong, J. H., Leung, A. C. W. & Luong, J. H. T. 2012. Applications of functionalized and nanoparticle-modified nanocrystalline cellulose. *Trends in Biotechnology*, 30, 283-290.
- Lee, B.-S., Lee, C.-C., Wang, Y.-P., Chen, H.-J., Lai, C.-H., Hsieh, W.-L. & Chen, Y.-W. 2016. Controlled-release of tetracycline and lovastatin by poly(d,l-lactide-co-glycolide acid)-chitosan nanoparticles enhances periodontal regeneration in dogs. *International Journal of Nanomedicine*, 11, 285-297.
- Peng, B. L., Dhar, N., Liu, H. L. & Tam, K. C. 2011. Chemistry and applications of nanocrystalline cellulose and its derivatives: A nanotechnology perspective. *The Canadian Journal of Chemical Engineering*, 89, 1191-1206.

- Rathod, M., Haldar, S. & Basha, S. 2015. Nanocrystalline cellulose for removal of tetracycline hydrochloride from water via biosorption: Equilibrium, kinetic and thermodynamic studies. *Ecological Engineering*, 84, 240-249.
- Roman, M. & Winter, W. T. 2004. Effect of Sulfate Groups from Sulfuric Acid Hydrolysis on the Thermal Degradation Behavior of Bacterial Cellulose. *Biomacromolecules*, 5, 1671-1677.
- Ruka, D. R., Simon, G. P. & Dean, K. M. 2013. In situ modifications to bacterial cellulose with the water insoluble polymer poly-3-hydroxybutyrate. *Carbohydrate Polymers*, 92, 1717-1723.
- Sacui, I. A., Nieuwendaal, R. C., Burnett, D. J., Stranick, S. J., Jorfi, M., Weder, C., Foster, E. J., Olsson, R. T. & Gilman, J. W. 2014. Comparison of the Properties of Cellulose Nanocrystals and Cellulose Nanofibrils Isolated from Bacteria, Tunicate, and Wood Processed Using Acid, Enzymatic, Mechanical, and Oxidative Methods. *ACS Applied Materials & Interfaces*, 6, 6127-6138.
- Tang, J., Sisler, J., Grishkewich, N. & Tam, K. C. 2017. Functionalization of cellulose nanocrystals for advanced applications. *Journal of Colloid and Interface Science*, 494, 397-409.
- Wammer, K. H., Slattery, M. T., Stemig, A. M. & Ditty, J. L. 2011. Tetracycline photolysis in natural waters: Loss of antibacterial activity. *Chemosphere*, 85, 1505-1510.

Chapter 7

7 Conclusions and Recommendations

7.1 Conclusions

Bacteria-derived cellulose offers key advantages when compared to other sources of nanocellulose. In particular, the possibility to tailor the bacterial cellulose properties during synthesis is unique to bacterial cellulose (BC). The use of cellulose nanocrystals (CNs) in many applications has been widely investigated in the past decades, with relatively few reports on bacterial cellulose nanocrystals (BCNs).

Limited understanding on how the culturing conditions applied during cellulose biosynthesis affects the yield and characteristics of BCNs was the primary motivation for this research. In addition, the resultant BCNs were used to study the effect of acid hydrolysis on BCNs properties and their capacity to adsorb the model drug antibiotic tetracycline hydrochloride (TCH).

Longer cultivation time and higher agitation rate led to an increase in BC fiber produced. Comparison between shake flasks with and without baffles emphasized the advantages of mixing on the bacterial cellulose production. On the other hand, longer cultivation time and higher agitation rate produced BC fiber with lower crystallinity. Thus, selection of shake flask geometry, shaker speeds, and cultivation time need to be considered during the design of a bioprocessing system to enhance the yield of BC fiber.

A 3L stirred-tank bioreactor, offering a means to scale-up BC production, was used to study the effect of agitation rates on the kinetics of growth and oxygen uptake of *K. xylinus* cells. Similar to the shake flask study finding, higher agitation rate resulted in higher production yields of BC fiber. In addition to allowing the monitoring and control of process parameters during cultivation, the bioreactor system allowed the possibility to tailor the BC properties during synthesis, which is unique to bacterial-derived cellulose.

A screening study using fractional factorial design was applied to identify the parameters that significantly affected the production of BC fiber and nanocrystals. As expected, a

higher BC production (g/l) was found to generate a higher BCNs yield (g) per liter of liquid culture medium. In addition, adsorption studies on BCNs obtained with different initial medium pH and rotational speeds suggest that, the impact of these culturing conditions were overridden by chemical modifications introduced during acid hydrolysis. BCNs produced from different fermentation runs exhibited comparable adsorption capacity towards TCH.

The use of BCNs as a nano drug carrier for controlled drug delivery was explored. Based on methodologies from previous studies using wood-derived CNs, the amount of TCH that was bound to BCNs was determined, as were the morphologies of BCNs. BCNs exhibited a higher length distribution than wood-based CNs. The amount of TCH bound to BCNs was comparable to that found on wood-derived CNs. Adsorption studies on solutions of different pH and BCNs dosage were performed, and was found that pH 3 and 0.5 mg BCNs/ml solution resulted in maximum adsorption capacity. Moreover, adsorption kinetics of TCH on BCNs demonstrated a behavior that followed pseudo-second order model. In addition to providing insight into the effect of BC production methods on the yield and characteristics of BCNs, this study demonstrated the use of bacterial derived-CN as bioadsorbent and as an alternative to that of plant-derived CNs.

In brief, this thesis contributed to the following findings:

- There was a tradeoff between BC production and cellulose crystallinity. Longer cultivation time and higher agitation rate led to an increase in BC fiber produced and lower cellulose crystallinity.
- BC cultivation conditions affected the yield of BCNs. Higher rotational speed promoted higher BC production and resulted in higher BCNs per volume of liquid medium.
- BC cultivation conditions did not affect BCNs surface characteristics due to the overriding acid hydrolysis.

- Adsorption of TCH on BCNs is comparable to the adsorption of TCH on plant based CNs.
- BCNs showed burst release kinetics and is applicable for anesthetic and fast release, but not applicable for controlled drug delivery.

7.2 Recommendations

Based on the findings of this research, it is recommended that further studies focus on addressing the following:

- Develop a model to study the impact of scaling up to a different bioreactor type or different mode of operation (like fed-batch) on BC production and cellulose crystallinity.
- Addition of water soluble polymers to the liquid medium during BC culturing has been reported to modify the properties of BC fibers, however there is no literature on its impact on altering the surface properties of BCNs.
- Further studies to optimize acid hydrolysis conditions can result in an increase in BCNs yield. Limiting the amount of acids used and shortening hydrolysis time is essential. Optimization of acid hydrolysis can help lower the cost, which can augment the growth of BCNs in many applications.
- Different acid hydrolysis conditions, presented in Appendix C, can influence the CNs size distribution and surface charge. More work should be done in exploring the effect of size distribution and surface charge of BCNs for different applications, such as: drug adsorbent and emulsion stabilizer.
- Although tetracycline hydrochloride was selected as the model drug for adsorption to pristine BCNs and for comparing with previously published research work, different drugs that are ionizable and water soluble could be explored. Other

studies have modified the surface of CNs for enhancing adsorption of hydrophobic drugs.

- Explore the use of pristine BCNs in oil-in-water emulsion for oil recovery, or for Pickering emulsion stability. Studies on the effect of BCNs concentration, oil viscosity, and oil fraction will provide an insight on how BCNs adsorption onto oil stabilizes Pickering emulsions.

Appendices

Appendix A: Pictures of bacterial cellulose and bacterial cellulose nanocrystals

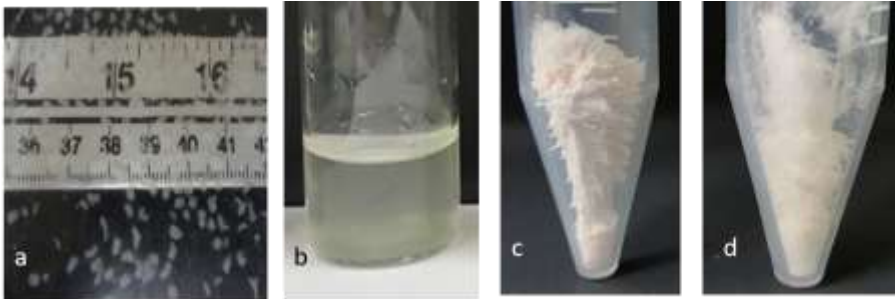


Figure A.1 Pictures of bacterial cellulose (BC) obtained from shake flasks experiment rotated at 250 rpm, (a) before homogenization and freeze drying and (c) after freeze drying. Pictures of bacterial cellulose nanocrystals (BCNs) after acid hydrolysis, (b) before freeze drying and (d) after freeze drying.

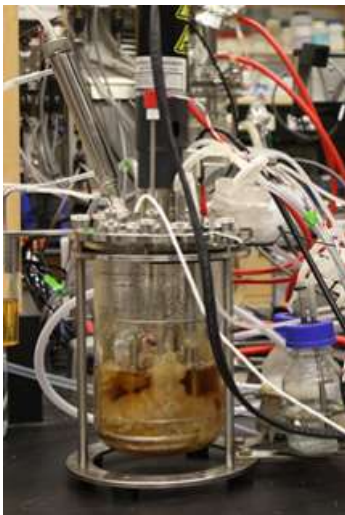


Figure A.2 Bacterial cellulose fibers production in fructose and corn steep solid solution medium in a 3 L BioFlo bioreactor with dual Rushton turbine impellers. Bacterial cellulose fibers clumps were visible near the wall, baffles, and probes area rendering non-homogeneous fluid.

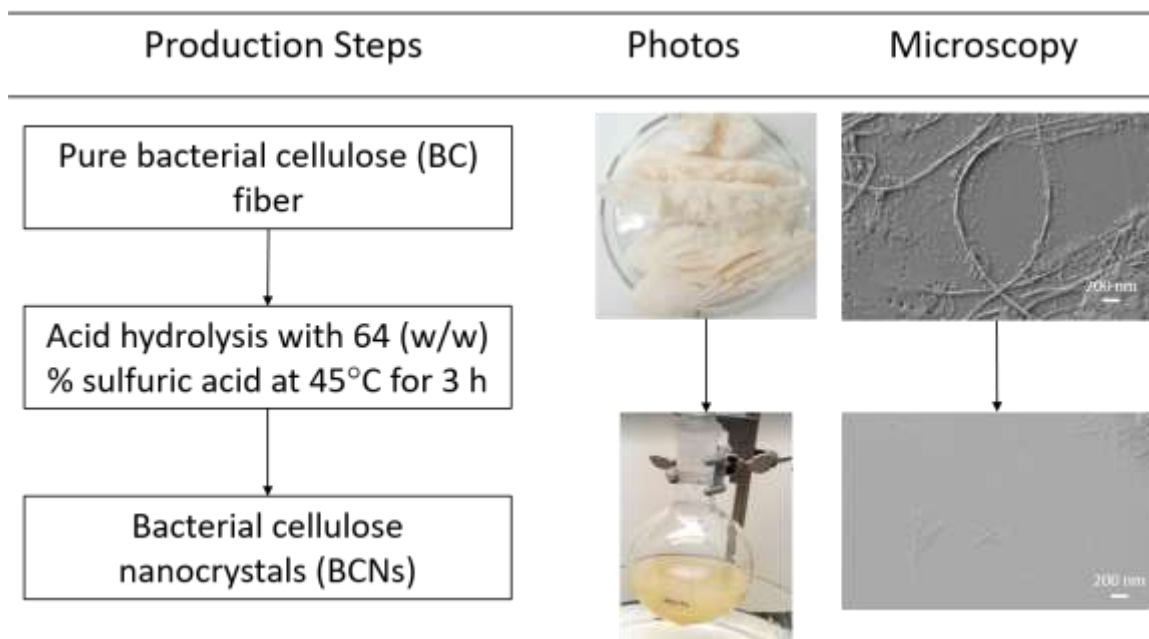


Figure A.3 The schematic diagram on bacterial cellulose nanocrystals production steps, the photos of freeze-dried BC and BCNs suspension during acid hydrolysis, and the corresponding scanning electron microscopy images.

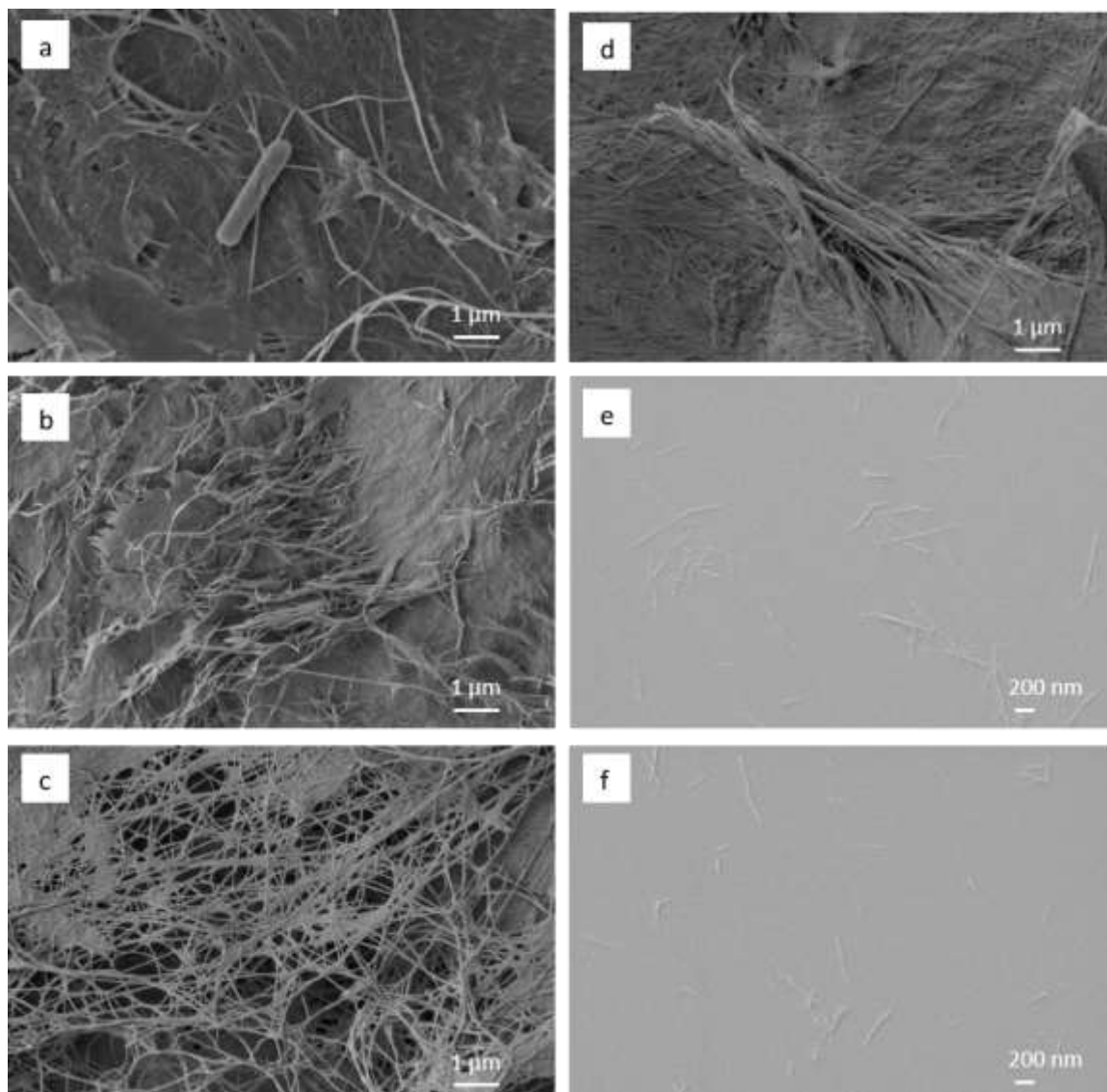


Figure A.4 SEM images of bacterial cellulose fibers: a) BC before purification showing *K. xylinus* producing BC nanofibril, b) BC-Ag c) BC-Bioreactor, and d) BC-Static. The bar corresponds to 1 μm and magnification is 10 k x. SEM images of bacterial cellulose nanocrystals: e) BCN-Ag, and f) BCN-Bioreactor. The bar corresponds to 200 nm and magnification is 20 k x. BCNs-Bioreactor: BCNs obtained from BC grown in bioreactor for 3 days at 700 rpm. BCNs-St: BCNs obtained from BC grown in static culture for 60 days. BCNs-Ag: BCNs obtained from BC grown in shake flasks incubated in shaker incubator at 250 rpm for 5 days. Hydrolysis conditions: acid: 64%(w/w) sulfuric acid; temperature: $^{\circ}\text{45C}$; acid to BCNs ratio: 100 ml/g.

Appendix B: Characterization of bacterial cellulose nanocrystals via sulfuric acid hydrolysis

Appendix B1: Bacterial cellulose nanocrystals (BCNs) production

Effect of acid hydrolysis time and acid to BCNs weight ratio were examined to investigate the length and width distribution of BCNs with the following parameters (Table B.1). Figure B.1 and Figure B.2 show the length and width distribution of BCNs, respectively.

The higher acid to BCNs ratio generally produced BCNs with a slightly smaller width. Different acid hydrolysis conditions, reaction time and acid to BCNs ratio, did a little variation on the width of BCNs. On the other hand, the length of BCNs is greatly affected by the hydrolysis time and the acid to BCNs ratio.

Table B.1 The mean width and length of BCNs from 150-200 individual nanocrystals and the standard deviation.

Hydrolysis time (h)	Acid to BCNs ratio: (ml sulfuric acid/g BCNs)			
	40 ml/g	100 ml/g	40 ml/g	100 ml/g
	Width (nm)		Length (nm)	
0.75	22.8 ± 8.8	-	390.4 ± 196.4	-
1.5	16.6 ± 6.6	16.6 ± 4.5	204.0 ± 121.1	211.3 ± 125.9
2	-	14.5 ± 3.8	-	212.5 ± 141.3
3	16.2 ± 4.7	14.1 ± 3.7	315.7 ± 212.6	252.5 ± 128.1
24	-	12.6 ± 3.8	-	210.1 ± 107

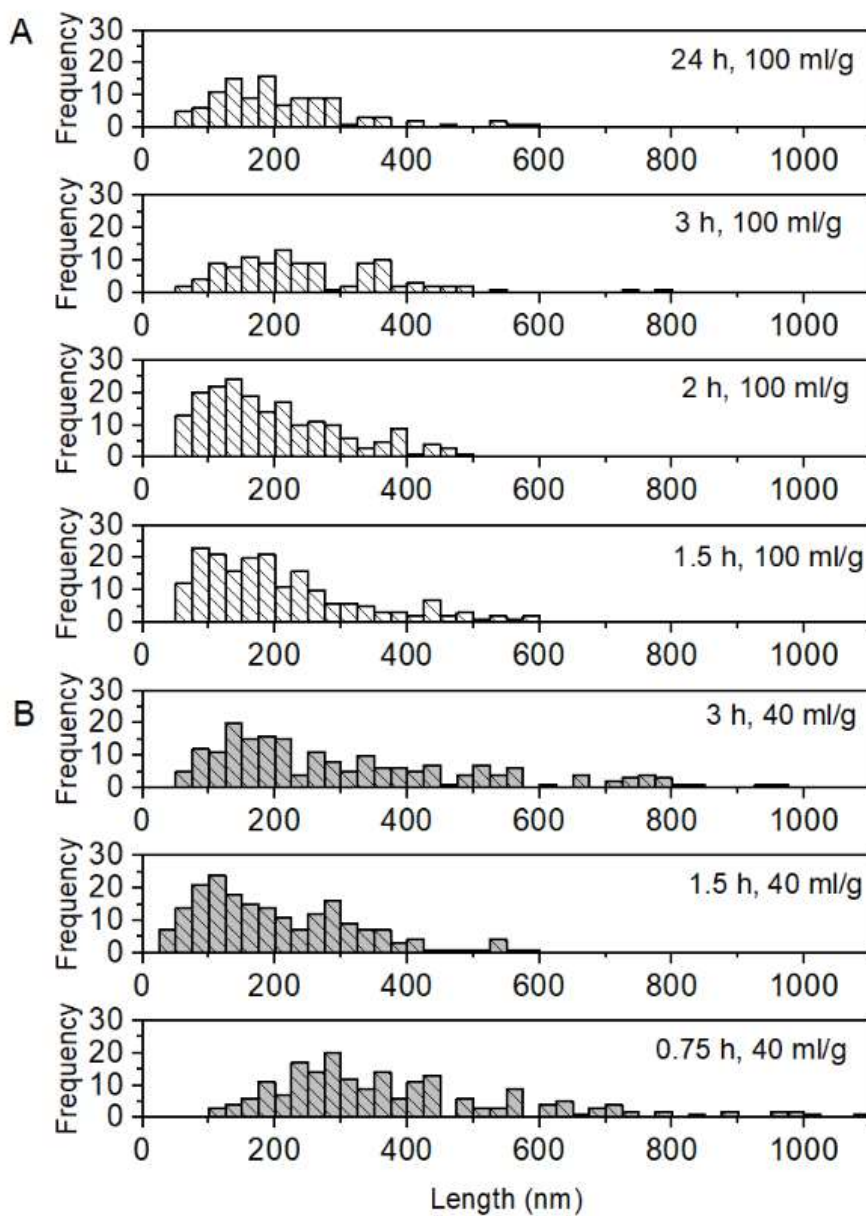


Figure B.1 The length distribution of BCNs obtained at several acid hydrolysis times and two acid-to-BCNs ratios: A) 40 and B) 100 ml of sulfuric acid/g BCNs.

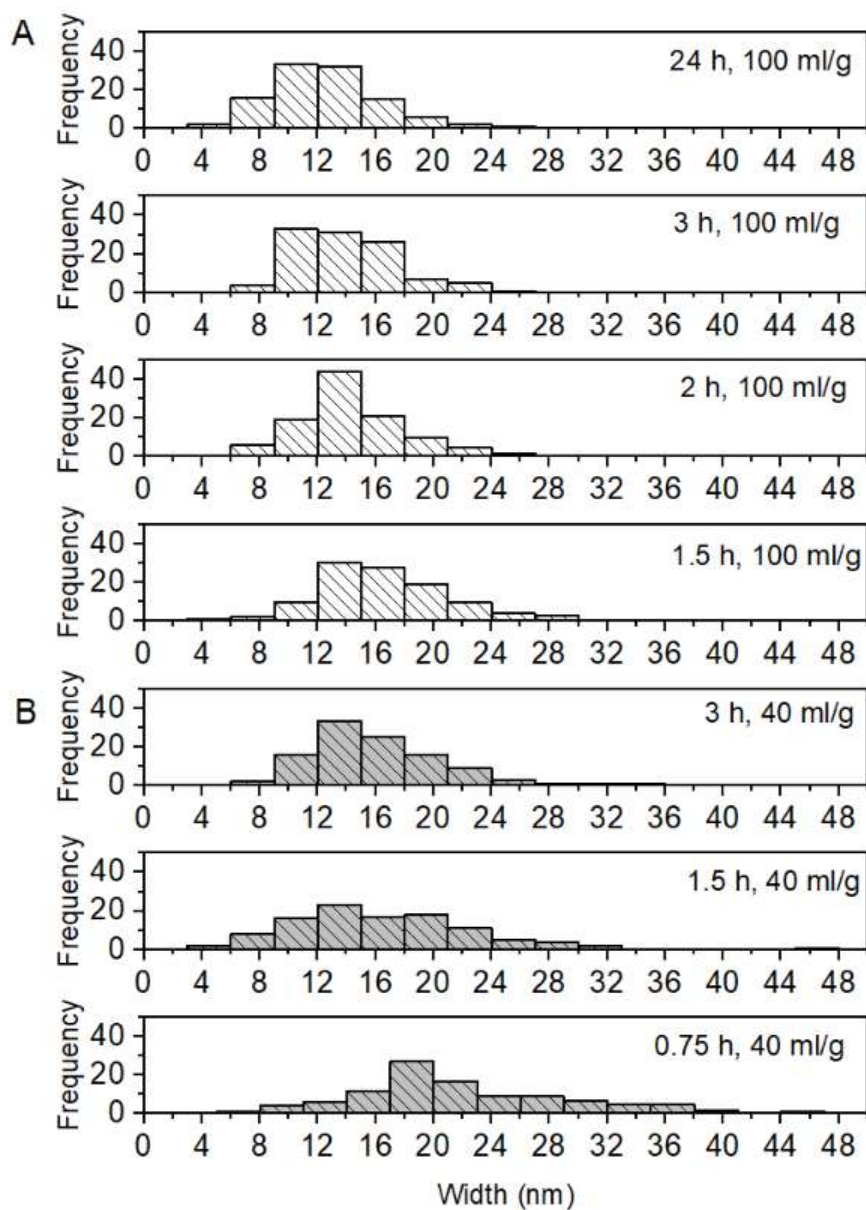


Figure B.2 The width distribution of BCNs obtained at several acid hydrolysis times and two acid-to-BCNs ratios: A) 40 and B) 100 ml of sulfuric acid/g BCNs.

Appendix B2: Size distribution of bacterial cellulose nanocrystals (BCNs) and Avicel cellulose nanocrystals (Avi-CNs) obtained at different acid hydrolysis times.

The length distribution of BCNs obtained from different culturing methods (static and shake flask rotated in an orbital incubator at 250 rpm) are compared to CNs obtained from acid hydrolysis of Avicel (as shown in Figure B.3 and Figure B.4). Data to generate the histograms were obtained by measuring at least 150 individual nanocrystals on TEM images using ImageJ software.

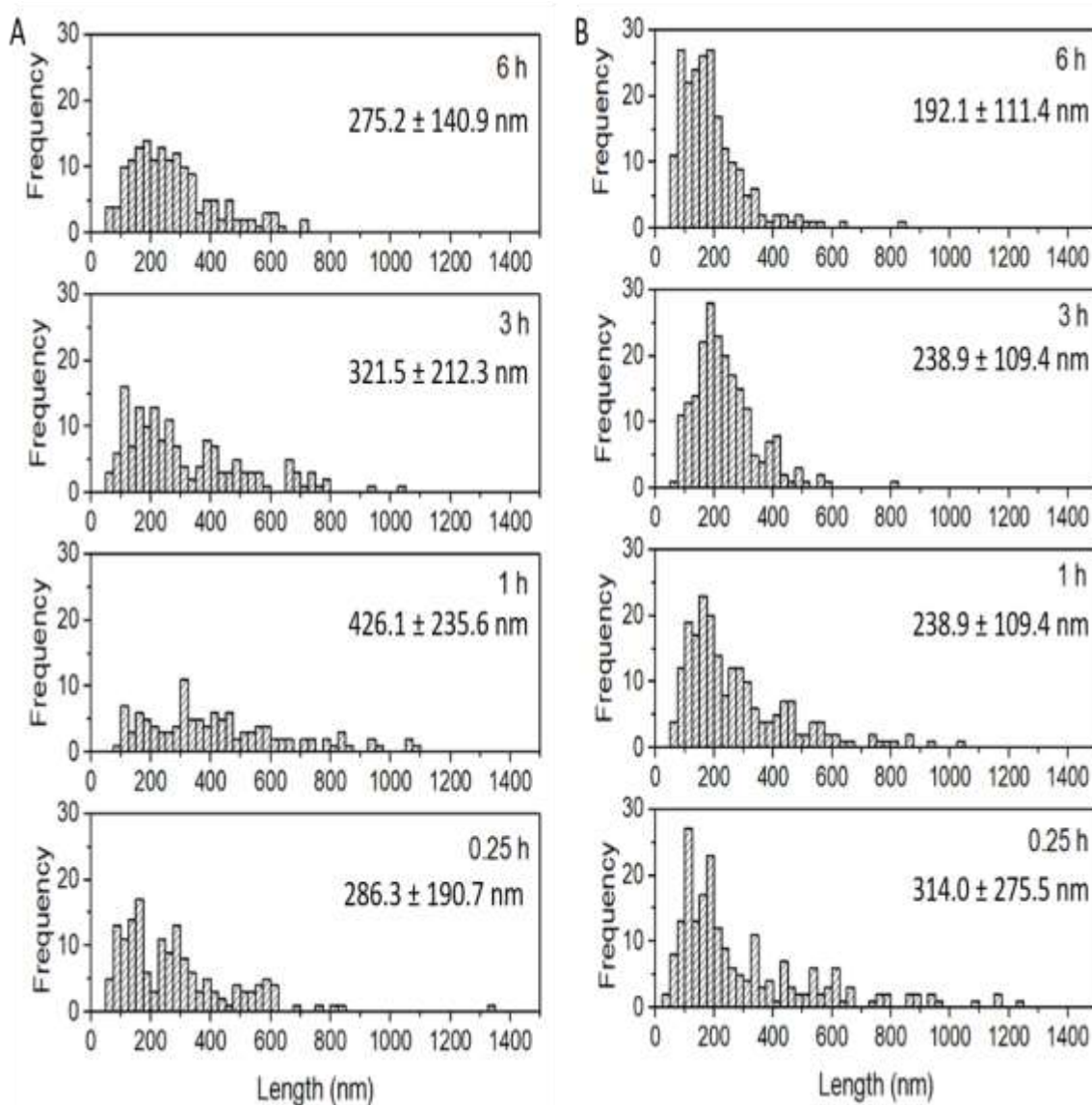


Figure B.3 Size distribution of BCNs and the mean length \pm standard deviation at varying acid hydrolysis times for A) BCNs-St and B) BCNs-Ag (Hydrolysis condition:

acid: 64%(w/w) sulfuric acid; temperature: °45C; acid to BCNs ratio: 100 ml/g). BCNs-St: BCNs obtained from BC grown in static culture for 60 day. BCNs-Ag: BCNs obtained from BC grown in shake flasks incubated in shaker incubator at 250 rpm for 5 days.

Although 3 h and 6 h of acid hydrolysis time of Avicel resulted the same average of CNs length, the longer acid hydrolysis time produced CNs with a narrower length distribution.

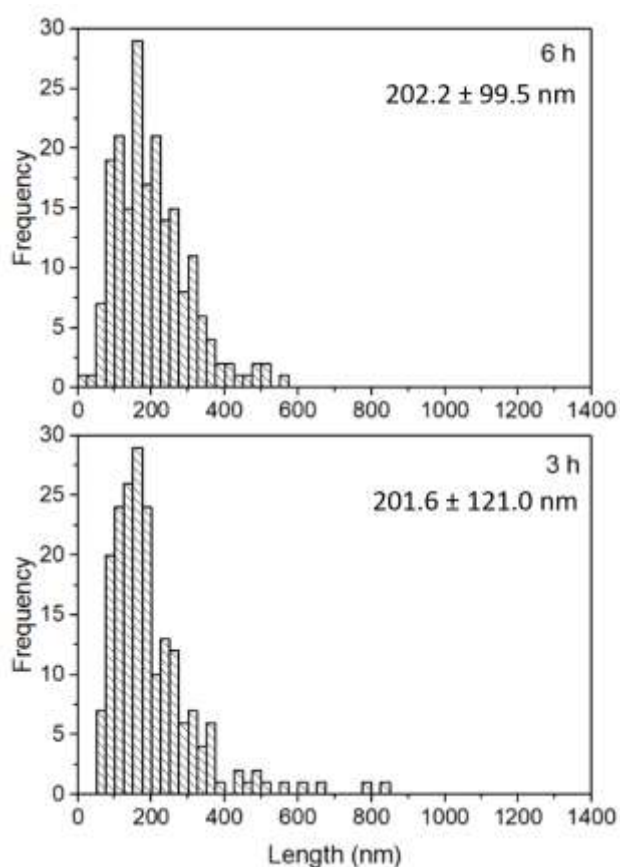


Figure B.4 Size distribution of Avi-CNs and the mean length \pm standard deviation at varying acid hydrolysis times. (Hydrolysis condition: acid: 64%(w/w) sulfuric acid; temperature: 45°C; acid to Avicel ratio: 100 ml/g). Avi-CN: CNs obtained from Avicel.

Appendix C: Calibration curves for TCH in 10 mM PBS at pH 7 and in deionized water at pH 3 to 7

Table C.1 Slope and R² values for the calibration curves of TCH solution in 10 mM PBS at pH 7.4 and in deionized water at pH 3 to 7.

Medium	Slope	R ²
10 mM PBS, pH 7.4	0.0319	0.9999
dH ₂ O, pH 3	0.0335	0.9999
dH ₂ O, pH 4	0.0348	0.9996
dH ₂ O, pH 5	0.0353	0.9999
dH ₂ O, pH 6	0.0349	0.9980
dH ₂ O, pH 7	0.0356	0.9999

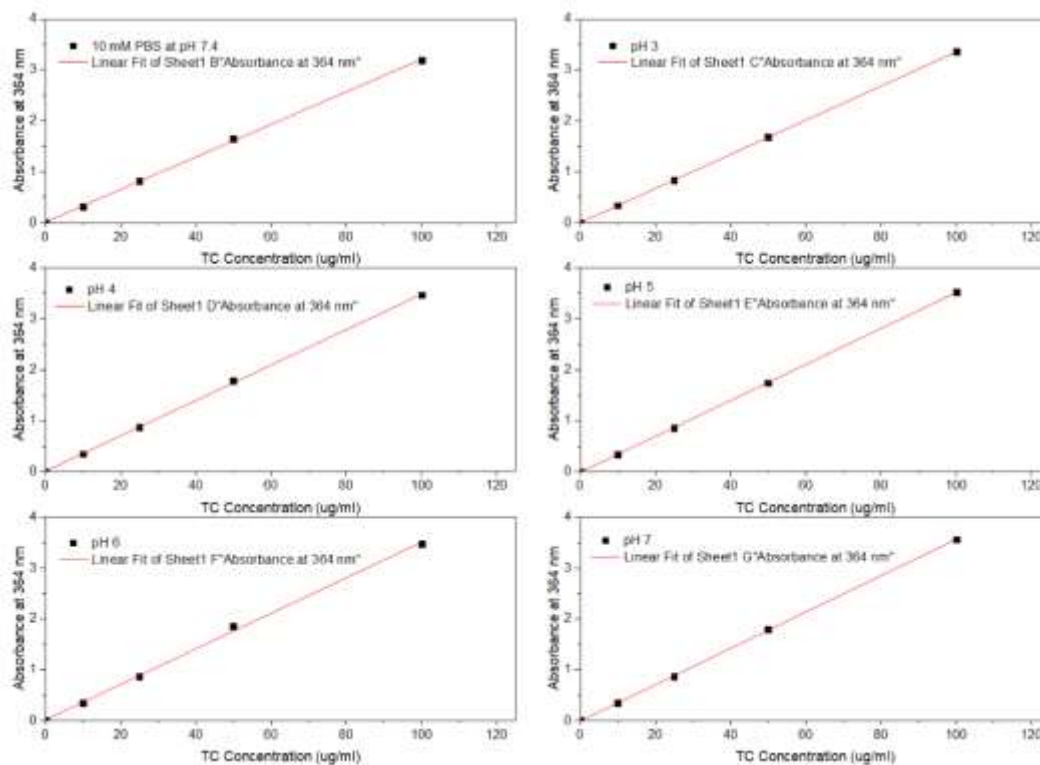


Figure C.1 Calibration curves of TCH in solution in PBS and in deionized water at pH 3 to 7.

Curriculum Vitae

ISABELA REINIATI

EDUCATION

Doctor of Philosophy in Chemical and Biochemical Engineering. The University of Western Ontario, London, Ontario Canada, Department of Chemical and Biochemical Engineering.	2011-2017
Master of Science in Chemical Engineering. Washington State University, Pullman, WA, USU, The Gene and Linda Voiland School of Chemical Engineering and Bioengineering.	2007-2009
Bachelor of Science in Chemical Engineering. Washington State University, Pullman, WA, USA, The Gene and Linda Voiland School of Chemical Engineering and Bioengineering.	2004-2007

RESEARCH EXPERIENCE

Chemical and Biochemical Engineering PhD Candidate, Western Ontario, London, Ontario, Canada.	2011-2017
Graduate Research Assistant The Gene and Linda Voiland School of Chemical Engineering and Bioengineering, Washington State University, Pullman, WA, USA	2007-2009
Research Assistant Composite Materials and Engineering Center, Washington State University, Pullman, WA, USA	2006-2007

TEACHING EXPERIENCE

Teaching assistant, Western Ontario, London, Ontario, Canada.	2011-2016
Chemical Engineering Thermodynamics	2015
Engineering Solutions – Environmental Sustainability	2013-2015
Fundamentals of Biochemical and Environmental Engineering	2014
Chemical Process and Plant Design	2012-2014

ENGINEERING EXPERIENCE

Sales Engineer, NATS Inc., Middletown, Connecticut	2010-2011
<ul style="list-style-type: none"> Created and delivered proposals for up to \$500,000 worth of tenders. Provided pre-sales technical assistance, product education, and after-sales support services. 	
Outreach Specialist, Claretian Associates, Chicago, Illinois	2009-2010
<ul style="list-style-type: none"> Conducted outreach for green building sustainable design to resource-limited communities. 	

PUBLICATIONS

Reiniati, I., Hrymak, A., and Margaritis, A. 2017. Kinetics of Cell Growth and Crystalline Nanocellulose Production by *Komagataeibacter xylinus*. *Biochemical Engineering Journal*, In Press, 22 July 2017. (<https://doi.org/10.1016/j.bej.2017.07.007>).

Reiniati, I., Hrymak, A., and Margaritis, A. 2017. Recent developments in the production and applications of bacterial cellulose fibers and nanocrystals, *Critical Reviews in Biotechnology*, 37, 4, 510-524. (doi:10.1080/07388551.2016.1189871).

Reiniati, I., Osman, N.B., Mc Donald, A.G., and Laborie, M.-P. 2015. Linear viscoelasticity of hot-pressed hybrid poplar related to densification and to the in situ molecular parameters of cellulose, *Annals of Forest Science*, 72, 693-703. INRA and Springer-Verlag: France. (doi: 10.1007/s13595-014-0421-1)

Reiniati, I., 2009. Chemical, Physical, and Visioelastic Properties of Hotpressed Hybrid Poplar. M.S. Thesis. Washington State University: USA.

Gupta, B., Reiniati, I., and Laborie, M.-P., 2007. Surface properties and adhesion of wood fiber reinforced thermoplastic composites, *Colloids and Surfaces A: Physicochemical and Engineering Aspects* 302 (1-3) 388-395.

CONFERENCES AND WORKSHOPS

Reiniati, I., Hrymak, A.N., and Margaritis, A. Adsorption of Antibiotic Tetracycline Hydrochloride on Bacterial Cellulose Nanocrystals. Nano Ontario 2016, University of Guelph, Guelph, ON, Nov. 10-11, 2016.

Reiniati, I., Hrymak, A.N., and Margaritis, A. Characterization of Cellulose Fibers and Nanocrystals from *Gluconacetobacter xylinus*. Annual Research Bridge of Chemical and Biochemical Engineering of University of Western Ontario, Sarnia-Lambton, ON, July 9, 2015.

Reiniati, I., Hrymak, A.N., and Margaritis, A. Characterization of Bacterial Cellulose Nanofibers and Nanocrystals. 64th Canadian Chemical Engineering Conference, Niagara Falls, ON, Oct. 19-22, 2014.

Reiniati, I., Hrymak, A.N., and Margaritis, A. Production and Purification of Bacterial Cellulose Nanocrystals. 13th International Symposium on Bioplastics, Biocomposites & Biorefining – Moving Towards Sustainable Bioeconomy, Guelph, ON, May 19-24, 2014.

Business Acumen, Ivey School of Business, University of Western Ontario, London, ON. 2015.

Fundamental of Project Management, MITACS STEP Workshop, London, ON, 2014.

Essentials of Productive Teams, MITACS STEP Workshop, London, ON, 2013.

The Teaching Assistant Training Program. Teaching Support Services, University of Western Ontario, London, ON. 2011.